Applications of coupled gas chromatography-atomic emission detection.

WEBSTER, Caroline S.

Applications of Coupled Gas Chromatography-Atomic Emission Detection

Caroline S Webster, MSc

A thesis submitted in partial fulfilment of the requirements of
Sheffield Hallam University
for the degree of Doctor of Philosophy

June 1995

ACKNOWLEDGEMENTS

I would like to thank my Supervisor, Professor Michael Cooke, for his help and encouragement throughout this project.

I am also grateful to Mrs Joan Hague for her technical support and advice, and to Sally for her patience and hard work in typing this thesis.

I would also like to thank all my colleagues in the laboratory for their friendship and understanding.

Special thanks go to my parents for their constant support and encouragement over the last few years, without which none of this would have been possible.

Finally, I must thank Fergus for putting up with me during my writing-up stage, and for keeping me going for the last 3½ years.

ABSTRACT

This thesis describes the evaluation and application of the atomic emission detector as a detector for capillary gas chromatography.

Chapter 1 is a general introduction to the technique, describing the development of the atomic emission detector, the theory of its operation, and some of its applications. This chapter also includes a detailed description of chromatography theory.

Chapter 2 describes the experimental conditions used throughout the course of this work.

Chapter 3 concentrates on compound independent calibration, beginning with a general introduction to the area and a discussion of studies already made. Four groups of compounds were used to determine the ability of the atomic emission detector to perform compound independent calibration. Initial studies with a group of similar hydrocarbons showed little or no compound/structure dependence. However, results from the same study with a group of phenols did indicate some structure dependence for carbon and oxygen, but when chloroanisoles were tested, this compound dependence was not apparent.

A group of different nitrogen-containing compounds was then studied. Here structure dependence was observed on all channels, ie carbon, oxygen and nitrogen. It was also noted that the responses became non-linear at higher concentrations. This would normally indicate detector overload, but not in this case as non-linearity occurred to different extents for the same element in different compounds.

A study was also made on the effect of discharge tube ageing on response. Clean and dirty discharge tubes were used for the phenols and the nitrogen-containing compounds. The phenol, carbon and chlorine results showed a decreased sensitivity with the old tube, but the oxygen responses were not affected. The same drop in sensitivity was seen with the nitrogen-containing compounds, but here oxygen was also affected.

Chapter 4 describes the use of the atomic emission detector and mass spectrometry as complementary techniques. Perfume samples were analysed using both instruments. A comparison of 'real' and 'fake' perfumes was also made. Results indicated that the atomic emission data was useful in deciding whether to accept or reject mass spectral library guesses.

Chapter 5 describes the application of the atomic emission detector for the analysis of refinery streams. The use of the 'backamount' correction facility was also effectively demonstrated.

Chapter 6 is a general discussion of the instrument including operational problems encountered and possible modifications to overcome these problems.

The overall objective of the thesis is to place the GC-AED combination in the context of the commonly used chromatographic techniques.

TABLE OF CONTENTS

CHAPTER 1
INTRODUCTION

CHAPTER 2
EXPERIMENTAL DETAILS

CHAPTER 3
COMPOUND INDEPENDENT CALIBRATION

CHAPTER 4
PERFUMES

CHAPTER 5
SULPHUR TRACE ANALYSIS

LIST OF FIGURES

LIST OF TABLES

1.1 Introduction to Chromatography and Detectors

The ability to determine very small amounts of an analyte, possibly present in a complex matrix, is a basic requirement for analytical chemists. The problems encountered in fulfilling this requirement led to the development of two main types of analytical technique.

The first of these is the use of highly selective methods which only respond to the species of interest, therefore ignoring all other components which may be present. An example of this type of method is atomic absorption spectroscopy.

The second approach involves the separation of a mixture into its individual components before detection, and forms the basis of a range of analytical techniques. The simplest of these include filtration or crystallisation methods where a compound is separated as a solid from a liquid matrix. Other techniques are based on the partitioning of samples between two immiscible phases. Methods which utilise two phases moving relative to each other are broadly termed 'chromatographic' methods.

Usually one phase is held in position in a tube or column, and is termed the stationary phase. The second 'mobile' phase then moves over the stationary phase, carrying the analyte with it. The stationary phase can be a solid or a liquid and is spread on the walls of a column or over an inert support. The mobile phase can be a gas, a liquid or a supercritical fluid.

This basic idea has developed into a wide range of methods. These can be divided into two broad groups depending on whether the mobile phase is a gas or a liquid, ie gas chromatography/liquid chromatography/high performance liquid chromatography.

Separation and retention of components occurs via the interaction of the analyte with the stationary phase. The degree of interaction, and therefore the retention time is characteristic of the individual compound, and will be the same whether that compound is present as a single component or in a mixture. The retention properties of a compound can also be used for identification of unknowns by comparison with standards. Retention times can be altered, however, by changing the stationary phase in gas chromatography, the mobile phase in liquid chromatography or the temperature in either technique.

Once components are separated, they are passed to a detector which produces a variable electronic output which is recorded as a chromatogram.

Detectors for gas chromatography may be broadly divided into three categories. Firstly, universal detectors which are virtually unselective. An example is the thermal conductivity detector.

Secondly, selective detectors. These are used when it is necessary to discriminate specific components, or to analyse for one particular class of compound. Selective detectors may be element selective such as the nitrogen/phosphorus detector; structure/functionality selective, eg Fourier Transform Infrared Spectroscopy; or property selective, eg the flame ionisation detector, the electron capture detector.

Thirdly, specific detectors which are those sufficiently selective to be effectively blind to eluates other than the target analyte, eg a mass spectrometer set to a specific mass number.

1.2 History of Chromatography

Probably the earliest work on chromatographic separations was carried out in the mid-nineteenth century. Friedrich Runge (1795 - 1867) published books in 1850 and 1855 in which he described how solutions of mixtures of coloured compounds formed concentric rings when spotted onto filter paper.

Separations were also carried out by David Talbot Day (1859 - 1925) while he was investigating the origins of different crude oils. In 1897 he showed that when crude oil was passed through Fullers earth, fractionation took place, the early fractions differing in composition from the latter. However, Day did not fully realise the potential of the technique, and it was left to Michael Tswett (1872 - 1919) to coin the term 'chromatography'.

Tswett was a Russian botanist working on the separation of plant pigments, particularly chlorophyll. In a paper presented in 1903, Tswett summarised his work on the separation of pigments, describing chromatography, but not actually naming the technique. Three years later he reported a method in which extracts of plants were placed on top of a calcium carbonate column and washed through with a solvent, producing different bands of colour. He named the technique, chromatography saying "I call such a preparation a chromatogram, and the corresponding method a chromatographic method" (1).

The methods described by Tswett were not widely adopted however, and no further work was done in the area until 1931 when Kuhn, Winterstein and Lederer brought Tswett's work back to the fore by applying it successfully to the separation of carotene and xanthophylls (2). After publication of this work, methods involving a solid stationary phase and a liquid mobile phase became widely used.

No further developments occurred until 1941 when Martin and Synge made a huge advance (3). They had been working on a very complex liquid-liquid partitioning system in which two solvents moved in opposite directions in a tube, when it occurred to them that it was not necessary for both liquids to move. They discovered that by coating one of the liquids onto a solid inert support, better separations could be achieved. Martin and Synge also noted that the mobile phase need not be a liquid, but could be a gas. This statement alone predicted the possibility of gas liquid chromatography, but was not picked up on at the time, as World War II was at its height.

For the following ten years, no significant advances were made in the area until Martin began work with A. T. James at the National Institute for Medical Research. The project they were involved in was not progressing, so Martin suggested attempting some separations using gas liquid chromatography. The results of the subsequent fatty acid analysis were published in 1952 (4), and gas liquid chromatography took off as a new technique. In the same year Martin and Synge received the Nobel Prize for chemistry.

At this time, Denis Desty, a scientist with British Petroleum, approached Martin and James about hydrocarbon separation (5). Up until the advent of gas chromatography, liquid chromatography was widely used for the analysis of crude oil and its products. However, the equipment and technique used were relatively old-fashioned. Glass columns packed with coarse silica gel or aluminia were used and required large volumes of solvent. The hydrocarbons could only be separated into saturates and, mono-, di-, tri-, and polyaromatics. Separation of individual compounds was not usually possible, therefore the petroleum industry became very interested in the possibility of separating complex hydrocarbon mixtures into individual compounds automatically and quickly. The industry, therefore, supported the research, and the first commercial instrument became available in 1955.

By the late 1960s and early 1970s, instrumentation for gas chromatography was well established, but by contrast liquid chromatography had hardly advanced at all. It soon became clear, however, that the instrumental techniques developed for gas chromatography could be adapted for liquid chromatography. The early work in this area was so successful that the resulting technique of high performance liquid chromatography was quickly adopted by the pharmaceutical industry, just as gas chromatography had been by the petroleum industry.

1.3 Basic Concepts of Chromatography

Since the emergence of chromatography as a major separation technique attempts have been made to derive equations to explain the processes occurring during separation. The basic concepts of chromatography were established early on, and these theories are effectively the same for all areas of chromatography, and can therefore be described by a common set of equations.

When establishing and optimising a chromatographic system there are four factors that must be considered. The first of these is **resolution**, Rs. This is defined as the ability to separate components of a mixture and is closely related to retention times and peak shapes. Secondly, the **sensitivity** of the instrument must be optimised. Thirdly, the technique must give **reproducible** results, and finally the **analysis time** should be reasonable.

However, in practice it may be necessary to compromise on the optimum conditions. For example, maximum resolution may require a long analysis time which could be expensive in terms of operator time and instrument maintenance.

In order to select the optimum conditions for a particular analysis the factors which influence retention, peak shape, sensitivity and efficiency must be considered.

1.3.1 **Retention**: In theory the retention of a compound is defined as the volume of the mobile phase required to elute that compound compared with the volume of the column. This value however would be almost impossible to measure in GLC, so time is used instead, with retention time, t_R, being the time after injection to elution of the peak (Figure 1).

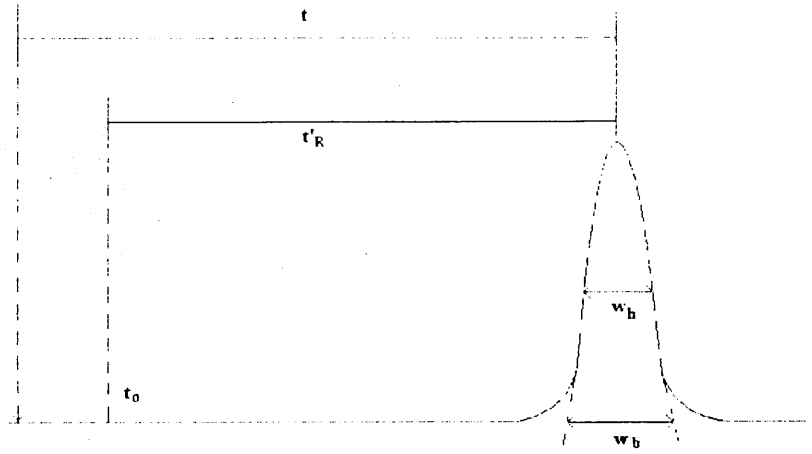

FIGURE 1

The column void volume, t_o, is the volume accessible to the eluent, and is usually determined as the time taken for an unretained compound to travel through the column. The adjusted retention time, t'_R, is therefore the difference between the retention time and the void volume

$$t'_R = t_R - t_o$$

This value is therefore the time the analyte is retained on the column compared with an unretained compound, and is directly related to the interaction of the sample with the stationary phase.

The fundamental factor which governs retention is how the sample is distributed between the stationary and mobile phases. Different analytes interact and are distributed in different ways, giving them different retention times and bringing

about separation. The distribution of a sample between a stationary and mobile phase is best shown as the distribution constant K where

$$K = \frac{\text{Concentration in unit volume of stationary phase}}{\text{Concentration in unit volume of mobile phase}}$$

K therefore depends solely on the structure of the analyte and the nature of the phases.

The proportion of the analyte present in each phase is the capacity factor k' and is the product of the distribution constant and the phase ratio, $\alpha = Vs/Vm$.

$$\therefore \quad k' = K \frac{Vs}{Vm}$$

where Vs and Vm are the volumes of stationary and mobile phase respectively. The capacity factor can also be shown to be related to retention time, ie:-

$$k' = \frac{t_R - t_o}{t_o} \qquad \text{ie} \quad \frac{t'_R}{t_o} = K\frac{Vs}{Vm}$$

There is, therefore, a direct relationship between the distribution constant and retention time of an analyte. As the distribution constant is a property of the analyte, then the retention time for that particular compound should be independent of other compounds present in the sample. Therefore the retention time of a compound on a particular column will be the same whether the compound is injected in a pure form or in a mixture.

For two different analytes to be separated on the same column they must have different distribution constants, the magnitude of this constant dictating the length of time a compound is retained, ie a large distribution constant will lead to a long retention time.

However, some analytes have the same or very similar distribution constants, and will therefore have the same or very similar retention times. To overcome this problem the separation conditions can be changed, eg mobile phase, stationary phase or temperature. In HPLC the mobile phase is usually changed, as this can have a great effect on separation. In GLC helium or hydrogen are most often used as mobile phases. However, their partition properties are very similar, so changing one for the other would have little or no effect on separation.

Changing the temperature of a GLC run does affect separation though. Increasing the temperature makes the sample more volatile, therefore it favours the gaseous phase more and the distribution constant is reduced. The most useful way of altering the temperature of a GLC separation is to change the ramp rate of a temperature programmed run. If the ramp rate is decreased the analytes have more time to interact with the stationary phase, so separation should improve. However, slower ramp rates can cause peak broadening and affect resolution. If the run is isothermal changing the temperature would be unlikely to affect separation unless the compounds involved had very different structures, and therefore different interactions with the stationary phase. Changing the temperature for similar compounds would not affect separation, as distribution constants would be altered to the same extent.

1.3.2 **Efficiency**: Ideally, when a sample is placed on the column the analyte band should spread as little as possible during the separation to give sharp peaks. The efficiency of a column is defined as a measure of the broadening of a sample peak during a separation. Efficiency is expressed as the number of theoretical plates on the column, n, and is determined experimentally as the square of ratios of the retention time over peak broadening, σ. Peak broadening is defined as the standard deviation of the retention times of individual molecules. However, in

practice σ is normally replaced by the base peak width, Wb or the peak width at half height, Wh, ie

$$n = \left(\frac{t_R}{\sigma}\right)^2 = 16\left(\frac{t_R}{Wb}\right)^2 = 5.54\left(\frac{t_R}{Wh}\right)^2$$

If a Gaussian peak shape is assumed, Wb is 4σ and Wh is 2.35σ, leading to the factors 16 and 5.54 in the above equations. It can be difficult to measure the width of the base of a peak as it requires extrapolation of the sides of the peak. The width at half-height, Wh is therefore most frequently used.

Typical values of efficiency for packed GLC columns would be n = 500 - 2,000 and for open tubular columns, n = 30,000 - 100,000.

For open tubular columns an alternative way of expressing efficiency is as the effective efficiency N or Neff. where:-

$$N = 16\left(\frac{t'_R}{Wb}\right)^2 = 5.54\left(\frac{t'_R}{Wh}\right)^2$$

Effective efficiency calculations are based on adjusted retention times, t'_R, because of the long void volumes of open tubular columns.

Often it is necessary to compare the efficiencies of columns of different lengths. In these cases the efficiencies can be expressed as the height equivalent to a theoretical plate (HETP), h where:-

$$h = \frac{L}{n}$$

1.3.3 **Resolution**: If a chromatogram contains two components their resolution, Rs, is determined from the difference in their retention times and peak widths,

$$Rs = \frac{2(t_{R2} - t_{R1})}{(Wb_1 + Wb_2)}$$

An Rs value of 1.0 indicates 98% separation or 2% overlap, whereas a value of 1.25 represents 99.4%, or almost complete separation. Ideally the resolution of 2 peaks should be 1.0 or greater. Resolutions of less than 1.0 indicate severe overlap, making quantification difficult. If resolution is very poor there may not be a valley between the two peaks, and one may appear as a shoulder on the other.

The equations for efficiency and resolution can be combined, ie

$$Rs = \frac{\sqrt{n}}{4}\left(\frac{\alpha - 1}{\alpha}\right)\frac{k'_2}{1 + k'_2}\left(\alpha = \frac{k'_2}{k'_1}\right)$$

where α is the ratio of the capacity factors of the 2 peaks.

The above equation shows that the resolution of a separation depends on the square root of the efficiency. As efficiency is directly proportional to column length, to double the resolution of a separation, the column length would have to be increased four fold.

1.3.4 **Optimisation of separation**: As shown previously, resolution can be improved by changing separation conditions. However, if peak spreading can be reduced, better resolution can be achieved without having to alter the separation parameters.

There are several factors which can contribute towards band spreading during a separation. Part of the spreading occurs on the column. The peaks can also spread because of dead volumes in the injector, detector, connecting tubing and column fittings. However, these effects can be largely ignored in GLC because high diffusion rates in the gases result in rapid mixing.

In GLC there is also band spreading due to the pressure drop across the column which causes expansion of the gaseous analyte. However, most band spreading occurs on the column because of the kinetics of the separation processes.

Probably the most often used model for the causes of band spreading on the column is the equation derived by van Deemter *et al* (6). The equation has three components which are related to the average mobile phase flow rate, u:-

$$h = A + \frac{B}{u} + Cu$$

The three components are eddy diffusion (A term), molecular diffusion (B term) and mass transfer effects in stationary and mobile phases (C term). The contributions of the three terms can be thought of as separate sources of variance. Therefore in optimising the system the reduction of a particular term will decrease its associated variance.

1.3.5 **Eddy diffusion**: Analyte molecules travelling through a column can follow different pathways around the particles of the stationary phase, some of these pathways being shorter than others. The variations in the distances travelled therefore cause the bands to spread out:-

$$\sigma^2 = 2L\lambda dp$$

where λ is a geometrical packing factor whose value increases with decreasing particle size, dp. For open-tubular columns this term is effectively zero as the liquid stationary phase is only coated on to the walls of the column.

1.3.6 **Molecular diffusion**: The molecules of an analyte dissolved in a liquid matrix can diffuse in all directions, part of this diffusion being along the axis of the column, resulting in axial spreading of the peak. The extent of the spreading is directly proportional to the coefficient of diffusion of the analyte in the mobile phase, Dm, and the time the sample is in the mobile phase, L/u.

$$\sigma^2 = \frac{2DmL\gamma}{u}$$

where γ is a geometrical factor dependent on the nature of the stationary phase. The diffusion rate, Dm, depends on the temperature and pressure of the mobile phase, so spreading is decreased by reducing temperatures and increasing column pressures. In GLC this spreading can also be decreased by using a higher molecular weight carrier gas, as their diffusion rates are lower.

1.3.7 **Resistance to mass transfer**: This term is the most important for both GLC and HPLC. It is usually split up into two components, the resistance to mass transfer in the stationary phase, CsU, and in the mobile phase, CmU.

The transfer of analyte molecules between the stationary and mobile phases continually takes place to maintain distribution ratios. However, this transfer can only take place at the interface between the two phases.

As a compound passes down a column the concentrations in the mobile phase at the front and back edges of the peak will be changing. The analyte molecules can diffuse a certain amount into the phases, and therefore must diffuse back to the interface to respond to changes in the mobile phase. This causes a time-

delay before the concentration distribution between the phases can be re-established.

At the front edge of a peak the mobile phase will be rich in analyte compared to the stationary phase. If the diffusion of the analyte to the interface is slow, the analyte concentration in the mobile phase can 'get ahead' of the concentration in the stationary phase, causing peak broadening. The extent of the broadening will depend on the diffusion rates of the analyte, and is therefore time-dependent. The broadening therefore increases as the mobile phase flow rate increases.

At the back edge of the peak, the stationary phase will be relatively analyte rich. The opposite effect to that described above therefore occurs, and the tail of the peak is stretched.

The effect due to a liquid stationary phase depends on the film thickness (df), the diffusion coefficient of the analyte on the stationary phase (Ds) and a geometric factor (q) whose value depends on the nature of the packing.

$$\sigma^2 = \frac{Lqk^1 d_1^2 u}{(1+k^1)^2 Ds}$$

The second part of the C term is the resistance to mass transfer in the mobile phase, Cm

$$\sigma^2 = \frac{Lwf(k^1) dp^2 u}{Dm}$$

where $f(k^1)$ is the affinity of the analyte for the mobile phase, and is a function of the capacity factor. This parameter has been precisely described for open-tubular columns and indicates that increased retention can cause band

broadening. The parameter dp is the diameter of the stationary phase particles and represents the average path length between particles in the column. This term is usually replaced for open tubular columns by the column diameter, dc. The parameter w is a constant.

The most important term in the above equation is Dm, the coefficient of diffusion of the analyte in the mobile phase. However, in GLC this term can usually be ignored because the mobile phase effects are much smaller than the stationary phase effects. This is because gaseous diffusion rates are higher than those in liquids.

However, Dm is important in HPLC as the mobile phase effects are quite significant. Dm in a liquid is temperature dependent and can be approximated by the Wilke-Change equation:-

$$Dm = \frac{7.4x10^{-12} T(\psi M_{eluent})^{0.5}}{\eta V_{solute}^{0.6}}$$

where T is temperature in Kelvins
ψ is the eluent association factor
M_{eluent} is the molecular weight of the eluent
η is eluent viscosity
V_{solute} is solute molecular volume

so this term depends mainly on the size of the analyte molecule.

The combination of the above terms give the van Deemter equation:-

$$h = A + \frac{B}{u} + Cu$$

However, as exact numerical values are difficult to calculate for some of the terms, a graphical illustration of HETP versus flow rate can be useful (see Figure 2).

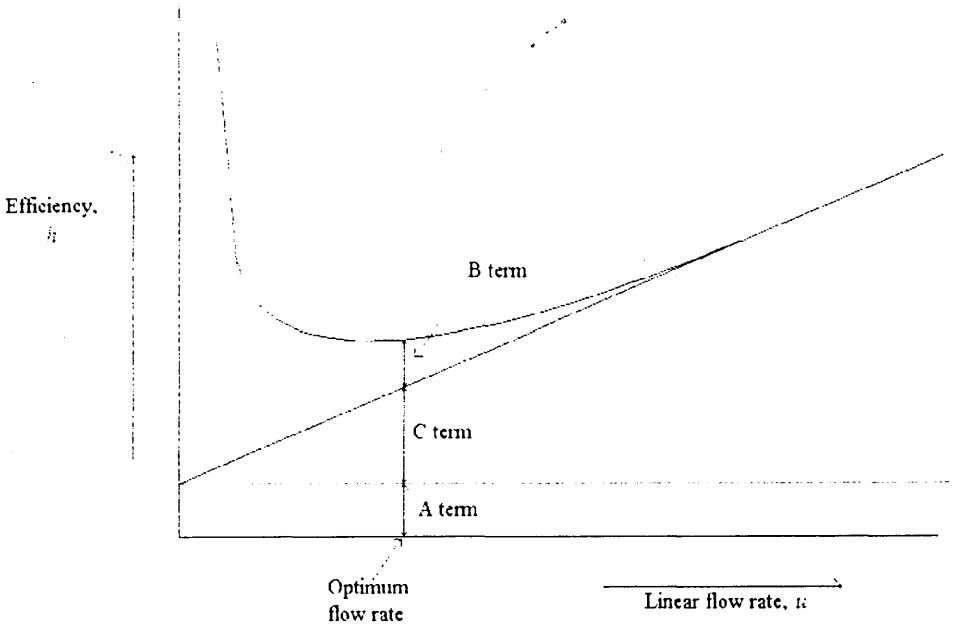

FIGURE 2

REALTIONSHIP BETWEEN ELUENT FLOW RATE AND EFFICIENCY BASED ON THE VAN DEEMTER CURVE

As the graph shows, the A term (eddy diffusion) is independent of flow rate. At low flow rates the B term (molecular diffusion) dominates, but as the rate increases the C term (mass transfer) becomes more important. Therefore there is an optimum flow rate for a chromatographic separation which should give maximum efficiency.

1.4 Columns

The column plays a vital role in any chromatographic separation as it determines the efficiency and selectivity which can be achieved.

Columns for Gas-Liquid Chromatography have greatly changed over the last 15 years or so. Up until the early 1980s most separations were performed on

packed columns where the liquid stationary phase was coated on to an inert support and packed into a metal or glass tube. A few separations were carried out on open-tubular columns in which the stationary phase was coated onto the column walls. However, the relatively high price of these columns at the time precluded their wide-spread use.

Glass and fused silica open tubular columns were then introduced in which a cross-linked polymer acted as the stationary phase. These columns give much higher efficiencies and reproducibility.

1.4.1 Packed Columns

The first component of a packed column which must be considered is the tubing. Ideally this should be chemically inert, thermally stable and flexible enough to be wound into a coil. The most often used materials are copper, stainless steel or glass. Glass columns are popular because the stationary phase is visible and can therefore be easily checked for the build-up of contamination, decomposition of the phase or settling of the packing. The inner surface of the glass is usually silylated to prevent interaction with polar samples. Metal columns generally have less inert surfaces. One of the biggest problems with packed columns is that different makes of gas chromatographs often require columns of different dimensions and shapes, so columns are rarely interchangeable between instruments.

The second component of a packed column is the support material on to which the liquid stationary phase is coated as a thin film. The support material must therefore be inert towards both the stationary phase and the analytes. It should also have a large surface area so that the liquid phase can be spread as thinly as possible. Mechanical strength is also important in with-standing packing procedures. To achieve the optimum efficiency for a separation the particles of

the support material should have a uniform particle and pore size so that they can be evenly packed.

Most supports are based on diatomaceous earths or kieselguhrs. These are obtained from geological deposits of the skeletons of single-cell algae or diatoms, and are mainly composed of silica. To increase particle size the diatomaceous earths are calcinated alone to give red firebrick or with sodium carbonate flux to give a grey or white filter aid. The Chromosorbs are probably the most widely used support materials. Chromosorb P (pink) is made from calcinated firebrick and is a hard support with a large surface area, mainly used for the separation of hydrocarbons and moderately polar compounds.

Chromosorb W (white) and Chromosorb G (grey) are formed from flux-calcinated material and are suitable for polar samples. Chromosorb W is brittle and easily broken up and so requires careful handling. However, it has a larger surface area than the harder Chromosorb G and can therefore accept a higher load of liquid phase.

Support materials are available in a wide range of particle sizes, with 80-100 or 100-120 mesh supports being used for analytical columns and 40-60 or 60-80 for preparative work. However, it is more difficult to pack small particles uniformly, therefore the columns can have high back pressures.

1.4.2 **Open-tubular columns**

Open-tubular columns are unlike packed columns in that they contain no support material, the liquid stationary phase being coated directly on to the column wall. Such columns are called wall-coated open-tubular columns, WCOT, and therefore have a greater inertness than packed columns because there are no support affects. These columns also have very low back pressures and can

therefore be longer for the same pressure drop. However, in order to increase efficiency open-tubular columns must be very narrow. This reduces mass transfer effects and band spreading. Open-tubular columns therefore have a greater separating power than packed columns, giving narrower peaks and faster analysis times. Open-tubular columns are often called capillary columns because of their small diameter. Typical diameters are of the order of 0.18 to 0.32mm id.

Unfortunately, because capillary columns only contain a small amount of liquid stationary phase relative to their cross-sectional area, they have a greatly reduced sample capacity compared with packed columns (ng vs μg). The columns can easily be overloaded, therefore small injection volumes are required. This in turn leads to lower operating pressures and flow rates. These factors restricted the application of capillary columns until the late 1970s.

Support-coated open-tubular (SCOT) columns were then introduced in an attempt to increase sample capacity. These columns had a wide diameter (0.5mm) and the liquid film was coated on to a thin layer of a diatomaceous support which was spread on the column walls. This gave the liquid phase a larger surface area. However, these columns have now largely been replaced by wide-bore columns with thick films. Wide bore usually means 0.53mm id (530μ m).

Initially capillary columns were made from borosilicate glass, but such columns were brittle, and coating procedures were not particularly reproducible. An important development therefore was the replacement of the borosilicate glass with flexible fused silica or quartz tubing. The columns were therefore flexible and more robust, and fitted easily into injectors or detectors. This meant that the same column could be used in different instruments.

The next major step forward was the introduction of chemically bonded liquid phases. Here, the liquid phase bonded, usually by cross-linking between vinyl groups initiated by photolytic or free-radical reactions. There is usually some degree of bonding to the column wall so that the liquid phase is permanently held in place. The columns therefore have very low bleed, reducing tailing of polar compounds. Bonded columns can also be rinsed with organic solvents without stripping off the stationary phase.

Fused silica columns are coated with an external polyimide layer to protect the outside of the column from scratches.

Capillary columns are available in a wide range of internal diameters (0.18 - 0.32 mm), lengths (5 - 100m) and film thicknesses (0.1 - 5.0 μm). The best efficiencies are achieved using small diameters, but these columns cannot cope with large sample volumes. In general the column capacity increases with internal diameter or film thickness, but efficiency decreases.

1.4.3 **Stationary Phases**

Usually the same types of stationary phases are used for both open-tubular and packed columns. There are a vast number of different phases available, but in practice only a few are widely used. Generally, a liquid phase should be chemically stable, unreactive towards the sample, involatile, and stable to thermal decomposition. However, as the temperature of a separation increases the phase may become unstable and start to decompose causing column bleed. All phases therefore have a maximum recommended operating temperature, (MAOT: Maximum Allowable Operating Temperature).

Liquid phases can be broadly grouped into non-polar, polar and special phases. Each phase has a different selectivity, ie different phases retain and separate

compounds in different ways.

Non-polar phases have no groups capable of hydrogen bonding or dipole interactions with analytes, therefore compounds are eluted according to their boiling points. An example of a non-polar phase is Apiezon L which is hydrocarbon based (n - alkanes). These phases are used for packed columns mainly. Other non-polar phases are based on polymers with a silicon-oxygen-silicon backbone. These compounds are very stable and can be used up to about 320°C without bleeding. Another group of non-polar phases are the dimethylsilicones such as SE-30, OV-1 and OV-101. OV-101 is less viscous than other silicones and so is preferred for packed columns. The more viscous phases such as OV-1 are used for capillary columns as a more even coating of the liquid phase on the column wall can be achieved, and the higher viscosity confers some physical stability to the film at high temperatures. Many different nomenclatures now exist for these silicone polymers as most column manufacturers have generated their own naming systems for these phases to imply individuality of performance.

However, non-polar phases can often cause peak tailing in polar samples, so polar phases are usually used in these cases. Also poor solubility of polar analytes in the non-polar stationary phase means that the analytes and stationary phase are mismatched giving an apparent low capacity.

Polar liquid phases contain polar functional groups such as halogen, hydroxyl, nitrile, carbonyl or ester groups, so that analytes containing polar groups will interact with the phase more than non-polar analytes. Polar separations are therefore dependent on polar-polar interactions as well as boiling points.

Substituted silicones are used to form some polar phases. Different proportions of polar groups can be added to the silicone skeleton to give a range of column

polarities. For example, phases substituted with the trifluoromethyl group have strong electron accepting properties and are particularly useful for analytes containing carbonyl and nitro groups. Examples are OV-210 for packed columns and OV-215 for capillary columns.

Cyano substituted phases are also used. These groups are electron attracting and interact with π-bonded groups, eg phenyl ring, ester, and carbonyl groups. These phases tend to be very polar and OV-275 is regarded as one of the most polar phases available.

A range of specialised phases have been developed for use with particular techniques or groups of compounds. For example, carboxylic acids produce peak tailing on most packed columns, and to a lesser extent on open-tubular columns. A separation of a series of acids (C_1 - C_7) can be carried out however on a Carbowax 20M column impregnated with terephthalic acid.

There are also special phases for basic compounds. For example amines, which react badly with silica support materials can be separated on a Carbowax 20M column to which ≈ 2% of potassium hydroxide has been added.

Another area of interest is the development of phases which can separate enantiomers. These are chiral phases. A number of these phases have been developed which incorporate amino-acid derived chiral centres. Examples are phases derived from cyano-bonded siloxane polymers such as König's material and Chirasil-Val.

1.5 Hyphenated Techniques

All chromatography is a hyphenated technique. First there is separation, then detection. However, over the years the need for more information about samples

has grown, as have demands for better selectivity and sensitivity.

The first major hyphenated development was gas chromatography-mass spectrometry (GC/MS). The mass spectrometer has been used in analytical chemistry since about 1900, but the first quantitative analysis of mixtures by mass spectrometry was performed in 1927 when gaseous organic compounds were studied. Mass spectrometry was first coupled to gas chromatography in 1957 by R S Gohlke.

One major development which has greatly increased the ease of use of GC/MS was the introduction of capillary gas chromatography columns. The small flow required by these columns compared with packed columns, meant that they could be directly connected to the mass spectrometer without a special interface. Sub-picogram levels of detection have been reached using this set-up. The development of relatively inexpensive bench-top systems has helped make GC/MS a popular technique by making it available to a wider range of users. Large spectral libraries are incorporated into the software used to operate the systems. The mass spectra of unknown compounds are then compared with the library spectra. However, there is sometimes the possibility of a misidentification or non-identification if the unknown compound is not in the library. An alternative spectroscopic technique is therefore needed to provide more information.

Atomic emission spectroscopy can provide quantitative atomic information in the form of empirical formulae. Fourier Transform Infrared Spectroscopy can also be used to provide molecular structural information.

1.6 Atomic Spectroscopy

In the late 17th century Sir Isaac Newton (1642 - 1727) laid down the principles

of spectroscopy when studying prisms and rainbows. Before Newton's time it was accepted that white light was changed into colours by the prism and that colour was made up of light and darkness. Newton noted that when sunlight from a small hole in a shutter passed through a prism it was dispersed to form a series of coloured images of the hole. Newton called these images a spectrum. He then performed experiments in which the dispersed light was passed through a second prism. He observed that the light was not further dispersed by the second prism, only further refracted. He also noted that there was no colour change when an isolated colour passed through the second prism. Therefore, Newton concluded that the colours could not be produced by the prism.

Spectrochemical analysis was first reported by Talbot in 1820. He devoted much of his research to the study of the alcohol flame spectra sodium, potassium, lithium and strontium salts, and the spark spectra of silver, copper and gold. In 1826 (7) he wrote "This red ray (from the flame of potassium nitrate) appears to possess a definite refrangibility, and to be characteristic of the salts of potash and soda....If this should be permitted, I would further suggest that whenever the prism shows a homogeneous ray of any colour to exist in a flame, this ray indicates the formation or presence of a definite chemical compound".

In 1834 Talbot reported that strontium and lithium could be distinguished spectroscopically. However, Talbot did not fully recognise the significance of his findings, so the technique developed no further until the 1850s when Kirchhoff and Bunsen established that the spectra emitted from a metallic salt were characteristic of the metal itself. They placed various salts of the alkali elements and alkali earths on a platinum wire and introduced them into a flame. It was noted that the position of a particular element's spectral lines was independent of the excitation source used.

The work done by Kirchhoff and Bunsen led to the discovery of cesium (1860) and rubidium (1861) (8). Other elemental discoveries using spectroscopic evidence included Crookes' (9) discovery of thallium, Reich and Richters discovery of indium, de Boisbaudran's discovery of gallium and the establishment of helium as a terrestrial element by Ramsey (10).

The use of spectroscopy as an analytical tool rapidly declined after the initial interest generated by Kirchhoff and Bunsen's findings. The technique regained its popularity around the turn of the century, but progressed very slowly. One of the main reasons was that the technique was too sensitive for most work done at the time. Also, the use of low temperature flames as sources limited workers to a small range of elements because the excitation energy was not high enough to excite all elements. As electrical facilities grew, arc and spark sources became more available and were capable of exciting a broader range of elements. These sources, however, produced very complex spectra, making line identification more time consuming than with other methods.

In the 1950s plasmas were developed as new excitation sources for atomic emission spectroscopy. These plasmas were created from a high frequency electrical discharge in an inert gas. These plasmas have since developed into three popular high power discharges which are exceptional atomisers due to their high temperatures and inert gas atmospheres.

The first of these sources are the DC plasmas (Figure 3). These are formed between two or more electrodes which are cooled by argon gas. The plasma is very stable due to the position of the electrodes, and can tolerate large volumes of liquid samples. However, very high gas flows are required to prevent the samples coming into contact with the electrodes. The second type of plasma sources are inductively coupled plasmas (Figure 4). This plasma uses a coil wrapped around concentric quartz tubes. The coil carries a current which

DIRECT CURRENT PLASMA

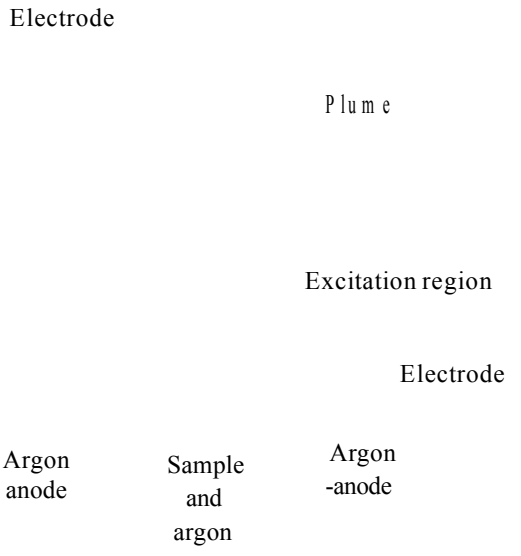

FIGURE 3

INDUCTIVELY COUPLED PLASMA SOURCE

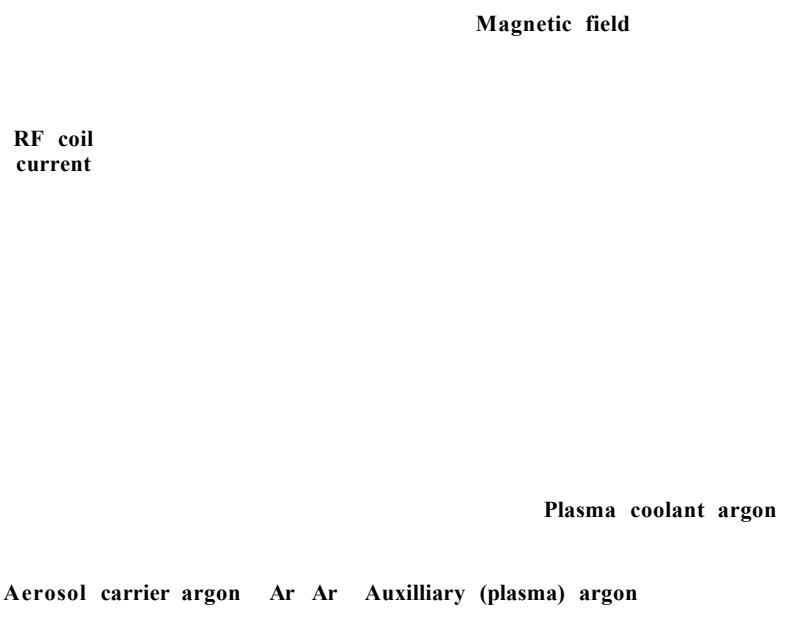

FIGURE 4

generates an inductive field to energise the plasma. The torch-like plasma is formed at the end of the tube and is cooled by flowing argon. Again, very high flow rates are required. Both these plasmas can cope with large sample volumes such as nebulised liquids or powders. This is often an advantage but can cause problems when dealing with small sample volumes, as in gas chromatography.

The third type of plasma source is the microwave induced plasma.

1.7 Development of the Atomic Emission Detector

Two types of microwave plasma systems have been considered as excitation sources for spectroscopy (11).

In the first type, microwave energy supplied by a magnetron is conducted to the tip of an electrode, forming a flame-like plasma. This is termed a capacitively coupled system. The second type consist of electrodeless systems. These are termed microwave induced plasmas, MIPs. Here the microwave energy is coupled to a gas stream, usually argon or helium. The plasma is formed inside a non-conductive discharge tube contained in an external cavity.

The development of the MIP as a detector began in earnest in the mid 1960s. At this stage several cavities were under evaluation (12). The cavity design was known to be crucial to the efficient operation of the plasma. The function of the cavity is to transfer power from the generator to the plasma support gas (13). The efficiency of the system, therefore, depends on how well the cavity transfers the power. To optimise the system a coupling device is usually used to match the impedance of the cavity and plasma to that of the power supply. The resonant frequency of the plasma must also be tuned to match that of the power supply. The reflected power from the cavity is therefore minimised and the power available to sustain the plasma is maximised.

However, the plasma itself changes the frequency of the cavity, therefore detuning it. As the properties of the plasma were known to change with support gas and pressure, frequency tuning and impedance matching adjustments were necessary to ensure efficient operation over a range of plasma conditions.

Various cavities were evaluated, but the two that became popular were the tapered cavity and the Evenson cavity (12, 13) (Figures 5 and 6).

The tapered cavity consisted of a rectangular waveguide tapered at one end. Cavity coupling was achieved via a screw. The most useful feature of this cavity was that it could be positioned without disturbing the discharge tube via the slot at the tapered end. This was particularly useful if the discharge tube was attached to a vacuum system.

The Evenson cavity differed from the tapered cavity in that it had two tuning adjustments giving it a wider operating range. The discharge tube was also held in the transverse configuration.

In 1965 McCormack (14) described a detector for gas chromatography based on electronic emission spectra produced by excitation of the gas chromatography eluents in a 2450 MHz plasma. This frequency was chosen as it was the one used by the medical diathermy units which provided the microwave power in early cavities.

Originally McCormack used low pressure helium as the plasma support gas, because helium produced fewer spectral lines than argon and therefore gave a lower background. However, it was subsequently discovered that a stable argon plasma could be sustained at atmospheric pressure. The argon plasma was therefore used to avoid the complicated vacuum system associated with the helium discharge.

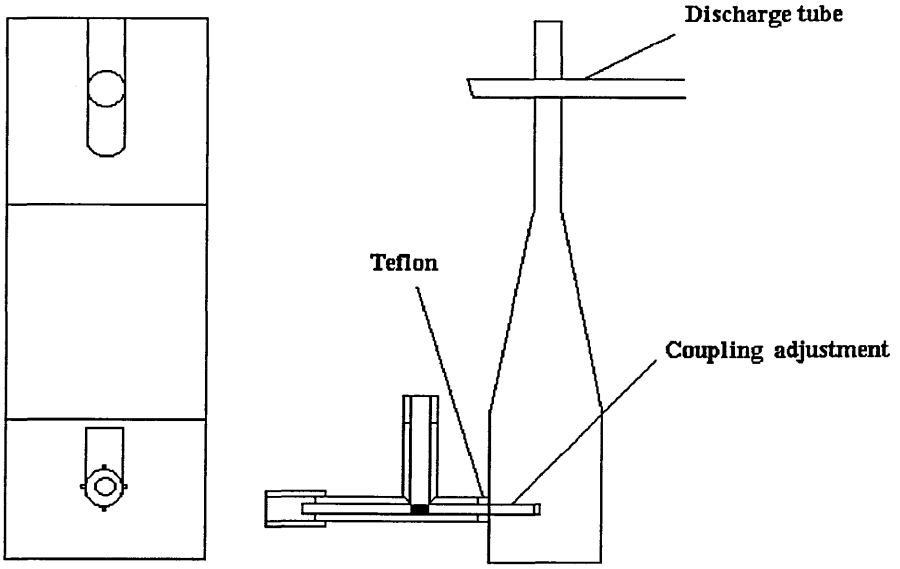

TAPERED RECTANGULAR CAVITY

FIGURE 5

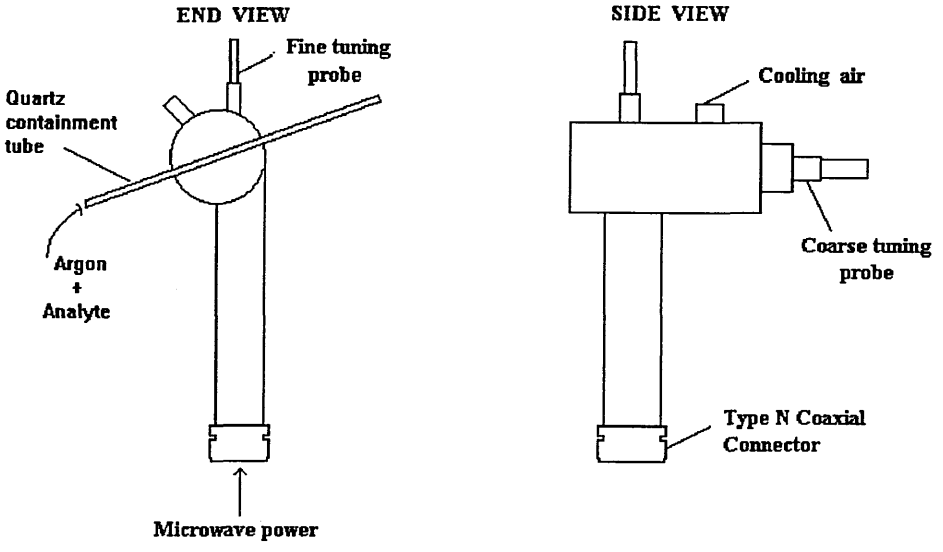

EVENSON 1/4 WAVE CAVITY

FIGURE 6

McCormack noted that using the above system the eluted compounds were not completely atomised, and therefore the spectra obtained arose from both atomic and molecular emissions. This caused an increased spectral background, and meant that the sensitivity for a particular element strongly depended on the compound present.

It was also noted that atomic lines were not produced for sulphur, chlorine and bromine in the argon plasma. Only band emission was observed for these elements. Recombination of atoms was also suspected due to the cyanogen band emission seen for all organic compounds in the presence of nitrogen.

McCormack used both the Evenson and tapered cavities. The latter was found to give better sensitivity, but the Evenson cavity could cope with larger sample volumes.

Bache and Lisk (15) used this arrangement to determine organophosphorus residues to the ppm level. The following year the same authors used a low pressure argon plasma which improved sensitivity by an order of magnitude (16).

Attempts were then made to initiate atomic emission lines from sulphur, chlorine and bromine. Bache and Lisk succeeded using a low pressure helium discharge (17).

In 1967 Moye (18) described an improved detector which used an argon/helium mixture at low pressure to sustain the plasma. This detector showed an increased sensitivity and selectivity for phosphorus, chlorine and iodine. Mage also compared the Evenson and tapered cavities, and found the Evenson cavity to be less sensitive. He also found it difficult to tune, despite the double tuning adjustments. The greatest problems, however, were high noise levels and low

discharge tube life-time. These difficulties were caused by 'hotspots' in the discharge tube which led to a high background and eventual etching and decomposition of the tube. Attempts were made to cool the tube using forced air, but this led to a drop in sensitivity due to deposition of effluent, in particular carbon, on the walls of the tube. Carbon is not volatile below 3500°C, and therefore was found to plate out on the relatively cold discharge tube walls.

Deposition of carbon continued to be a problem until McClean (19) found that the addition of small amounts of oxygen or nitrogen to the plasma dramatically reduced these deposits. These gases were termed carbon 'scavengers'. When organic compounds entered the plasma the scavenger gases held the carbon as volatile carbon oxides and nitrides, preventing build-up on the tube walls. As either oxygen or nitrogen could act as scavenger, either element could be included in the analysis by using the other as scavenger.

However, the minimum level of scavenger gas required seemed to vary, with values quoted of between 0.1 and 5% v/v. Also, the effect of these gases on elemental responses was unclear. These problems were addressed by van Dalen (20) who studied the spectral background and element specific response as a function of scavenger gas concentration. These results showed that below 0.5% v/v, the spectral background remained largely unchanged, but that the sensitivity for sulphur and the halogens decreased with increasing oxygen concentration. A maximum level of 0.25% v/v was therefore set for oxygen.

Oxygen obviously could not be used as a scavenger if oxygen was the element to be detected, so nitrogen was used. However, nitrogen was found to give strong molecular bands throughout the spectrum leading to a high background and serious spectral interferences. The only elements not affected by these interferences were carbon, phosphorus and oxygen. It was therefore suggested that nitrogen only be used as a scavenger for the specific detection of oxygen.

These scavenger gases worked well to stop carbon build-up in the tube from normal gas chromatography eluents, but could not cope with solvents. In most cases it was found that solvents extinguished the plasma, or overcame the scavenger gases leaving massive carbon deposits. Previously this problem had been overcome by allowing the solvent to pass through the discharge tube before igniting the plasma (15). However, the subsequent warming up period made the detector response unstable. It was therefore suggested that the plasma should be maintained by introducing a bypass behind the column outlet (20) which could be triggered automatically by a simple detector such as a katharometer. This procedure was termed solvent venting.

The use of scavenger gases and solvent venting greatly improved the performance of the detector, but the cavities were still limited to relatively slow sample introduction rates to prevent the plasma being extinguished. This factor therefore limited the useful range of the detector, specifically for the direct analysis of aqueous samples. A design change in the Evenson quarter wave cavity was therefore proposed which allowed the analysis of desolvated aqueous samples using an atmospheric argon plasma (21).

The main modification was the positioning of the discharge tube axially through the cavity instead of the usual transverse configuration. This cavity evolved into the Evenson quarter wave cavity and allowed for end-on viewing of the plasma, therefore overcoming the problems of effluent deposition associated with transverse viewing through the walls of the tube. The axial configuration permitted maintenance of the plasma even when the support gas was saturated with water vapour. This was because the plasma support gas was subjected to the maximum microwave field strength over a greater linear range in the axial position than in the transverse.

At this stage in the development of the MIP detector there were conflicting

opinions as to which cavity design was the most efficient. It was however apparent that a helium sustained plasma gave the highest degree of atomisation, although it was only stable at reduced pressure due to inadequate transfer of power to the plasma. The added complication of the vacuum system required led to the atmospheric argon plasma being more popular.

A major breakthrough occurred in 1976 when Beenakker introduced the TM010 cavity which was efficient enough to sustain either a helium or argon plasma at atmospheric pressure (22, 23).

The Beenakker cavity differed from the open-ended Evenson and tapered cavities in that it consisted of a cylindrical wall with a fixed base and a removeable lid. The cavity was constructed from copper because of its high conductivity (Figure 7).

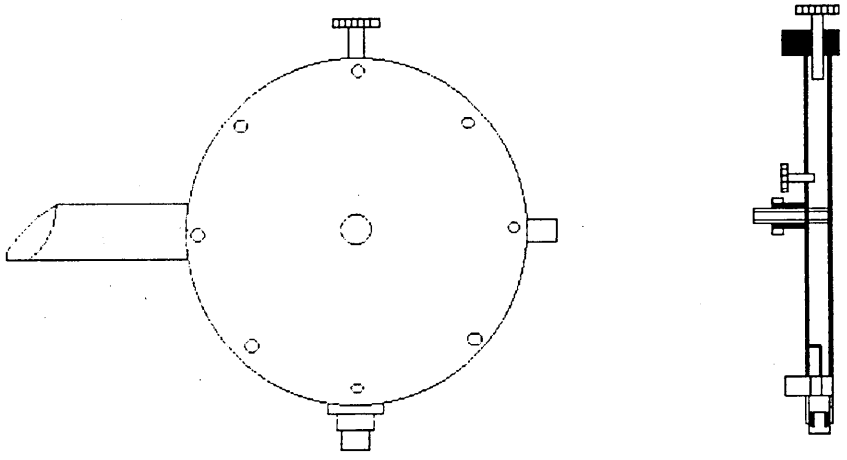

THE BEENAKKER CAVITY

FIGURE 7

The discharge tube was situated axially at the centre of the cavity, again at the point of maximum field strength. As in the previous axial configuration (21), the problems caused by transverse viewing were avoided, and meant that frequent replacement of the discharge tube was not as important.

However, comparisons of axial and transverse viewing (19) showed a reduction in linear dynamic range and limit of detection for the axial configuration, while Dingjan and de Jong reported a six-fold increase in signal with end-on compared with side-viewing (24).

Beenakker's initial studies showed that the detection limits for several elements improved by one or two orders of magnitude using the atmospheric helium plasma compared to those for the low pressure helium and atmospheric argon plasmas. It was also found that for the atmospheric helium plasma the reflected power from the cavity was less than 1% without the need for tuning or impedance matching.

Although a helium plasma was preferred for element selective detection, it was found that an argon plasma was more efficient for the analysis of aqueous samples via a nebulizer, as the nebulization efficiency of argon is higher than that of helium (25).

Impedance matching was more of a problem for the atmospheric argon plasma. The lowest reflected power was obtained by placing the discharge tube off-centre in the cavity. The disadvantage of this was that the plasma was no longer formed at the point of maximum field strength. Since an atmospheric helium plasma could not be formed at this point, a cavity to be used for either argon or helium plasmas had to have either two holes or a slot so that the discharge tube could be aligned as required.

Although the Beenakker cavity allowed for the production of an atmospheric helium plasma, there was still no system for cooling the cavity. In 1990 Hewlett Packard (26) described a reentrant cavity which was a modification of Beenakker's design. The main modification was the addition of a water jacket which was sandwiched between the two halves of the cavity. The water circulated through the system from a water bath. The water cooling path was kept narrow to avoid excessive power dissipation, and the wall of the discharge tube was kept thin to allow efficient cooling of the tube's inner surfaces.

In the same year Hewlett Packard also described the use of a photodiode array in the spectrometer of the AED (27). Previous detectors had used conventional optical spectroscopic equipment such as scanning monochromators for single wavelength detection. The photodiode array, however, allowed for simultaneous multi-wavelength detection, making multi-element analysis a reality. Combining effective capillary gas chromatography, a well engineered cavity and a diode array detector gives gas chromatography-microwave induced plasma-atomic emission spectrometry (GC-MIP-AES).

1.8 The HP5921A

Capillary gas chromatography and atomic emission spectroscopy when coupled together provide a powerful hyphenated technique for the separation and characterisation of complex mixtures. The low gas temperature of the MIP allows small amounts of sample compatible with those of gas chromatography eluents to be introduced without extinguishing the plasma. Also, sample introduction is easy, as the carrier and plasma gases are the same.

The HP5921A is the first fully automated system capable of routinely detecting a wide range of elements in gas chromatography effluents. The instrument consists of a capillary gas chromatograph interfaced to an atomic emission

detector via a heated transfer line, an autosampler and a Chemstation from which the system is controlled (Figure 8).

The AED has become a popular technique with several advantages over other gas chromatography detectors.

For example, it can selectively detect oxygen (777nm) which has been a particular problem in the past. Sulphur can also be monitored (181nm) over a greater linear range than with the flame photometric detector.

The atomic emission detector can also be used to detect halogens. Its major advantage here over the electrolytic conductivity detector and the electron capture detector is its ability to discriminate between individual halogens rather than giving a total halogen response.

Organomercury, lead and tin compounds can also be detected at the appropriate wavelengths, 253.6 nm for mercury, 303.4 nm for tin and 405.8 nm for lead.

Deuterated compounds can also be detected as can the presence of ^{13}C labelled compounds. Time consuming methods such as radiochemical detection can therefore be avoided.

The software incorporated into the Chemstation makes the calculation of elemental ratios possible, leading to the formation of partial empirical formulae. The calculation of elemental ratios is prone to error however. Elemental spectral response should be independent of the structure from which the atoms originate. This does appear to be the case for compounds with similar structures, but responses for different compounds can be structurally related (18).

Reagent gases

*s» ft

\ /

36

8

FIGURE 8 - GC-AED BLOCK DIAGRAM

The technique can therefore provide composition information complementary to the structural information given by gas chromatography-mass spectrometry. The AED can also be of use by providing valuable data to aid mass spectral analysis in eliminating certain library guesses. For example, if the mass spectrometry data shows a certain compound contains nitrogen, but the AED shows no nitrogen is present, then all library guesses containing nitrogen can be eliminated.

The helium carrier gas passes the gas chromatograph eluent into the cavity housing the plasma via a heated transfer line. Very high purity helium must be used, as any impurities would lead to a high spectral background and interference. Helium flow rates are in the range 20-100 ml min^{-1}. These flow rates are much lower than the 10-20 l min^{-1} flows needed for inductively coupled plasma sources.

The cavity shown (Figure 9) is a reentrant cavity which is similar to Beenakker's cavity, except that there is a pedestal in the centre of the cavity and the diameter of the cavity is smaller.

The helium plasma is formed in a narrow quartz discharge tube (1mm id x 1.25mm od x 40mm long) into which the end of the gas chromatograph column passes (Figure 10).

The discharge tube is the most delicate part of the system, and several features have been incorporated into the detector to prolong the tube's lifetime.

REENTRANT CAVITY

FIGURE 9

(I) pedestal, (2) quartz jacket, (3) coupling loop, (4) main cavity body, (5) cavity cover plate, (6,7) cooling water inlet and outlet, (8,9) water plates, (10) silica discharge tube, (II) polyimide ferrule, (12) exit chamber, (13,14) window purge inlet and outlet, (15) sparker wire, (16) spectrometer window, (17) gas union, (18) threaded collar, (19) column, (20) capillary column fitting, (21) makeup and reagent gas inlet, (22) purge flow outlets, (23) stainless steel plate, (24) heater block, (25) ferrule purge vent, (26) air filter, (27) solvent vent switch

Solvent Makeup and

FIGURE 10 - AED DISCHARGE TUBE

Firstly a water jacket surrounds the discharge tube. Water circulates through this jacket from a water bath thermostated at 60°C. This decreases erosion of the inner surfaces of the tube. Background emission is also reduced. For example a reduced cavity temperature reduces oxygen and silicon emissions by decreasing volatilization from the tube itself. Cooling of the tube also reduces peak tailing on some channels, eg sulphur. Clearly these observations and modifications to operating conditions point to a relatively complex plasma chemistry.

Secondly, a solvent vent procedure is used to stop solvents entering and extinguishing the plasma (Figure 11). If the plasma is extinguished due to incorrect solvent venting, the detector will automatically try to relight itself, weakening the discharge tube in the process. The solvent vent is controlled by a solenoid valve which is operated from the Chemstation and diverts the column flow away from the detector when the solvent comes off the column.

Thirdly, reagent gases are automatically added to the plasma support gas when the elements to be monitored have been chosen. They are added in small concentrations to prevent carbon deposits on the walls of the discharge tube. Any such deposits would lead to severely distorted peaks and affect the sensitivity of the instrument.

The compounds entering the plasma are atomised and the outer shell electrons are raised to an excited state. As they return to the ground state they emit light of a wavelength characteristic of the element present.

The light produced by the atoms then passes through the spectrometer window to the detector which in this case is a photodiode array.

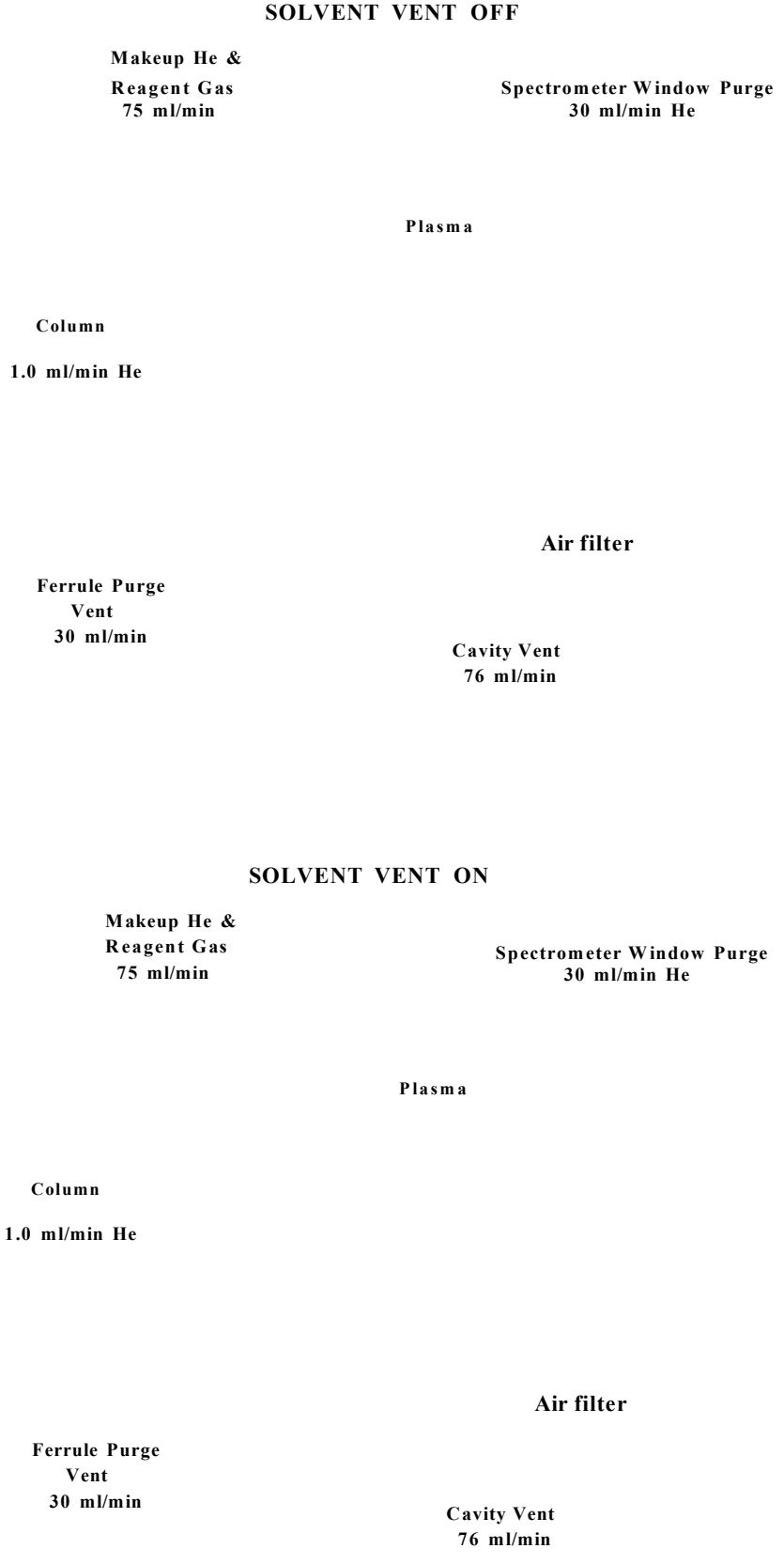

FIGURE 11
SOLVENT VENTING

As light enters the spectrometer it is focused through a slit by a mirror, and then dispersed into its component wavelengths by a curved holographic grating. The grating is curved to allow dispersion onto the flat focal plane along which the photodiode array slides. The full spectral range of the diode array is 165-780 nm, but in order to achieve the desired resolution, only a small window within this range can be monitored at any one time. So when the elements of interest are chosen prior to an analysis, the photodiode array is positioned to cover the emission wavelengths of those elements.

The diagram (Figure 12) shows the groups of elements which can be monitored in one injection. For example nitrogen, phosphorus, sulphur and carbon can be monitored simultaneously. However, if oxygen were present a second injection would be necessary. The Chemstation then merges the data from the two chromatographic runs.

It is therefore possible to identify all the elements present in compounds leaving the gas chromatograph. The data can be presented in two ways. The plot of the detector output, ie light intensity at a certain wavelength over time, gives a chromatogram; and the spectral detectors output across a range of wavelengths at a specific moment in time produces an emission spectrum. Hence the spectrum or 'snapshot' shown in Figure 13 is the full UV spectrum of the peak specified on the chromatogram. The snapshot shows the spectral lines of the element monitored and confirms elemental identity.

The snapshot is best represented as a 3-D plot (Figure 13). The spectrum shown is that of a chlorine containing compound and shows the chlorine elemental lines around 479 nm, giving conclusive proof of the presence of chlorine.

43
05
Ti.
OS
SPECTROMETER - FIGURE 12

$\mapsto$

The atomic emission detector can therefore provide quantitative data from the chromatograms, and qualitative data from the snapshot spectra.

1.9 Analyte Excitation Mechanisms

A full explanation of the production of spectra from a microwave induced plasma requires a knowledge of the nature and energies of all species present in the plasma, eg atoms, ions and molecules, and the excitation processes they are involved in. The excitation energies of the analyte atoms and ions must also be considered. In the following discussion the inert gas species are denoted by 'G' and the analyte atoms by 'X'. The superscripts m, *, and + refer to metastable, excited and singly ionised species, and $h\nu$ is the continuum.

In both low and high pressure plasmas the species present are metastable molecules and atoms, ions and low and high energy electrons (23). The low energy electrons are in abundance and take part in recombination excitation processes

$$e + G + X^+ \rightarrow G + X^* + h\nu \qquad 1)$$

or

$$e + G^+ \rightarrow G^* + h\nu \qquad 2)$$

The high energy fast electrons sustain the plasma by the following process:-

$$e + G \rightarrow G^+ + 2e \qquad 3)$$

However, the high energy electrons can also be involved in direct excitation processes:-

$$e + X \rightarrow X^* + e \qquad 4)$$

or

$$e + X^+ \rightarrow X^{+*} + e \qquad 5)$$

Ions can also take part in excitation processes by:-

$$G^+ + X \rightarrow G + X^{+*} \qquad 6)$$

The condition for the above process is:-

$$E_{ion}(G) \cong E_{ion}(X) + E_{exc}(X) \qquad 7)$$

ie the sum of the ionisation and excitation energies of the analyte must be almost equal to the ionisation energy of the support gas.

All the inert gases possess metastable levels (atoms in lowest triplet state) which appear to take part in excitation. Helium has two levels at 19.73 and 20.53 eV. The gas atoms can reach these levels by excitation followed by collisional de-excitation with another ground state support gas atom, or from the sequence of reactions 3) and 4).

The population of metastable atoms decreases with pressure up to 20 Torr. However, above 20 Torr the population increases with pressure. An increase in applied microwave power also causes the metastable population to increase.

Metastables, Gm, can be involved in ionisation or excitation as shown below:-

$$Gm + X \rightarrow G + X^+ + e \qquad 8)$$

$$Gm + X^+ \rightarrow G + X^{++} + e \qquad 9)$$

$$Gm + X \rightarrow G + X^* \qquad 10)$$

$$Gm + X^+ \rightarrow G + X^{+*} \qquad 11)$$

Reactions 8 and 9 are well known ionisation processes and occur if the energy of the particles before collision is greater than the first or second ionisation energy of X ie:-

$$E_m(G) \geq E_{ion}(X) \qquad 12)$$

The difference between the energy of the metastable atom and the ionisation energy of X is dispersed as kinetic energy of the electron.

Reactions 10 and 11 are relatively improbable and can only occur if the excitation of the analyte atom is approximately equal to the metastable energy, ie:-

$$E_m(G) \cong E_{exc}(X) \qquad 13)$$

In addition to metastable atoms, metastable molecules and molecular ions are known to exist in inert gas plasmas (23), and may also be involved in some excitation processes.

It is generally agreed that direct excitation of the analyte atoms and ions by electron collision is not the dominant process in microwave induced plasmas. Fewer lines are seen than would be expected from the continuous range of energies available with electrons. Also, the characteristics of the spectra do not

change with pressure as would be expected considering that electron temperatures generally decrease as pressure increases (23).

A more likely excitation process involves a sequence of steps starting with impact by metastables leading to ionisation of the analyte as in reactions 8 and 9, followed by ion recombination with low energy electrons, giving excited analyte atoms as in equations 1 and 2.

Following this mechanism, an increase in pressure would lead to an increase in analyte emission, as the metastable population increases at pressures above » 20 Torr. Increasing pressure would also decrease the electron temperature which in turn would give an increase in analyte emission through promotion of electron-ion recombination.

1.10 The Spectrometer

The photodiode array consists of 211 pixels or detecting diodes, which are active 100% of the time (Figure 14).

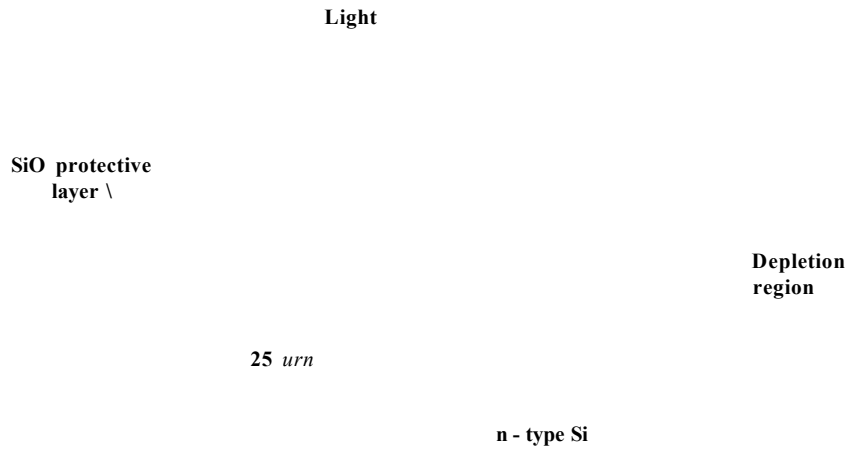

CROSS SECTION OF PHOTODIODE ARRAY - FIGURE 14

As shown on the previous page, bars of p-type silicon are formed on a base of n-type silicon, forming a series of p-n junction diodes. A reverse bias is applied to each diode which draws electrons and holes away from the junction. The junction behaves as a capacitor with charge stored on either side of the depletion layer. At the beginning of each measurement the diode/capacitor is fully charged.

When light strikes the semiconductor, free electrons and holes are created which migrate into regions of opposite charge and partially discharge the capacitor. The more light that hits each diode the less charge is left at the end of the measurement cycle. The capacitor is then recharged ready for the next measurement.

The detectable wavelength range of the spectrometer is 160-800 nm. However, because of the number of pixels it is not possible to detect the whole range all at once. Therefore, elements with fairly close emission wavelengths are monitored together. Carbon (193 nm), nitrogen (174 nm), sulphur (181 nm) form such a group.

Each element has its best response at a certain pixel, for example pixel 82 is the most sensitive for nitrogen, and pixel 91 is the most sensitive for sulphur. However, these pixels are not the only ones available. For example in the sulphur snapshot (Figure 15a), 6 pixels are aligned with the sulphur elemental lines around 181 nm. Usually, all the relevant pixels are used for optimal sensitivity. Each pixel is given a different 'weighting' which is proportional to the relative signal levels, and each element has its own set of optimal weights. A set of pixels arranged according to their optimum weights is called a matched filter.

The filters used in the atomic emission detector are not like the conventional

glass order sorters. They are in fact software algorithms. The filter multiplies several pixel signals by their weights and totals the results. This calculation is usually done every 10 seconds.

Figure 15b shows the matched filter for sulphur, ie pixels at 91, 92, 97, 98 and 100. The amplitudes of the pixels represent the relative weights used to detect sulphur. In a matched filter the pixel weights are selected to match the shape of the signal. The plot of pixel weights, therefore, resembles the spectrum it is designed to detect. This can be shown by comparing the sulphur matched filter Figure 15b with the sulphur snapshot Figure 15a.

If this matched filter is used for sulphur, the chromatogram shown in Figure 15c is obtained, indicating a poor selectivity for sulphur due to the presence of a hydrocarbon. As Figure 15e shows the spectrum of the hydrocarbon overlaps with the sulphur matched filter, giving the large peak on Figure 15c. It is therefore necessary to cancel out the hydrocarbon response by a process called background correction.

The pixels used for this are the ones shown in Figure 15b with the negative amplitudes. These pixels are weighted to produce a matched filter for the hydrocarbon interference on the sulphur channel. The output of this background filter is kept separate from the sulphur chromatogram as shown in Figure 15d. The background chromatogram is then subtracted from the sulphur chromatogram.

Care must be taken to subtract the correct amount of background. If too much is subtracted the interferences are over-corrected leading to negative peaks. If not enough is subtracted not all the interferences are removed. The amount subtracted is called the background amount and can be adjusted using the Data Editor software after recording the chromatogram.

FIGURE 15a - SULPHUR 'SNAPSHOT'

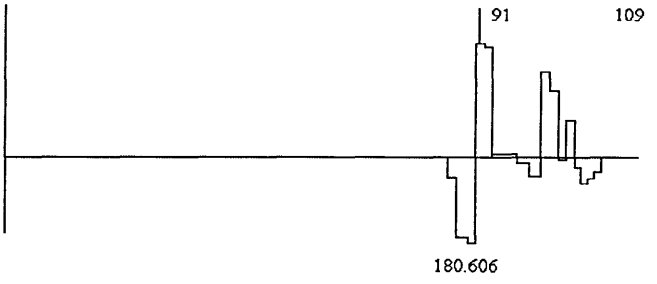

FIGURE 15b - SULPHUR MATCHED FILTER

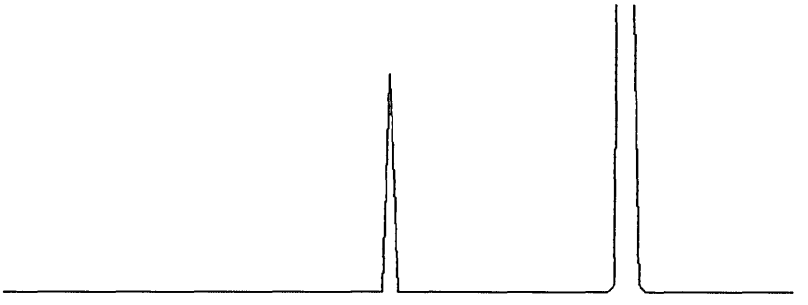

FIGURE 15c - SULPHUR CHROMATOGRAM - ELEMENT FILTER

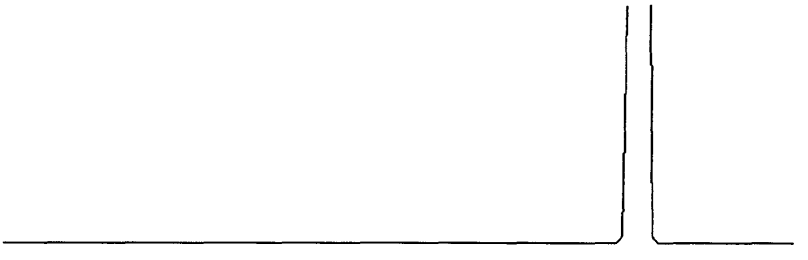

FIGURE 15d - BACKGROUND CHROMATOGRAM

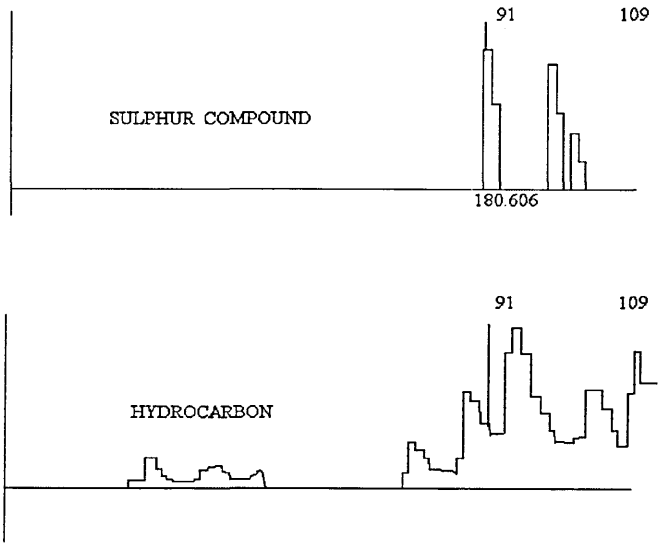

FIGURE 15e - HYDROCARBON SPECTRUM

This type of adjustment is called a 'real-time multipoint' correction. The term 'real-time' is used because the background measurements are made at the same time as the signal measurements so that the interferences in the sample signal can be accurately traced. The term 'multipoint' refers to the many pixels used to match the background signal into a filter.

The combination of wavelength, element pixels, element filter, background pixels, background filter and background amount is called a recipe, each element having its own particular recipe.

1.11 Applications of the Atomic Emission Detector

The early analyses performed using a microwave induced plasma in the 1960s and early 1970s were mostly on simple organic compounds or pesticide residues (14, 15, 16, 17). For the following decade or so researchers then concentrated on the development of the technique rather than its application.

Once the main instrumental problems had been ironed out, however, work began on evaluating the performance of the atomic emission detector (AED) using various compounds and elements.

Several general applications have been published (28), but one of the most popular areas was halogen analysis (14, 17). The monitoring of halogenated compounds is very important due to the environmental and health implications of their presence. Quimby (29) used the AED for the detection of trihalomethanes in drinking water. The performance of the instrument with respect to chlorine, bromine and fluorine was investigated in terms of selectivity, linearity and limit of detection.

In comparing the AED with the electron capture detector (ECD) and the

electrolytic conductivity detector (ELCD) it was found that similar or better sensitivities were achieved with the AED. However, the main advantage of the AED over the other two detectors is its ability to selectively detect individual halogens rather than giving a total halogen response.

The AED also became immediately popular for measuring oxygen and oxygenated (30) compounds as no oxygen selective detector had been previously available. The petroleum industry was particularly interested in this new oxygen detector, and immediately applied it to the analysis of oxygen and sulphur compounds in gasoline (31).

The AED was also an invaluable tool in fingerprinting petroleum products (32). For example, fingerprint chromatograms of spillages could be obtained using the AED and compared to either likely source samples or a database of refined product types. The AED's sensitivity to metals was also utilised by the petrochemical industry, for example in the detection of metal porphyrins (33) in crude oils. The ability to monitor for the presence of metalloporphyrins is important as their presence in the distillate can cause problems in refinery operations. Lead analysis is also very important in the petroleum industry. For example, alkyl lead compounds used as octane boosters for leaded petrols have been rapidly measured using the AED (34, 35).

As a consequence of the petrochemical and other industries, lead is now recognised as an environmental pollutant, and in recent years interest has been growing in the environmental pathways of organolead compounds. Such studies involve monitoring organolead species at ultratrace levels. This has been difficult in the past, but is possible using the AED which has been used to do sensitive speciation analysis of lead in environmental waters (36). Another metal which is important in environmental monitoring is tin, and several speciation studies have been carried out on tin using the AED (37, 38, 39).

Other metals monitored have included selenium, arsenic (40) and antimony (41).

A further environmental application of the AED has been in pesticide analysis (42). Pesticides usually contain heteroatoms and often have several in a single molecule. Frequently encountered elements are C, H, O, P, S, N, Cl, Br, F and metals such as As, Hg and Zn. The ability of the AED to give a complete profile of all elements present in a pesticide greatly aids identification.

In the applications described above atomic emission detection has been coupled to gas chromatography. However, the technique has also been interfaced with supercritical fluid chromatography (SFC) for the detection of ferrocene (43). In this case a modification is required as the microwave induced plasma has a low tolerance for molecular species. For example the introduction of the SFC mobile phase (CO_2) into the microwave induced plasma causes suppression of analyte emission. A microwave plasma torch was therefore developed which resembled an inductively coupled plasma the sample being introduced into a central channel in the plasma.

The GC-AED has also been used to analyse for compounds following supercritical fluid extraction (SFE) (44). This method has been used for the determination of elemental sulphur in coal (45) and for the analysis of organotin compounds in environmental samples (46).

More recently, the AED has been evaluated as an on-line detector for capillary zone electrophoresis (CZE) (47). To couple CZE to the AED an ion exchange membrane was used to connect the separation capillary to the interface capillary. The outlet of the interfacing capillary was then placed directly into the discharge tube of the AED. The system was evaluated using methyl tins and carbonyl compounds and it was demonstrated that the AED could be used in CZE to provide element selective detection.

Another recent application has been the use of pyrolysis GC-AED for polymer analysis (48). The polymers are degraded in the pyrolyser and the volatile pyrolysates are swept into the gas chromatograph. The advantage of this system is that both monomer and polymer composition can be investigated. This idea has also been extended to the analysis of geopolymers (49).

A lot of interest has also been shown in the empirical formulae determinations possible using the AED software. Elemental response should be independent of the molecular structure from which the atoms originate. However, opinions are divided over whether this is actually the case. As far back as 1977 van Dalen (20) found that carbon responses varied up to 25% between different compounds and that variations of up to 200% were seen with other elements. Several other workers have demonstrated that for mixtures containing a homologous series the relative responses are independent of structure (50, 51), but that for non-homologues the structure of the original compound has a significant effect on the response (51, 52). It has also been stated that improvements in the precision of empirical formula determinations can be made if the internal standard used has a similar structure to the analyte to be determined (51, 52, 53).

However, other results have shown that empirical formula (54, 55) determinations and compound independent calibration are possible within certain error limits (56, 57, 58, 59).

The AED has also been applied to the analysis of essential oils (35). This has been successful as sensitivity is very important in the analysis of these oils since compounds which are present at very low levels may contribute strongly to the properties of the extract.

The use of the AED as a detector for radioisotopes has also been examined. It

has been used to determine ^{13}C (60) labelled compounds and also deuterated reagents (61).

Table 1 summarises a further range of AED applications.

APPLICATIONS OF ATOMIC EMISSION DETECTION.

ANALYTE	TITLE	REFERENCE
Metals	Element-selective Atomic Emission Detection for Capillary GC of Metal Containing Compounds.	62
	Capillary G.C. Determination of Copper and Nickel Using MIP-AED.	63
	Quality Control of a Recently Developed Analytical Method for the Simultaneous Determination of Methyl Mercury and Inorganic Mercury in Environmental and Biological Samples.	64
	Characterisation of a Moderate Power MIP for Direct Solution Nebulisation of Metal Ions.	65
General	Element-selective Detection using Capillary G.C. with Atomic Emission Detection.	66
	Characterisation of an Element Specific Detector for Combined G.C./AED.	67
Polymers	Characterisation of Polymer additives using High Temperature Capillary G.C. - Possibilities of Atomic Emission Detection.	68
Speciation	MIP as an Element-specific Detector for Speciation Studies at the Trace Level - Speciation of Organic and Organometallic Compounds.	69
Comparison to other techniques.	Analysis of Volatile Organic Compounds in Air by G.C. with Thermal Desorption Cold-trap Injection and Atomic Emission and Mass Selective Detection.	70
	Comparison of GC/MSD and GC/AED for the Determination of Organotin Compounds in the Environment.	71
Halogens	Determination of the Aqueous Chlorination Products of Fluorine Substances by G.C. with Microwave Emission Detection.	72
	Continuous-flow Determination of Trace Iodine by Atmospheric Pressure Helium MIP-AES using Generation of Iodine from Iodide.	73

Applications	**cont.**	
	Application of an MIP-AED for Quantification of Halogenated Compounds by G.C.	56
	Moderate Power Helium Plasma as an Element-selective Detector for G.C. of Dioxins and Other Halogenated Compounds.	74
Compound Independent Calibration	Use of Microwave-induced Plasma Atomic Emission Detection for the Quantification of Oxygen Containing Compounds.	75
	Use of an Atomic Emission Detector to Study the Variation in Response for Chlorine, Carbon and Oxygen in Phenols.	76
Trace Analysis	The AED in G.C. Trace Analysis - Some Studies on the Performance and Applications.	77
	Large-volume Injections in G.C./AED - an Approach for Trace Level Detection in Water.	78
	Trace Analysis for Steriodal Carbanes via GC/MIP Emission Spectroscopic Detection.	79
Radio-labels	Detection of ^{13}C Labelled Compounds by G.C. Coupled to AED - Applications to Caffeine Metabolites.	80
Multi-element Detection	Simultaneous Multi-element Detection in Microlitre Samples by Rapid-scanning Spectrometry Coupled to an MIP.	81
	Nitrogen - oxygen - phosphorus Selective On-column Atomic Emission Detection in Capillary G.C.	82
	Detection of Sulphur and Carbon Containing Compounds Using Capillary G.C./AED	83

TABLE 1

CHAPTER 2

EXPERIMENTAL DETAILS

2.1 Analysis of Hydrocarbons

A 1 x 10^{-3}M test mix was prepared in hexane, and a range of dilutions (5 x 10^{-5} - 2 x 10^{-4}M) were made up.

Instrumental Configuration:

Gas Chromatograph:	HP 5890A
Autosampler:	HP 7673A
Detector:	HP 5921A

Gas Chromatograph Parameters:

Injection port temp:	250°C
Column:	HP-5 - 5% diphenyl - 95% dimethyl polysiloxane
	25m x 0.32mm id x 0.52 µm film
Oven program:	50°C (4 min), 20°C/min to 280°C (5 min)
Column flow rate:	1 ml min^{-1} He
Split ratio:	Splitless
Injection volume:	1 µl

AED Parameters:

Elements analysed:-

Element	Wavelength (nm)	Reagent Gas
C	193.031	H_2, O_2

Transfer Line Temp:	300°C
Cavity Temp:	300°C
Water Temp:	65°C
Makeup Flow:	60 ml min^{-1}
Spectrometer Purge Flow:	2 l min^{-1}
Ferrule Purge Flow:	40 ml min^{-1}

2.2 Analysis of Phenols

A 1 x 10^{-3}M test mix was prepared in dichloromethane, and a range of dilutions (5×10^{-5} - 5×10^{-4}M) were made up.

Instrumental Configuration:

Gas Chromatograph: HP 5890A

Autosampler: HP 7673A

Detector: HP 5921A

Gas Chromatograph Parameters:

Injection port temp: 250°C

Column: HP-5 - 5% diphenyl - 95% dimethyl polysiloxane
25m x 0.32mm id x 0.52 µm film

Oven program: 80°C (4 min), 20°C/min to 280°C (5 min)

Column flow rate: 1 ml min^{-1} He

Split ratio: Splitless

Injection volume: 1 µl

AED Parameters:

Elements analysed:-

Element	Wavelength (nm)	Reagent Gas	Injection No
C	193.031	H_2, O_2	1
N	174.261	H_2, O_2	1
O	777.302	H_2, Aux	2

Transfer Line Temp: 300°C

Cavity Temp: 300°C

Water Temp: 65°C

Makeup Flow: 60 ml min^{-1}

Spectrometer Purge Flow: 2 l min^{-1}

Ferrule Purge Flow: 40 ml min^{-1}

2.3 Analysis of Chloroanisoles

A 1 x 10^{-3}M test mix was prepared in hexane, and a range of dilutions (5 x 10^{-5} - 1 x 10^{-3}M) were made up.

Instrumental Configuration:

Gas Chromatograph: HP 5890A

Autosampler: HP 7673A

Detector: HP 5921A

Gas Chromatograph Parameters:

Injection port temp: 250°C

Column: Rt x -35 - 35% diphenyl - 65% dimethyl polysiloxane
30m x 0.32mm id x 0.25 μm film

Oven program: 50°C (3 min), 4°C/min to 170°C, 10°C/min to 280°C

Column flow rate: 1 ml min^{-1} He

Split ratio: Splitless

Injection volume: 1 μl

AED Parameters:

Elements analysed:-

Element	Wavelength (nm)	Reagent Gas	Injection No
Cl	479.465	O_2	1
C	193.031	H_2, O_2	2
O	777.302	Aux, H_2	3

Transfer Line Temp: 300°C

Cavity Temp: 300°C

Water Temp: 65°C

Makeup Flow: 60 ml min^{-1}

Spectrometer Purge Flow: 2 l min^{-1} N_2

Ferrule Purge Flow: 40 ml min^{-1}

2.4 Analysis of Nitrogen Containing Compounds

A 1 x 10^{-3}M test mix was prepared in methanol, and a range of dilutions (5 x 10^{-5} - 4 x 10^{-4}M) were made up.

Instrumental Configuration:

Gas Chromatograph: HP 5890A

Autosampler: HP 7673A

Detector: HP 5921A

Gas Chromatograph Parameters:

Injection port temp: 250°C

Column: HP-5 - 5% diphenyl, 95% dimethyl polysiloxane
25m x 0.32mm id x 0.52 µm film

Oven program: 80°C (4 min), 20°C min^{-1} to 280°C (3 min)

Column flow rate: 1 ml min^{-1} He

Split ratio: Splitless

Injection volume: 1 µl

AED Parameters:

Elements analysed:-

Element	Wavelength (nm)	Reagent Gas	Injection No
C	193.031	H_2, O_2	1
N	174.261	H_2, O_2	1
O	777.302	H_2, Aux	2

Transfer Line Temp: 300°C

Cavity Temp: 300°C

Water Temp: 65°C

Makeup Flow: 60 ml min^{-1}

Spectrometer Purge Flow: 2 l min^{-1} N_2

Ferrule Purge Flow: 40 ml min^{-1}

2.5 Analysis of Perfumes

Perfumes were analysed by GC-AED followed by GC-MS.

Instrumental Configuration:

GC-AED

Gas Chromatograph: HP 5890A

Autosampler: HP 7673A

Detector: HP 5921A

GC-MS

Gas Chromatograph: HP 5890A

Detector: VG-Trio-1

Gas Chromatograph Parameters:

Injection port temp: 250°C

Column: HP-5 - 5% diphenyl, 95% dimethyl polysiloxane
25m x 0.32mm id x 0.52 μm film

Oven program: 50°C (5 min), 5°C min^{-1} to 200°C, 10°C min^{-1} to 280°C (10 min)

Column flow rate: 2.5 ml min^{-1}

Split ratio: 40:1

Injection volume: 1 μl

AED Parameters:

Elements analysed:-

Element	Wavelength (nm)	Reagent Gas	Injection No
H	486.113	O_2	1
Cl	479.465	O_2	1
C	193.031	H_2, O_2	2
S	181.354	H_2, O_2	2
N	174.261	H_2, O_2	2
O	777.302	H_2, Aux	3

Transfer Line Temp: 300°C

Cavity Temp: 300°C

Water Temp: 65°C

Makeup Flow: 60 ml min^{-1}

Spectrometer Purge Flow: 2 l min^{-1} N_2

Femule Purge Flow: 40 ml min^{-1}

Mass Spectrometry Parameters:

Mass range: 25 - 500 m/z

Scans/second: 0.90

Ionisation: Electron impact

2.6 Analysis of Pre- and Post-Catalytic Streams

Instrumental Configuration:-

Gas Chromatograph:	HP 5890A
Autosampler:	HP 7673A
Detector:	HP 5921A

Gas Chromatograph Parameters:-

Injection port temp:	250 °C
Column:	HP-5 - 5% diphenyl - 95% dimethylpolysiloxane
	25m x 0.32mm id x 0.52μm film
Oven program:	30 °C (15 min), 4 °C/min to 150 °C, 20 °C/min to 280 °C
Column flow rate:	1ml min^{-1} He
Split ratio:	100:1
Injection volume:	1μl

AED Parameters:

Elements analysed:-

Element	Wavelength (nm)	Reagent Gas
C	193.031	H_2, O_2
S	181.354	H_2, O_2
O	777.302	H_2, Aux

Transfer line temp:	300 °C
Cavity temp:	300 °C
Water temp:	65 °C
Makeup flow:	60 ml min^{-1}
Spectrometer purge flow:	2 l min^{-1}

CHAPTER 3

COMPOUND INDEPENDENT CALIBRATION

3.1 Introduction

The determination of empirical and molecular formulae via elemental analysis has been a vital step in the identification and characterisation of unknowns since Dalton first investigated stoichiometry in the early nineteenth century.

An empirical formula is usually obtained by various combustion methods. The molecular formula can then be determined from knowledge of the molecular weight which is usually obtained by mass spectrometry or vapour phase osmometry. If an accurate mass determination can be made using high resolution mass spectrometry, then only a limited amount of elemental data is required to calculate the molecular formula. However if only a low resolution mass is available, accurate microanalytical data must be obtained for all but one of the elements present in the compound.

Various highly accurate and reliable microanalytical methods are available for common elements, but these usually require between 1 - 10 mg of pure sample for each elemental determination. Such classical methods cannot be used therefore for materials which are components of a mixture, in limited supply, or cannot be purified in sufficient quantity.

In order to determine the empirical formulae of components of a mixture a separation step such as gas chromatography is required. Ideally it should be coupled to a highly specific element selective detector, suited to elemental ratioing. The AED is one such system and has been widely used in an attempt to determine elemental ratios and empirical formulae. However the success of such determinations depends on the elemental response being independent of the original structure of the parent molecule.

Therefore, in theory, if analysing for a particular element in a compound, calibration can be carried out using any other substance which contains the element of interest. For example, any sulphur containing compound could be used for quantitatively analysing for any other sulphur containing compound. This would be particularly useful if no pure standard of the compound of interest was available. This type of calibration which is dependent only on elemental content has been termed 'compound independent calibration'.

The determination of elemental ratios and empirical formulae have become the subject of many studies. Dagnall *et al* (84) were the first to report on the determination of elemental ratios using an atmospheric argon microwave induced plasma (MIP). They examined the ratios of chlorine, iodine, bromine, sulphur and phosphorus emissions to carbon. A two detector system was used in which one monochromator was set to monitor the carbon 247.9 nm line and the second was set to the wavelength of the element being monitored, eg 206.2 nm for iodine. It was found that, for a range of simple compounds (eg carbon tetrachloride, chloroform, dichloromethane, methyl iodide, chlorobenzene) the iodine-, sulphur-, phosphorus - to carbon elemental ratios deviated from the theoretical values by between 4-8%.

Dagnall also noted that for iodine and phosphorus the ratios to carbon were independent of concentration and carrier gas flow rate. This was also true for sulphur-carbon ratios, but only at lower concentrations. At higher levels the ratios tended to be lower than expected. This was put down to the deposition of carbon onto the discharge tube walls. Early evidence was obtained therefore that compound independent calibration might not be universally applicable. Hence the response curve was convex in appearance. The chlorine-bromine ratios were also examined, but these could not be obtained as the emissions seen for chlorine and bromine were molecular not atomic.

The following year (1973) McClean *et al* (19) reported H:C ratios using a low pressure helium MIP. Here the gas chromatography eluent was split between the MIP and a flame ionisation detector (FID). Elemental ratios were then obtained by comparing the MIPs' responses to those from the FID. The majority of the ratios calculated were higher than the theoretical values, deviating by about 3% from the ideal, arguably within the limits of experimental error.

An MIP was then used by Gough *et al* (85) to determine the empirical formula of the product of a pyridine catalysed reaction of N-nitrosodimethylamine with heptafluorobutyric anhydride. Gough simultaneously detected carbon, hydrogen, nitrogen and fluorine. Oxygen could not be monitored as it was used as the scavenger gas. The values obtained for carbon, nitrogen and fluorine in the empirical formula agreed with the mass obtained by GC-MS. However, the hydrogen values produced were not as accurate.

Later van Dalen (20) questioned the reliability of empirical formula determinations. Using a low pressure helium MIP he found that responses for carbon, hydrogen, nitrogen, oxygen, chlorine, bromine, iodine and fluorine in a range of different compounds showed considerable variation indicating a marked structure dependence. For carbon this variation was estimated at 25%, but van Dalen concluded that for other elements the variation could be up to 200%. The discrepancy with previous results is dramatic.

Van Dalen also observed that on a linear scale the analytical curve for hydrogen was concave, and that at high concentrations the signal fell below the expected straight line, while at low concentrations it ran above this line. Several causes of this were investigated. Incomplete dissociation of hydrogen molecules was suggested, but this would produce a convex curve not a concave one as observed. Traces of water in the discharge tube were also considered as a

reason, but degassing of the connecting lines and discharge tube did not improve the curve. Reaction of hydrogen with the oxygen scavenger gas was also ruled out as the effect was still seen with a helium only environment.

Brenner used a MPD-850 (low pressure helium MIP) to study polychlorinated biphenyls (PCBs), diols and sulphur containing compounds (86). Empirical formulae were calculated for these compounds using the MIP and compared with those obtained by GC-MS. The hydrogen and chlorine results for PCBs were poor compared with those from GC-MS. The results obtained for some of the sulphur containing compounds also deviated from the true values. However, better results were obtained for hydrogen and oxygen atoms in the diols mixture. Also, the number of nitrogens in phthalodinitrile isomers were comparable with the theoretical values.

Tanabe *et al* (87) determined relative sensitivities in hydrocarbons, chloro- and bromohydrocarbons, methanol, ethanol and acetonitrile. For cyclohexane, benzene, hexane, and carbon tetrachloride the carbon sensitivities were much the same, but for methanol, ethanol and acetonitrile they were approximately 50% lower. Tanabe suggested that these differences in relative sensitivities could be due to the presence of nitrogen or oxygen in methanol, ethanol and acetonitrile, and that this somehow caused incomplete decomposition of the compounds in the plasma. It was also noted that a low hydrogen sensitivity was obtained for hydrogen in methanol. The suggestion was that this could be due to incomplete decomposition, however the sensitivity for hydrogen in ethanol was comparable with values obtained for the other compounds.

The relative sensitivities of chlorine and bromine in the various compounds were similar. Tanabe suggested that sensitivities could be improved by operating the plasma at a higher microwave power to aid decomposition. However, the

system used here was operated at 75W similar to the 50W power used to operate the HP5921A.

Dingjan and de Jong (88) looked at a range of carbon, chlorine, bromine, iodine and sulphur containing compounds (eg CH_2Cl_2, CCl_4, $CHBr_3$, C_6H_5I, CS_2, etc) and found that when the number of halogen atoms per molecule increased, the deviation from the expected theoretical value increased, and that in general the results tended to get worse with increasing numbers of atoms per molecule. It was suggested that these observations could be due to rate limiting fragmentation reactions in the plasma and interactions with the walls of the discharge tube, eg exchange reactions. Dingjan and de Jong therefore concluded that the use of a thermochemical cracker or pyrolysis unit in front of the MIP could overcome structure effects.

Yu *et al* (89) looked at a range of halogenated hydrocarbons and found no significant matrix effects on the responses for carbon and hydrogen in these compounds.

Hagen *et al* (90) monitoring fluorine containing metabolites in blood found that, although C/F ratios appeared to be unrelated to structure, the peak shape on the fluorine channel was poor. It was suggested that this was due to chemical effects such as the interaction of fluorine species with the quartz discharge tube. This interaction appeared to produce a fluorine containing entity which is momentarily retained on the wall of the tube. It was thought that this could cause the peak tailing or broadening seen on the fluorine channel. This effect was not seen on the carbon channel, and increased as the tube wall became more eroded.

Zerezghi *et al* (58) showed that for some chlorinated aromatics, hydrocarbons and pesticides, the carbon and chlorine responses were effected by structure, and that the responses decreased as the number of carbon and chlorine atoms increased. The compounds which gave lower responses were early eluters, so Zerezghi suggested that their anomalous results could be caused by the plasma not attaining steady state conditions after the solvent vent period.

Slatkavitz (91) used a low power atmospheric helium plasma to determine empirical and molecular formulae. He looked at a range of carbon, chlorine, phosphorus and silicon containing compounds, but only calculated empirical formulae for the hydrocarbons undecene, undecane, dodecane, dodecene, and tridene and the chloro-compounds chlorotoluene, dichlorobenzene, and trichlorobenzene. The formulae calculated from the MIP results matched the known formula in all cases to between 2-4% accuracy.

Haas and Caruss (74) used a moderate power (190W) helium MIP to calculate C/Cl elemental ratios for methoxychlor, 1,2,3,4-tetrachlorodioxin, and hexachlorocyclohexane. The values obtained varied from the actual ratios by between 2.7 - 8.3%. Ratios were improved to within 1% of the theoretical value by using a multi-element off-line correction process. However, the sensitivity achieved with this moderate power plasma was poor compared with the low pressure MIPs.

Hagen *et al* (92) then used a multi-element tagging (chlorofluoroalkylation) with a reduced pressure helium MIP to improve element ratioing. The multi-element tagging derivatisation used the element specific characteristic of the MIP to enhance quantitative and qualitative analysis of compounds containing various functional groups. This derivatisation also increased the reliability of element ratioing. Using this system Hagen showed good linearity in carbon response for

mixed homologues of alkanes and perfluoroalkanes, and reliable C/Cl and F/Cl ratios for chlorodifluoroacetic anhydride derivatives of straight chain aliphatic alcohols and amines. However, he stated that in practice deviations in linearity of elemental ratios in homologous series did occur for some elements. It was suggested that this was due to variations in pressure within the Evenson cavity used, and that a suitable internal reference should be used to obtain reliable results.

Zeng (30) used a low pressure helium plasma with a ¼λ coaxial cavity to investigate the response of the MIP to oxygenated compounds, and to determine their empirical formulae. The linear dynamic range of the oxygen channel was determined using different amounts of air, propanol, dioxane, and diethyl ketone. Results showed that different types of oxygenated compounds could be atomised quantitatively. Several groups of compounds were then used to study empirical formula determination, eg primary butanol, secondary butanol, tertiary butanol and ethanol. Most of the experimental values obtained corresponded to the theoretical formulae.

Uden *et al* (93) evaluated a low power (50 - 100W) atmospheric helium MIP for the determination of empirical formulae of various compounds including a series of alkanes (C_{10} - C_{24}), alkanes/alkenes, and chlorinated organics. The relative standard deviations (RSDs) for the known and experimental C/H ratios and empirical formulae ranged from 0.4 - 2.4%, the mean error for all results being 1.3%. Decane was the only exception to this. Uden suggested that because decane eluted just after the solvent vent, the plasma may not have fully regained stability.

For the chlorinated compounds the rounded values agreed with the expected empirical formulae, but the RSDs were higher than those for hydrocarbons, ie

0.2 - 3.3%. Also the mean RSD was 1.8%, again high compared with 1.3% for the hydrocarbons. It was suggested that this could reflect a minor structural dependence. It was also noted that the mean RSD of hydrogen (1.8%) was double that of chlorine (0.9%).

Evans *et al* (94) compared the performance of a low pressure helium plasma in a Beenakker type cavity to a MPD-850. Empirical formula were determined for n-alkanes, aromatic hydrocarbons and sulphur containing compounds. Overall the H/C ratios for the sulphur compounds were not as accurate as those for the alkanes, suggesting a certain degree of structure dependence.

In 1988 Wei-Le Yu (95) used a low pressure helium plasma to establish the accuracy of elemental ratioing and empirical formula calculation. A range of compounds were analysed and favourable formulae calculated.

More recently Yie-ru *et al* (51) used an atmospheric helium MIP to study the effect of structure on formula determinations. He stated that for homologous hydrocarbons (eg a series of alkanes) response is unaffected by structure, so any homologous compound could be used as a reference. Also, for mixtures of alkenes and alkanes either could be used as a reference, as structure again did not seem to affect response. However for non-homologous mixtures such as alkenes and polycyclic aromatic hydrocarbons (PAHs) the structure of the reference did effect the response. For example, when an alkene was used as a reference the results for alkenes in the mixture were more accurate than the PAH results, but when a PAH acted as reference the results for PAHs improved while those for alkenes deteriorated. It was also noted that overall, aromatic hydrocarbons gave lower hydrogen responses than alkenes.

Responses for halogenated hydrocarbons also showed a significant structure dependency. In these compounds it was found that the more chlorine atoms present, the larger the error in the H/C ratios. It was therefore suggested that for such hydrocarbons the reference compounds should have a similar C-H skeleton and similar number of halogen atoms to the test compound.

Yie-ru also suggested that errors in multi-element detection could be due to background intensity shifts at specific elemental lines when carbon containing compounds are eluted from the column. He stated that these shifts were due to emission from molecular species such as CN, CO and C_2^+ which caused deviations of heteroatom to carbon ratios. However, the implementation of on-line background correction had previously been found to overcome this problem, as Haas and Caruso had demonstrated (74). It was also noted that the lines used to monitor for bromine (470.49nm) and chlorine (479.5nm) were the second order or ionic lines in the uv/vis regions. These were chosen because they have a higher excited energy than the atomic emission lines for these elements. Yie-ru therefore suggested that if the chlorine and bromine atoms were not completely ionised in the plasma, partly excited ions could be produced. The responses detected by the ionic lines would not therefore be a reliable representation of the amount of chlorine and bromine present. The effect could therefore become more pronounced as the numbers of halogen atoms in the compound increased.

Another suggestion was that because the H/C ratios worsened as the number of chlorine atoms increased, the presence of heteroatoms may affect the state of carbon and hydrogen in the plasma. This effect had been seen previously by Freeman and Hieftje (96) who found that the presence of nitrogen dramatically decreased the emission intensities of fluorine and chlorine lines, and that the

introduction of decane into the MIP reduced the helium emission intensity and excitation temperature.

A later paper by Yie-ru (50) confirmed the earlier results discussed above. Again he looked at the structural effects on the responses of alkanes, alkenes, PAHs and halogenated hydro-carbons. He showed that again the alkane/alkene response appeared to be independent of structure, but noted that the response per mole of carbon and hydrogen were higher for these simple hydrocarbons than for PAHs. Also, results for chlorinated compounds the carbon and hydrogen responses were higher than in unhalogenated hydrocarbons. This effect was also seen for brominated species.

Wylie *et al* (57) used the HP5921A to demonstrate the use of a software algorithm for empirical formula determination, looking at groups of methyl esters, phenols and pesticides. For each element in the formula 'inaccuracy' parameters have to be set up. For example, when the methyl ester mix was run, the C/0 ratios obtained were correct to within 3%, therefore the inaccuracy parameter was set to 3%.

The accuracy for the phenol moiety was poor by comparison, with pentachlorophenol showing the greatest error. The effect had been noted earlier by Yie-ru (50) who found that chlorine content in pentachlorophenol caused elevated hydrogen response. Even when pentachlorophenol was left out of the empirical formula calculations, the C/H accuracy had to be increased to 15% and the C/O accuracy to 10%. There were also large errors in the results obtained by Yie-ru for oxygen ratios in the pesticide analysis, with inaccuracy parameters of between 11 and 27%. Better ratios were found however for C/H, C/N and C/S. It was also noted that the hydrogen response factors were dependent on the amount of hydrogen present in the plasma.

This effect was also reported by Jelink and Venema (52) who also used the HP5921A. They investigated the C/H ratios for aromatic and aliphatic hydrocarbons. Their results showed that for alkanes the ratios obtained were very close to the theoretical values. For aromatic molecules (benzene, ethylbenzene, p-xylene and biphenyl) however a significant deviation from the theoretical values was observed. Also, compared with the alkanes, the experimental C/H ratios for the aromatics were higher than the theoretical values.

Jelink suggested that this could be caused by a low hydrogen yield in the plasma as a result of the larger dissociation energy of aromatic C-H bonds compared to aliphatic C-H bonds. A reduced hydrogen response would result, leading to a higher C/H ratio as seen above. He also noted that the C/H and C/O ratios of oxygen containing compounds changed with structure. For example the oxygen response for butanol decreased from primary to secondary to tertiary. The C/H ratios for oxygenated compounds was also low compared with those of hydrocarbons, and the C/O ratio was not as reproducible as the C/H ratio. One reason given for this poor oxygen reproducibility was the fact that carbon, hydrogen and oxygen cannot be monitored in one injection. Two injections had to be made which could account for any drift. The C/H ratios of nitrogen containing compounds were also found to be higher than those for the aliphatic hydrocarbons. The C/N ratio of these hetero-aromatic compounds was also seen to deviate from those of other non-aromatic nitrogenated species. Jelink therefore concluded that response was structure dependent, but he was unclear as to whether this was due to poor energy transfer or was affected by residence time in the plasma.

Pedersen-Bjergaard *et al* (53) recently investigated the effect of structure and analyte concentration on response using an HP5921A. Analysis of a mixture of

polycyclics showed that the ratio of $C_{(area)}/H_{(area)}$ decreased when the amount of analyte increased. The same effect was observed for the C/N peak area ratios nitrogen-containing polycyclics. It was suggested that this was more likely due to reactions between analyte atoms and plasma impurities rather than detector overload, as the non-linearity was more apparent at lower concentrations. When the structural effect on response was investigated it was found that C/H ratios for saturated polycyclics were higher than those for their unsaturated analogues, and that ratios for n-alkanes were higher still. The C/H ratio was also affected by the presence of halogens and nitro substituents, for example results for benzene were higher than for substituted benzene. Variations were also seen in C/N ratios, even for a group of PAHs each containing one nitro group. It was therefore concluded that C/H and C/N ratios were significantly effected by both structure and analyte concentration.

It is therefore obvious from the above summary that opinion is divided on the relative merits of using the AED to determine elemental ratios and empirical formula. Many of the conflicting reports however may stem from the lack of standard widely available equipment.

As stated earlier, if the GC-AED detector has a high enough temperature to atomise organic compounds and excite those atoms properly, then each elemental response should be independent of the original structure of the compound. Therefore, if plots are constructed of response versus concentration for a particular element in a range of compounds, all plots should have the same slope. For example, equimolar amounts of azobenzene and nicotine should give identical responses for nitrogen, as both contain two nitrogen atoms. It should therefore be possible to use azobenzene to calibrate for any other nitrogen-containing compound. Hence our initial intention was to use azobenzene as a calibration standard for nitrogen-containing drugs.

However, not only should the slopes be the same, but the y-intercepts should be the same, ie the plots should all be superimposable (Figure 16).

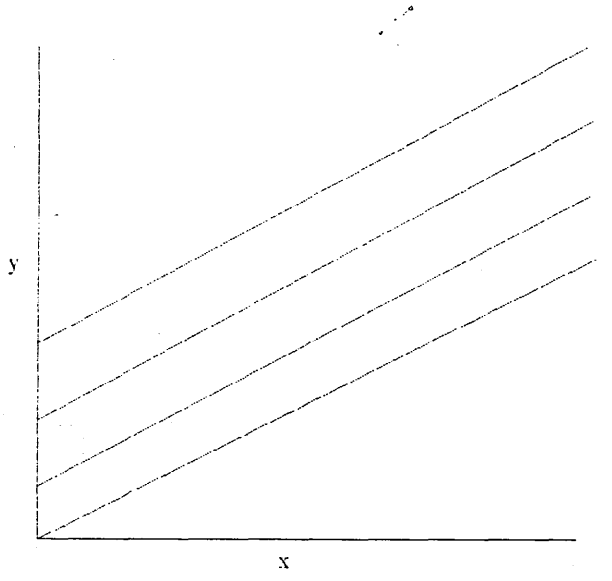

SAMPLE SLOPES

FIGURE 16

All the slopes in Figure 16 are equal, but the responses per unit atom are not, therefore identical slope does not necessarily mean identical elemental response.

3.2 Hydrocarbon Study

An initial study was undertaken to test compound independent calibration using a group of structurally similar aromatic hydrocarbons, bibenzyl, diphenylethylene, *cis*-stilbene, *trans*-stilbene and diphenylacetylene (see Figure 17).

The C(193 nm) line was monitored and the results obtained are summarised in Tables 2 and 3. Plots were constructed of response versus concentration for each compound (Figure 18). As these plots show the carbon response appears to be independent of structure, and all five relationships are linear, all but one giving a correlation coefficient of 1.0000. The *cis*-stilbene response is however consistently higher than the other four. It was initially thought that this could be due to steric hindrance as both benzyl groups are on the same side of the double bond. However, if this was the case, diphenylacetylene would be affected in a similar way. Also, if steric hindrance or other stereochemical effects were a factor it would probably prevent complete atomisation in the plasma, therefore causing a reduced response rather than an increased one as is observed. The hybridisation of the carbon atom does not appear to influence the spectroscopic yield for these compounds, as three different types of hybridisation are present, ie sp^3 in bibenzyl, sp^2 in the stilbenes and diphenylethylene and sp in diphenylacetylene.

BIBENZYL

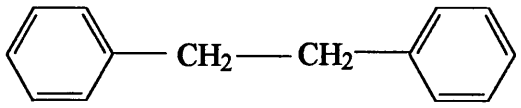

cis - STILBENE

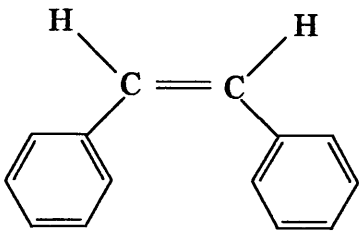

trans - STILBENE

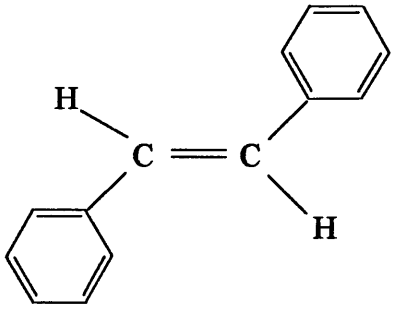

DIPHENYLACETYLENE

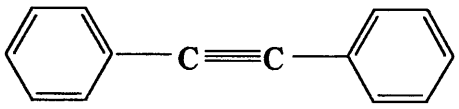

DIPHENYLETHYLENE

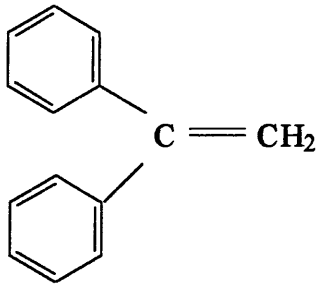

HYDROCARBON STRUCTURES

FIGURE 17

HYDROCARBON MIX

RESPONSE / CARBON

$1x10^{-5}$ M

	1	2	3	4	5	Average	RSD
Bibenzyl	1219	1362	1119	1113	1055	1174	10.3
Diphenyl-ethylene	1160	1303	1073	1073	1072	1026	9.7
c-Stilbene	1309	1476	1214	1206	1158	1273	9.9
Diphenyl-acetylene	1025	1189	941	932	886	995	12.1
t-Stilbene	1075	1238	982	964	905	1033	12.6

$5x10^{-5}$M

	1	2	3	4	5	Average	RSD
Bibenzyl	5838	5064	5371	5283	5896	5490	6.6
Diphenyl-ethylene	5852	5067	5353	5301	5893	5493	6.6
c-Stilbene	6454	5588	5905	5849	6503	6060	6.6
Diphenyl-acetylene	5486	4771	5117	4967	5616	5191	6.8
t-Stilbene	5524	4825	5173	5013	5666	5240	6.7

$1x10^{-4}$M

	1	2	3	4	5	Average	RSD
Bibenzyl	10521	11249	10054	10428	12156	10882	7.7
Diphenyl-ethylene	10313	11122	9896	10291	11982	10721	7.8
c-Stilbene	11233	11942	10741	11165	12885	11593	7.3
Diphenyl-acetylene	10186	10601	9568	9891	11680	10385	7.9
t-Stilbene	10359	10664	9676	9961	11827	10497	7.9

$2x10^{-4}$M

	1	2	3	4	5	Average	RSD
Bibenzyl	24066	18653	20647	20936	20789	21018	9.2
Diphenyl-ethylene	24024	18673	20697	20924	20848	21033	9.1
c-Stilbene	25350	19935	22070	22332	21949	22327	8.7
Diphenyl-acetylene	23586	18099	20097	20452	20020	20451	9.7
t-Stilbene	23878	18246	20245	20683	20199	20650	9.9

TABLE 2

$5x10^{-4}M$

	1	2	3	4	5	Average	RSD
Bibenzyl	53594	47082	59196	55086	49246	52841	9.1
Diphenyl-ethylene	54080	47388	58948	54937	49483	52967	8.7
c-Stilbene	56757	49903	62314	57961	52118	55811	8.8
Diphenyl-acetylene	52597	45931	59788	55442	48895	52531	10.3
t-Stilbene	52503	45896	60226	55892	48965	52696	10.7

TABLE 2 cont.

HYDROCARBON MIX - GRAPHICAL DATA

response/carbon plotted

	SLOPE ($x10^8$)	Correlation coefficient
Bibenzyl	1.052294	1.0000
Diphenylethylene	1.056211	1.0000
c-Stilbene	1.108800	1.0000
Diphenylacetylene	1.051240	0.9999
t-Stilbene	1.053794	1.0000

TABLE 3

FIGURE 18

For true compound independence the response per carbon should be the same for each compound. The RSDs for the responses here range from 12.6% at lower concentrations to 8.8% at higher concentrations. Concentration therefore does not seem to have an adverse effect on response for these compounds, as has been earlier observed (48), and which will be seen later in this chapter.

3.3 Phenol Study

The next group of compounds considered were the chloro- and nitrophenols 2-chlorophenol, 4-chloro-3-methylphenol, 2,4,6-trichlorophenol, 2-nitrophenol and 2,4-dinitrophenol (see Figure 19 for structures). Pentachlorophenol was to be included in this study but was difficult to get into solution and gave very low responses compared with the other phenols. This was seen earlier by Wylie (57) and Yie-ru (50). The poor response for pentachlorophenol is seen in Figure 20.

Carbon, nitrogen, chlorine and oxygen were monitored at 193, 174, 479 and 777nm respectively. Three injections were required. The results obtained are summarised in Tables 4 - 13. Plots were then constructed of response versus concentration for each element. This procedure was later repeated when the discharge tube had become contaminated with frequent use. The plot of carbon response versus concentration for the clean discharge tube (Figure 21) shows that 2-chlorophenol and 4-chloro-3-methylphenol give almost identical results and sensitivities. The response for 2,4,6-trichlorophenol is a little less however, and that for 2-nitrophenol is further reduced. Responses for 2,4-dinitrophenol overall were too low to be of quantitative value, and so were not plotted.

2-CHLOROPHENOL

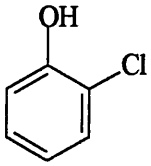

2,4-DICHLOROPHENOL

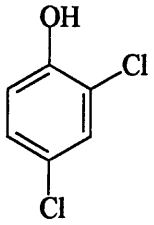

2,4,6-TRICHLOROPHENOL

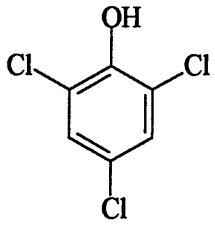

PENTACHLOROPHENOL

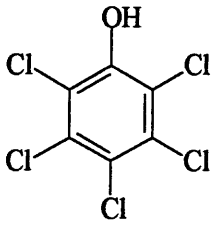

2,4-DIMETHYLPHENOL

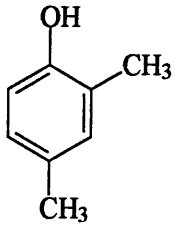

4-CHLORO-3-METHYLPHENOL

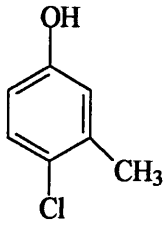

2-NITROPHENOL

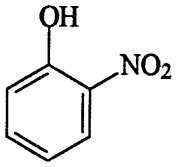

4-NITROPHENOL

2,4-DINITROPHENOL

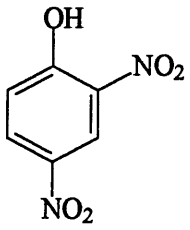

PHENOL STRUCTURES
FIGURE 19

FIGURE 20

PHENOL MIX - CARBON DATA
NEW DISCHARGE TUBE

	5E-5	5E-5	1E-4	1E-4	2E-4	2E-4	4E-4	4E-4	5E-4	5E-4
	C (193)	Resp./C	C (193)	Resp./ C	C (193)	Resp./ C	C (193)	Resp./C	C (193)	C (193)
2-chloro	14756	2459	51982	8664	92476	15413	228775	38129	279813	46636
2,4,6 tri-chloro	10535	1505	42670	7112	86330	14388	214003	35667	260079	43347
4-chloro-3-methyl	16935	2823	60042	8577	112435	16062	267659	38237	319153	45593
2-nitro	2885	481	31497	5250	73614	12269	203429	33905	250123	41687
2,4 di-nitro	------	------	-----	-----	-----	-----	29245	4874	58493	9749

TABLE 4

PHENOL MIX - OXYGEN DATA
NEW DISCHARGE TUBE

	5E-5	5E-5	1E-4	1E-4	2E-4	2E-4	4E-4	4E-4	5E-4	5E-4
	O (777)	Resp./O	O (777)	Resp./ O	O (777)	Resp./O	O (777)	Resp./O	O (777)	Resp./O
2-chloro	77	77	113	113	404	404	751	751	1399	1399
2,4,6 tri-chloro	120	120	204	204	494	494	1034	1034	1410	1410
4-chloro-3-methyl	128	128	216	216	593	593	1149	1149	1559	1559
2-nitro	83	28	357	119	1261	420	2824	941	3970	1323
2,4 di-nitro	---	----	----	----	----	----	179	36	903	181

TABLE 5

PHENOL MIX - CHLORINE DATA
NEW DISCHARGE TUBE

	5E-5	5E-5	1E-4	1E-4	2E-4	2E-4	4E-4	4E-4	5E-4	5E-4
	Cl(479)	Resp./ Cl	Cl(479)	Resp./Cl	Cl(479)	Resp./Cl	Cl(479)	Resp./Cl	Cl(479)	Resp./Cl
2-chloro	126	126	339	339	605	605	1450	1450	1958	1958
4-chloro-3-methyl	154	154	378	378	675	675	1525	1525	1939	1939
2,4,6 tri-chloro	328	109	993	331	1807	602	4276	1425	5478	1826

TABLE 6

PHENOL MIX - NITROGEN DATA
NEW DISCHARGE TUBE

	5E-5	5E-5	1E-4	1E-4	2E-4	2E-4	4E-4	4E-4	5E-4	5E-4
	N (174)	Resp./N	N (174)	Resp./N	N (174)	Resp./N	N (174)	Resp./N	N (174)	Resp./N
2-nitro	32	32	187	187	382	382	1109	1109	1349	1349
2,4 di-nitro	----	----	----	----	----		255	103	568	284

TABLE 7

PHENOL MIX - GRAPHICAL DATA
NEW DISCHARGE TUBE

response / carbon plotted

	SLOPE ($x10^7$)	Correlation coefficient
2-chlorophenol	9.877533	0.9978
2,4,6-trichlorophenol	9.399738	0.9985
4-chloro-3-methyl phenol	9.653035	0.9981
2-nitrophenol	9.340233	0.9980

response / chlorine plotted

	SLOPE	Correlation coeficient
2-chlorophenol	4004668	0.9965
2,4,6-trichlorophenol	3791335	0.9985
4-chloro-3-methyl phenol	3948334	0.9988

response / oxygen plotted

	SLOPE	Correlation coefficient
2-chlorophenol	2732334	0.9672
2,4,6-trichlorophenol	2855334	0.9975
4-chloro-3-methyl phenol	3163000	0.9975
2-nitrophenol	2849667	0.9975

TABLE 8

PHENOL MIX - CARBON DATA
OLD DISCHARGE TUBE

	5E-5	5E-5	1E-4	1E-4	2E-4	2E-4	4E-4	4E-4	5E-4	5E-4
	C (193)	Resp./ C	C(193)	Resp./ C	C (193)	Resp./C	C (193)	Resp./C	C(193)	Resp./C
2-chloro	23247	3875	44324	7387	84170	14028	154925	25821	183274	30546
2,4,6 tri-chloro	16430	2738	38265	6378	74914	12486	140939	24390	166023	27671
4-chloro-3-methyl	20110	2873	50268	7181	100943	14420	181519	25931	211363	30195
2-nitro	8395	1399	28919	4819	68411	11402	136746	22791	161368	26895
2,4 di-nitro	-------	------	------	------	------	------	7773	1296	24185	4031

TABLE 9

PHENOL MIX - OXYGEN DATA
OLD DISCHARGE TUBE

	5E-5	5E-5	1E-4	1E-4	2E-4	2E-4	4E-4	4E-4	5E-4	5E-4
	O (777)	Resp./O	O (777)	Resp./O	O (777)	Resp./O	O (777)	Resp./O	O (777)	Resp./O
2-chloro	116	116	192	192	328	328	636	636	1816	1816
2,4,6 tir-chloro	112	112	252	252	451	451	1030	1030	1696	1696
4-chloro-3-methyl	114	114	238	238	497	497	1180	1180	1836	1836
2-nitro	165	55	472	157	1184	395	2925	975	4780	1593
2,4 di-nitro	-----	-----	-----	-----	-----	-----	397	79	1353	271

TABLE 10

PHENOL MIX - CHLORINE DATA
OLD DISCARGE TUBE

	5E-5	5E-5	1E-4	1E-4	2E-4	2E-4	4E-4	4E-4	5E-4	5E-4
	Cl (479)	Resp./Cl	Cl (479)	Resp./Cl	Cl (479)	Resp./Cl	Cl (479)	Resp./Cl	Cl (479)	Resp./Cl
2-chloro	102	102	220	220	629	629	1120	1120	1617	1617
4-chloro-3-methyl	102	102	299	299	640	640	1136	1136	1606	1606
2,4,6 tri-chloro	228	76	734	245	1715	572	3134	1045	4437	1479

TABLE 11

PHENOL MIX - NITROGEN DATA
OLD DISCHARGE TUBE

	5E-5	5E-5	1E-4	1E-4	2E-4	2E-4	4E-4	4E-4	5E-4	5E-4
	N (174)	Resp./ N	N (174)	Resp./ N	N (174)	Resp./ N	N (174)	Resp./ N	N (174)	Resp./ N
2-nitro	52	52	127	127	311	311	642	642	783	783
2,4 di-nitro	-----	-----	-----	------	-------	------	64	32	208	104

TABLE 12

PHENOL MIX - GRAPHICAL DATA
OLD DISCHARGE TUBE

response / carbon plotted

	SLOPE ($x10^7$)	Correlation coefficient
2-chlorophenol	5.950134	0.9986
2,4,6-trichlorophenol	5.633101	0.9962
4-chloro-3-methyl phenol	6.043767	0.9957
2-nitrophenol	5.713102	0.9976

response / chlorine plotted

	SLOPE	Correlation coefficient
2-chlorophenol	3249334	0.9939
2,4,6-tirchlorophenol	297300	0.9957
4-chloro-3-methyl phenol	3164334	0.9951

response / oxygen plotted

	SLOPE	Correlation coefficient
2-chlorophenol	3206667	0.8887
2,4,6-trichlorophenol	3305001	0.9791
4-chloro-3-methyl phenol	3684334	0.9865
2-nitrophenol	3268000	0.9836

TABLE 13

PHENOLS CARBON CHANNEL 193nm - NEW DISCHARGE TUBE

FIGURE 21

When a contaminated discharge tube is used for the analysis, the 2-chloro and 4-chloro-3-methylphenols give a similar response again, and the overall pattern of slopes remains the same (Figure 22). However, the slopes and responses of all four compounds are reduced by about 35% compared with those obtained using a clean tube, although the correlation coefficients remain acceptable.

There are also differences in relative response with respect to molecular structure. For example, in both cases of new/old discharge tube the lines for 2-chloro and 4-chloro-3-methylphenol are almost identical and are superimposed, indicating a similar efficiency of element production in the plasma giving equal carbon elemental yield. However, the lines for 2-chloro and 2-nitrophenol are parallel not superimposed, even though they too have similar slopes. The vertical separation of these two lines indicates that the total response for carbon atoms in the 2-nitrophenol is less than that of the 2-chlorophenol. This therefore suggests that the carbon elemental yield differs for these two compounds.

A similar effect is seen in the chlorine response, ie the responses all decrease when using an old discharge tube. This can be seen from the plots for the new (Figure 23) and old (Figure 24) tube. The slopes decrease by approximately 20% with the old tube. Here however, although the slopes for the compound are not identical, the vertical separation between the lines is small compared with that of the carbon lines, indicating that the chlorine response is relatively independent of structure. This is expected, as chlorine is unlikely to form stable intramolecular species during atomisation of the parent molecule in the plasma.

PHENOLS CARBON CHANNEL 193nm - OLD DISCHARGE TUBE

FIGURE 22

PHENOLS CHLORINE CHANNEL 479nm - NEW DISCHARGE TUBE

FIGURE 23

PHENOLS CHLORINE CHANNEL 479nm - OLD DISCHARGE TUBE

FIGURE 24

However, when oxygen is considered the picture is different. Although the correlation coefficients appear to be acceptable (Tables 8 and 13), the responses are best represented as non-linear (Figures 25 and 26). There is only a small difference in responses and slopes between the new (Figure 25) and old (Figure 26) discharge tubes. The slopes are slightly higher for the old tube. The differences between individual compounds are more pronounced though, as the lines are not parallel. Differences are also highlighted by the intermolecular elemental response. For example, the oxygen atoms in 2-chloro and 2-nitrophenol give similar responses. However the carbon atoms in the same two phenols produce quite dissimilar slopes and give responses which differ by about 12% on average. This shows that the structure of the parent molecule affects different elemental responses in different ways.

Therefore, the elemental responses of carbon and chlorine in a group of phenols are related to the condition of the discharge tube, a dirty tube reducing responses for both elements. Oxygen responses are only slightly affected by the discharge tube.

Overall the chlorine response appears to be independent of structure, but the carbon and oxygen response do show some structural dependence. One explanation of this is the possible formation of carbon monoxide during breakdown of molecules in the plasma which could affect both the carbon and oxygen elemental yields. Carbon and oxygen could combine to form CO, but chlorine could not take part in such reactions. There is evidence that CO can be formed in the plasma. For example, the ^{13}CO lines at 171.0nm is used to monitor for labelled compounds.

FIGURE 25

PHENOLS OXYGEN CHANNEL 777nm - OLD DISCHARGE TUBE

FIGURE 26

Another factor which supports this suggestion of side reactions in the plasma is the relatively poor response for oxygen in the nitrophenols, especially at low concentrations. As this compound contains the $-NO_2$ group, it could easily break down in the plasma to form NO_2, therefore preventing complete oxygen yield. This effect is even more pronounced in 2,4-dinitrophenol which gives very low carbon and oxygen/nitrogen responses.

Therefore, the carbon response for an oxygen-containing compound will vary from that of a compound with no oxygen. This conclusion is borne out by the fact that the response per carbon atom for the phenols are between 25-55% lower than those for the aromatic hydrocarbons.

Discriminating loss of compounds due to a dirty injection port was also considered, but this would manifest itself on a compound dependent basis possibly related to polarity, not on an elemental dependent basis.

3.4 Chloroanisole Study

In order to check for polarity affects and positional substitution effects a series of eleven chloroanisoles was studied (Figure 27). Anisoles are methoxy aromatic compounds, whereas phenols are hydroxyaromatic compounds. Hence, they are much less polar and are unlikely to be adsorbed by active sites in the injection port or on the column.

Carbon, chlorine and oxygen were monitored at 193, 479 and 777 nm respectively. Three injections were required. The results obtained are summarised in Tables 14 - 17. Plots were then constructed of response versus concentration for each element.

3-CHLOROANISOLE

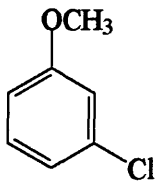

4-CHLOROANISOLE

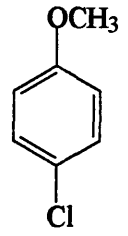

2-CHLOROANISOLE

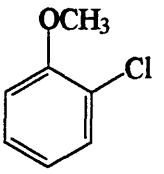

2,6-DICHLOROANISOLE

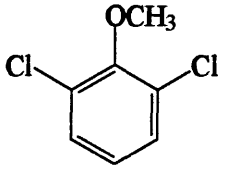

3,5-DICHLOROANISOLE

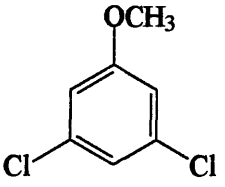

2,5-DICHLOROANISOLE

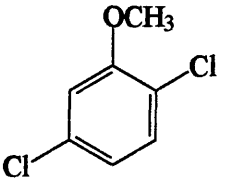

2,4-DICHLOROANISOLE

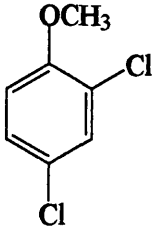

2,3-DICHLOROANISOLE

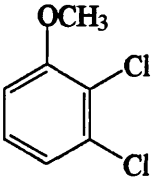

2,3,6-TRICHLOROANISOLE

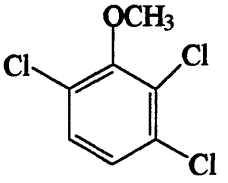

2,3,4-TRICHLOROANISOLE

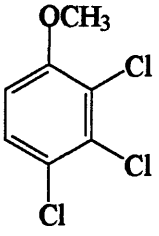

2,3,4,5-TETRACHLOROANISOLE

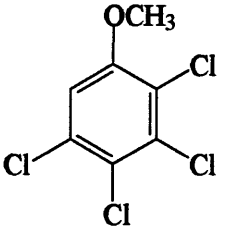

CHLOROANISOLE STRUCTURES
FIGURE 27

CHLOROANISOLE MIX - CARBON DATA

RESPONSE / CARBON

$5x10^{-5}M$

	1	2	3	4	5	Average	RSD
3,	4503	4514	4953	4225	4122	4463	7.2
4,	4637	4664	5112	4358	4245	4603	7.3
2,	4682	4681	5141	4389	4281	4635	7.2
2,6,	4523	4605	5035	4274	4179	4523	7.4
3,5,	4650	4780	5208	4414	4308	4672	7.6
2,5,	4459	4578	4978	4219	4118	4470	7.6
2,4,	4593	4749	5180	4371	4284	4636	7.7
2,3,	5939	6165	6710	5651	5527	5998	7.8
2,3,6,	4606	4840	5261	4438	4337	4696	7.9
2,3,4,	4331	4656	5037	4200	4131	4471	8.4
2,3,4,5,	2647	2937	3165	2622	2590	2792	9.0

TABLE 14a

$1x10^{-4}M$

	1	2	3	4	5	Average	RSD
3,	6762	8187	7282	6720	7001	7190	8.3
4,	6959	8482	7518	6973	7239	7434	8.5
2,	7031	8488	7549	6974	7272	7463	8.3
2,6,	6658	8293	7257	6828	7053	7218	8.9
3,5,	6724	8582	7400	7069	7272	7409	9.5
2,5,	6430	8237	7057	6779	6960	7093	9.6
2,4,	6645	8535	7316	7048	7249	7359	9.6
2,3,	8563	11055	9422	9110	9362	9502	9.8
2,3,6,	6589	8691	7312	7162	7328	7416	10.4
2,3,4,	6123	8367	6801	6889	6995	7035	11.6
2,3,4,5	3712	5260	4137	4340	4383	4366	13.0

TABLE 14b

RESPONSE / CARBON

$2x10^{-4}M$

	1	2	3	4	5	Average	RSD
3,	14147	14671	17636	16625	15542	15724	9.0
4,	14659	15221	18239	17191	16116	16285	8.9
2,	14619	15181	18233	17215	16093	16268	9.1
2,6,	14376	14953	17780	16761	15801	15934	8.6
3,5,	14919	15534	18263	17187	16365	16454	8.1
2,5,	14366	14972	17544	16519	15705	15821	7.9
2,4,	14919	15467	18186	17102	16298	16394	7.9
2,3,	19342	20084	23448	22072	21070	21203	7.7
2,3,6,	15242	15888	18341	17294	16594	16672	7.2
2,3,4,	14776	15511	17259	16512	16055	16023	5.9
2,3,4,5,	9332	9874	10560	10278	10119	10033	4.6

TABLE 14c

$5x10^{-4}M$

	1	2	3	4	5	Average	RSD
3,	56231	54254	49026	50919	51479	52382	5.4
4,	58211	56243	50983	52767	53214	54284	5.3
2,	57993	55956	50737	52541	53035	54052	5.4
2,6,	56869	55375	50306	51821	51402	53155	5.2
3,5,	58682	57462	52271	53542	52413	54874	5.5
2,5,	57478	56146	50867	52184	50851	53505	5.8
2,4,	57558	56616	51648	52755	51533	54022	5.3
2,3,	75624	74275	67196	68773	66600	70494	5.9
2,3,6,	59248	58593	53447	54380	52203	55574	5.7
2,3,4,	56561	56551	51845	52507	49481	53389	5.8
2,3,4,5,	35187	35263	33131	33328	30849	33552	5.4

TABLE 14d

RESPONSE / CARBON

$1x10^{-3}M$

	1	2	3	4	5	Average	RSD
3,	89955	75076	92570	71466	79581	81730	11.3
4,	92837	77658	95519	73677	82270	84392	11.2
2,	92447	77304	95231	73465	81833	84056	11.3
2,6,	90149	76166	93506	72021	80856	82540	11.0
3,5,	92390	78977	96449	74125	83930	85174	10.8
2,5,	91823	78198	96821	73064	83207	84623	11.5
2,4,	88135	76703	91727	71947	81128	81928	9.9
2,3,	117947	102009	123944	95098	108058	109411	10.7
2,3,6,	92312	80738	97534	75110	85669	86273	10.3
2,3,4,	87749	78289	92784	72356	83237	82883	9.7
2,3,4,5,	55254	50099	57785	45950	53106	52439	8.8

TABLE 14e

CHLOROANISOLE MIX - OXYGEN DATA

RESPONSE / OXYGEN

$5x10^{-5}M$

	1	2	3	4	5	Average	RSD
3,	220	235	234	231	239	232	3.1
4,	217	190	243	239	258	229	11.5
2,	225	206	215	228	187	212	7.8
2,6,	252	216	180	212	214	215	11.9
3,5,	186	228	219	205	262	220	12.9
2,5,	251	246	271	200	181	230	16.4
2,4,	290	213	194	231	171	220	20.5
2,3,	318	295	339	251	288	298	11.1
2,3,6,	230	245	297	276	211	252	13.8
2,3,4,	194	225	214	199	202	207	6.1
2,3,4,5,	122	133	182	172	150	152	16.7

TABLE 15a

$1x10^{-4}M$

	1	2	3	4	5	Average	RSD
3,	319	411	357	351	419	371	11.4
4,	406	372	411	310	377	375	10.7
2,	351	445	395	295	418	381	15.5
2,6,	319	396	375	323	351	353	9.4
3,5,	334	444	429	337	361	381	13.6
2,5,	342	387	338	310	394	354	10.0
2,4,	371	401	362	370	324	366	7.5
2,3,	471	504	486	476	556	499	6.9
2,3,6,	328	430	363	353	406	376	11.0
2,3,4,	333	375	346	319	360	347	6.3
2,3,4,5,	181	215	239	261	197	219	14.7

TABLE 15b

RESPONSE / OXYGEN

$2x10^{-4}M$

	1	2	3	4	5	Average	RSD
3,	634	813	785	565	734	706	14.8
4,	708	807	664	583	739	700	11.9
2,	715	755	682	688	724	713	4.1
2,6,	655	854	666	653	786	723	12.7
3,5,	729	796	618	622	776	708	11.9
2,5,	660	737	674	641	696	682	5.4
2,4,	666	802	689	680	756	719	8.1
2,3,	845	1051	925	812	995	926	10.8
2,3,6,	729	810	732	659	753	737	7.4
2,3,4,	594	895	647	570	760	693	19.4
2,3,4,5,	409	489	474	381	483	447	10.9

TABLE 15c

$5x10^{-4}M$

	1	2	3	4	5	Average	RSD
3,	1971	2426	1920	2082	2059	2092	9.5
4,	2017	2527	2004	2130	2182	2172	9.8
2,	2015	2631	1990	2192	2157	2197	11.7
2,6,	2014	2565	1974	2223	2091	2173	11.0
3,5,	2045	2583	1981	2163	2226	2200	10.7
2,5,	1971	2215	1883	2119	2102	2058	6.4
2,4,	2065	2433	1974	2183	2192	2169	8.0
2,3,	2669	3496	2582	2892	2835	2895	12.4
2,3,6,	2105	2667	2039	2247	2196	2251	10.9
2,3,4,	2006	2656	1896	2189	2159	2181	13.3
2,3,4,5,	1282	1627	1166	1258	1306	1328	13.2

TABLE 15d

RESPONSE / OXYGEN

$1x10^{-3}M$

	1	2	3	4	5	Average	RSD
3,	4097	3940	3581	3657	3828	3821	5.5
4,	4265	3996	3731	3733	3962	3937	5.6
2,	4297	4087	3799	3772	4025	3996	5.4
2,6,	4180	4062	3691	3729	3972	3927	5.4
3,5,	4203	4145	3795	3735	4036	3983	5.2
2,5,	4182	4013	3687	3653	3978	3903	5.8
2,4,	4077	3909	3694	3683	3941	3861	4.4
2,3,	5485	5354	4980	4972	5292	5217	4.4
2,3,6,	4355	4197	3798	3815	4076	4048	6.0
2,3,4,	4011	3978	3577	3617	3939	3824	5.5
2,3,4,5,	2422	2432	2181	2227	2370	2326	5.0

TABLE 15e

CHLOROANISOLE MIX - CHLORINE DATA

RESPONSE / CHLORINE

$5x10^{-5}M$

	1	2	3	4	5	Average	RSD
3,	214	204	226	194	209	209	5.7
4,	212	204	230	211	227	217	5.1
2,	210	203	216	216	214	212	2.6
2,6,	209	213	218	198	207	209	3.6
3,5,	209	218	224	204	213	214	3.7
2,5,	194	194	208	185	202	197	4.5
2,4,	212	214	231	204	227	218	5.2
2,3,	278	263	288	257	290	275	5.2
2,3,6,	204	209	222	205	227	213	4.8
2,3,4,	192	203	212	196	208	202	4.1
2,3,4,5,	117	121	134	121	131	125	5.8

TABLE 16a

$1x10^{-4}M$

	1	2	3	4	5	Average	RSD
3,	321	343	381	316	324	337	7.9
4,	350	355	381	333	346	353	5.0
2,	339	355	395	338	346	355	6.7
2,6,	334	342	373	317	329	339	6.2
3,5,	345	350	393	332	337	351	7.0
2,5,	323	323	361	312	313	326	6.2
2,4,	351	348	391	340	347	355	5.7
2,3,	442	449	499	426	441	451	6.2
2,3,6,	340	342	384	335	337	348	5.9
2,3,4,	321	319	365	318	316	328	6.4
2,3,4,5,	194	191	225	200	198	202	6.8

TABLE 16b

RESPONSE / CHLORINE

$2x10^{-4}M$

	1	2	3	4	5	Average	RSD
3,	743	711	777	779	683	739	5.7
4,	769	731	799	808	713	764	5.4
2,	768	737	797	809	703	763	5.7
2,6,	747	716	781	783	695	744	5.2
3,5,	769	742	818	803	724	771	5.2
2,5,	723	705	776	763	683	730	5.3
2,4,	774	745	823	809	725	775	5.3
2,3,	994	961	1062	1042	941	1000	5.1
2,3,6,	762	742	829	806	728	773	5.5
2,3,4,	726	718	812	757	708	744	5.6
2,3,4,5,	435	445	508	457	443	458	6.4

TABLE 16c

$5x10^{-4}M$

	1	2	3	4	5	Average	RSD
3,	2515	2044	2404	2756	2193	2382	11.6
4,	2588	2114	2508	2856	2265	2466	11.7
2,	2581	2110	2478	2832	2249	2450	11.5
2,6,	2532	2070	2443	2803	2220	2414	11.8
3,5,	2618	2147	2537	2900	2304	2501	11.6
2,5,	2534	2074	2472	2808	2237	2425	11.7
2,4,	2580	2140	2511	2859	2289	2476	11.2
2,3,	3370	2791	3300	3738	2997	3239	11.2
2,3,6,	2619	2783	2574	2907	2340	2525	11.0
2,3,4,	2490	2123	2487	2764	2267	2426	10.1
2,3,4,5,	1530	1343	1560	1701	1426	1512	9.0

TABLE 16d

RESPONSE / CHLORINE

$1x10^{-3}M$

	1	2	3	4	5	Average	RSD
3,	4468	4296	4582	3820	3504	4134	11.0
4,	4617	4438	4756	3934	3639	4277	11.1
2,	4583	4434	4728	3921	3605	4254	11.1
2,6,	4526	4314	4647	3788	3517	4158	11.7
3,5,	4695	4466	4847	3862	3658	4306	12.1
2,5,	4692	4476	4810	3785	3563	4265	13.1
2,4,	4504	4288	4667	3697	3546	4140	12.0
2,3,	6083	5807	6296	4903	4712	5560	12.8
2,3,6,	4746	4520	4930	3784	3675	4331	13.1
2,3,4,	4499	4351	4807	3525	3563	4149	13.9
2,3,4,5,	2781	2713	3046	2161	2245	2589	14.5

TABLE 16e

CHLOROANISOLE MIX - GRAPHICAL DATA

response / carbon plotted

	SLOPE ($x10^7$)	Correlation coeffiecient
3,	8.455829	0.9880
4,	8.733866	0.9877
2,	8.692278	0.9877
2,6,	8.544554	0.9875
3,5,	8.818866	0.9875
2,5,	8.775576	0.9890
2,4,	8.475739	0.9852
2,3,	11.32747	0.9875
2,3,6,	8.938079	0.9874
2,3,4,	8.592682	0.9874
2,3,4,5,	5.440204	0.9880

TABLE 17a

response / oxygen plotted

	SLOPE	Correlation coefficient
3,	3858835	0.9982
4,	3995372	0.9977
2,	4063383	0.9979
2,6,	3995923	0.9978
3,5,	4047994	0.9977
2,5,	3950340	0.9989
2,4,	3920632	0.9973
2,3,	5300244	0.9975
2,3,6,	4102622	0.9975
2,3,4,	3907622	0.9964
2,3,4,5,	2353172	0.9967

TABLE 17b

response / chlorine plotted

	SLOPE	Correlation coefficient
3,	4256603	0.9956
4,	4402040	0.9956
2,	4377217	0.9957
2,6,	4285551	0.9952
3,5,	4439466	0.9952
2,5,	4412686	0.9960
2,4,	4260066	0.9937
2,3,	5734791	0.9950
2,3,6,	4471279	0.9949
2,3,4,	4287331	0.9947
2,3,4,5,	2678366	0.9947

TABLE 17c

The plot of carbon response versus concentration (Figure 28) shows that nine of the chloroanisoles give almost identical responses and sensitivities. The plots obtained have very similar slopes and are almost superimposable. Two of the anisoles, however, give unexpected results. 2, 3-Dichloroanisole gives a much higher response and 2, 3, 4, 5-tetrachloroanisole gives a much lower response compared with the other nine compounds. The tetrachloroanisole appears to be behaving like pentachlorophenol which, as mentioned earlier, was disregarded from the previous study due to poor responses. The same overall pattern was observed for both the oxygen (Figure 29) and chlorine (Figure 30) channels. All responses were linear giving acceptable correlation coefficients. The structural dependence observed for the carbon and oxygen responses in phenols was not apparent here, except for the two anomalous results. The carbon responses for the chloroanisoles are similar to those of the phenols, but again are less than those for the aromatic hydrocarbons. This therefore reinforces the previous statement that carbon responses of oxygenated and non-oxygenated compounds differ. Overall the oxygen responses for these compounds were some 30% higher than the responses for the equivalent phenol compound, and no structural dependence was noted. The chloroanisole chlorine responses were also slightly higher than the phenol responses, but again were not structurally dependent.

CHLOROANISOLES
CARBON CHANNEL - 193nm

FIGURE 28

FIGURE 29

CHLOROANISOLES
CHLORINE CHANNEL - 479nm

CO C V I C M O O C M C V J C M C V I C M C M

O
O
O
CO
O
O
O
in
1
0
O
LO X
0
c
0
O
CO
"O
c
CO
CO
D
0
-C
h -
0
Q.
CO
CD
CL
0
CO
0
O
CO LO ^ CO CM

FIGURE 30

3.5 Nitrogen Based Study

The three studies described previously were carried out on groups of similar compounds, so the following analysis was undertaken on a series of compounds with markedly dissimilar structures. The mixed standard consisted of cotinine, lidocaine, pentobarbital, secobarbital, barbital, caffeine, nicotine and azobenzene. The original intention was to find a standard which could be used to calibrate for all nitrogen containing drugs. The structures are shown in Figure 31. Carbon, nitrogen and oxygen were monitored at 193, 174 and 777 nm respectively. Two injections were made. A sample chromatogram is shown in Figure 32. The analysis was later repeated when the discharge tube had become contaminated. The results obtained are summarised in Tables 18 - 25.

Cotinine is a major metabolite of nicotine and contains one oxygen in a carbonyl group adjacent to a nitrogen in a 5 membered ring. Nicotine has the same basic backbone, but does not contain any oxygen. Caffeine has a xanthene-type skeleton consisting of a 5 and a 6 membered ring, each containing two nitrogen atoms, three of which are amino and one of which is imino in character. The two oxygens are both in carbonyl groups on the 6 membered ring and are in similar environments as the oxygen in cotinine.

The three barbiturates have the same basic structure consisting of a 6 membered ring. Each barbiturate contains three oxygens which are all in carbonyl groups in barbital and in two carbonyl and one hydroxyl group in pentobarbital and secobarbital. Both seco- and pentobarbital also have relatively large alkyl side chains, and hence have a very similar overall structure. Lidocaine contains one tertiary amino nitrogen, one amido nitrogen and an oxygen in a carbonyl group which is not contained in a ring. Therefore the nitrogen and oxygen atoms in these compounds are in very different environments.

BARBITAL

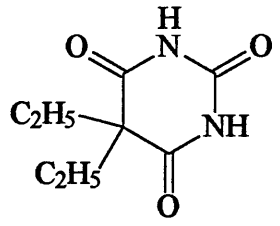

PENTOBARBITAL

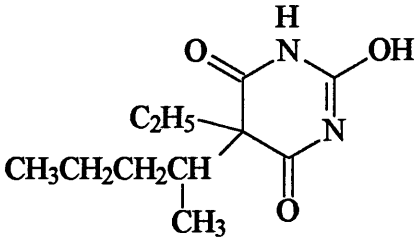

SECOBARBITAL

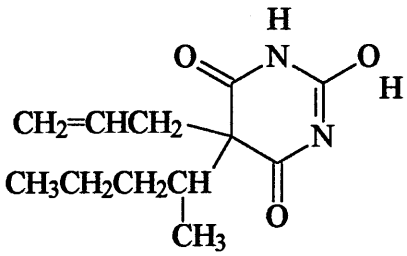

CAFFEINE

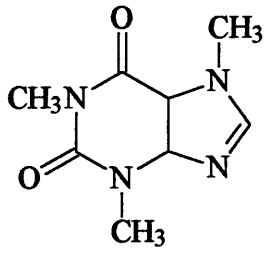

NICOTINE

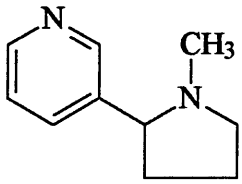

COTININE

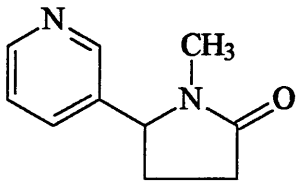

AZOBENZENE

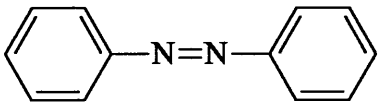

LIDOCAINE

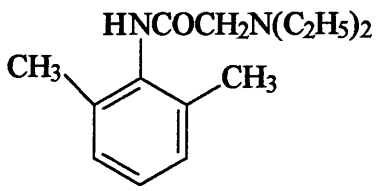

NITROGEN CONTAINING COMPOUNDS
FIGURE 31

NITROGEN CONTAINING COMPOUNDS

FIGURE 32

NITROGEN CONTAINING COMPOUNDS - CARBON DATA
NEW DISCHARGE TUBE

	5E-5	5E-5	1E-4	1E-4
	C (193)	Resp./ C	C (193)	Resp./ C
Azobenzene C12	44014	3668	113801	9483
Cotinine C10	26899	2690	85915	8592
Nicotine C10	35044	3504	102254	10225
Caffeine C8	26731	3341	76207	9526
Barbital C8	28927	3616	78622	9828
Secobarbital C12	40861	3405	112096	9341
Pentobarbital C11	39053	3550	104639	9513
Lidocaine C14	46973	3355	129676	9263

	2E-4	2E-4	4E-4	4E-4
	C (193)	Resp./ C	C (193)	Resp./ C
Azobenzene C12	195759	16313	495929	41327
Cotinine C10	154964	15496	440163	44016
Nicotine C10	180418	18042	469226	46923
Caffeine C8	130773	16347	371544	46443
Barbital C8	139546	17443	388587	48573
Secobarbital C12	196701	16392	542663	45222
Pentobarbital C11	178480	16225	486474	44225
Lidocaine C14	224305	16022	577651	41261

TABLE 18

NITROGEN CONTAINING COMPOUNDS - NITROGEN DATA
NEW DISCHARGE TUBE

	5E-5	5E-5	1E-4	1E-4
	N (174)	Resp./ N	N (174)	Resp./ N
Azobenzene N2	146	73	396	198
Cotinine N2	93	47	347	174
Nicotine N2	130	65	411	206
Caffeine N4	257	64	750	188
Barbital N2	138	69	403	202
Secobarbital N2	141	71	388	194
Pentobarbital N2	134	67	397	199
Lidocaine N2	132	66	390	195

	2E-4	2E-4	4E-4	4E-4
	N (174)	Resp./ N	N (174)	Resp./ N
Azobenzene N2	714	357	2128	1064
Cotinine N2	659	330	2114	1057
Nicotine N2	771	386	2305	1153
Caffeine N4	1358	340	4041	1010
Barbital N2	740	370	2250	1125
Secobarbital N2	708	354	2225	1113
Pentobarbital N2	707	354	2156	1078
Lidocaine N2	708	354	2091	1046

TABLE 19

47	342	174
65	411	206
64	750	188
69	403	202
71	388	194

2E-4	4E-4	8E-4
Kesp / N	N (1/4)	Kesp / N
357	2128	1064
330	2114	1057
386	2305	1153
340	4041	1010
370	2250	1125
354	2225	1113
354	2150	1076
354	2091	1046

TABLE 19

NITROGEN CONTAINING COMPOUNDS - OXYGEN DATA
NEW DISCHARGE TUBE

	5E-5	5E-5	1E-4	1E-4
	O (777)	Resp./ O	O (777)	Resp./ O
Cotinine O1	282	282	369	369
Caffeine O2	489	245	830	415
Barbital O3	754	251	1245	415
Secobarbital O3	754	251	1185	395
Pentobarbital O3	851	284	1167	389
Lidocaine O1	250	250	369	369

	2E-4	2E-4	4E-4	4E-4
	O (777)	Resp./ O	O (777)	Resp./ O
Cotinine O1	652	652	1301	1301
Caffeine O2	1674	837	3070	1535
Barbital O3	2697	899	5103	1701
Secobarbital O3	2374	791	4036	1345
Pentobarbital O3	2383	794	4161	1387
Lidocaine O1	773	773	1518	1518

TABLE 20

NITROGEN CONTAINING COMPOUNDS - GRAPHICAL DATA
NEW DISCHARGE TUBE

Carbon responses:-

	SLOPE ($x10^8$)	Correlation coefficient
Azobenzene	1.064597	0.9940
Cotinine	1.172233	0.9910
Nicotine	1.227155	0.9938
Caffeine	1.221644	0.9897
Barbital	1.277586	0.9909
Secobarbital	1.186651	0.9912
Pentobarbital	1.152016	0.9911
Lidocaine	1.070805	0.9937

Nitrogen responses:-

	SLOPE	Correlation coefficient
Azobenzene	2827131	0.9881
Cotinine	2880697	0.9870
Nicotine	3100871	0.9894
Caffeine	2693914	0.9888
Barbital	3012523	0.9879
Secobarbital	2980174	0.9859
Pentobarbital	2878262	0.9874
Lidocaine	2790435	0.9891

Oxygen responses:-

	SLOPE	Correlation coeffiecient
Cotinine	2971131	0.9971
Caffeine	3709914	0.9992
Barbital	4200001	0.9991
Secobarbital	3153045	0.9970
Pentobarbital	3221913	0.9975
Lidocaine	3694957	0.9989

TABLE 21

NITROGEN CONTAINING COMPOUNDS - CARBON DATA
OLD DISCHARGE TUBE

Conc.(M)	5E-5	5E-5	1E-4	1E-4
	C (193)	Resp./ C	C (193)	Resp./ C
Azobenzene C12	36367	3031	66317	5526
Cotinine C10	20115	2012	42246	4225
Nicotine C10	30995	3100	61245	6125
Caffeine C8	18924	2366	38263	4783
Barbital C8	19250	2406	37937	4742
Secobarbital C12	24308	2026	52978	4415
Pentobarbital C11	27050	2459	51559	4687
Lidocaine C14	36126	2580	66213	4730

Conc.(M)	2E-4	2E-4	4E-4	4E-4
	C(193)	Resp./C	C(193)	Resp./C
Azobenzene C12	127845	10654	37146	30946
Cotinine C10	94175	9418	332239	33224
Nicotine C10	125747	12575	384475	38448
Caffeine C8	78874	9859	273396	34175
Barbital C8	84140	10518	290797	36350
Secobarbital C12	111560	9297	397016	33085
Pentobarbital C11	106505	9682	362762	32978
Lidocaine C14	135039	9646	410015	29287

TABLE 22

NITROGEN CONTAING COMPOUNDS - NITROGEN DATA
OLD DISCHARGE TUBE

Conc.(M)	5E-5	5E-5	1E-4	1E-4
	N (174)	Resp./ N	N (174)	Resp./ N
Azobenzene N2	129	65	255	128
Cotinine N2	80	40	184	92
Nicotine N2	133	67	267	134
Caffeine N4	202	51	413	103
Barbital N2	101	51	206	103
Secobarbital N2	89	45	201	101
Pentobarbital N2	100	50	207	104
Lidocaine N2	111	56	210	105

Conc.(M)	2E-4	2E-4	4E-4	4E-4
	N (174)	Resp./ N	N (174)	Resp./ N
Azobenzene N2	500	250	1619	810
Cotinine N2	423	212	1640	820
Nicotine N2	580	290	1944	972
Caffeine N4	863	216	2826	707
Barbital N2	474	237	1767	884
Secobarbital N2	422	211	1669	835
Pentobarbital N2	430	215	1670	835
Lidocaine N2	450	225	1377	688

TABLE 23

NITROGEN CONTAINING COMPOUNDS - OXYGEN DATA
OLD DISCHARGE TUBE

Conc.(M)	5E-5	5E-5	1E-4	1E-4
	O (777)	Resp./ O	O (777)	Resp./ O
Cotinine O1	130	130	217	217
Caffeine O2	269	135	513	257
Barbital O3	350	117	800	267
Secobarbital O3	342	114	766	255
Pentobarbital O3	292	97	794	267
Lidocaine O1	181	181	296	296

Conc.(M)	2E-4	2E-4	4E-4	4E-4
	O (777)	Resp./ O	O (777)	Resp./ O
Cotinine O1	557	557	930	930
Caffeine O2	1454	727	2076	1038
Barbital O3	2439	813	3762	1254
Secobarbital O3	1917	639	2789	930
Pentobarbital O3	1941	647	2766	922
Lidocaine O1	736	736	1131	1131

TABLE 24

NITROGEN CONTAINING COMPOUNDS - GRAPHICAL DATA
OLD DISCHARGE TUBE

response / carbon plotted

	SLOPE ($x10^7$)	Correlation coefficient
Azobenzene	8.081967	0.9870
Cotinine	9.087288	0.9807
Nicotine	10.24724	0.9862
Caffeine	9.240472	0.9803
Barbital	9.892316	0.9810
Secobarbital	9.018280	0.9799
Pentobarbital	8.877394	0.9805
Lidocaine	7.757133	0.9856

response / nitrogen plotted

	SLOPE	Correlation coefficient
Azobenzene	2158088	0.9826
Cotinine	2272696	0.9773
Nicotine	2632871	0.9824
Caffeine	1904870	0.9833
Barbital	2431827	0.9780
Secobarbital	207263	0.9666
Pentobarbital	2016000	0.9679
Lidocaine	1652973	0.9834

response / oxygen plotted

	SLOPE	Correlation coeffiecient
Cotinine	2333566	0.9914
Caffeine	2624175	0.9690
Barbital	3300000	0.9790
Secobarbital	2332175	0.9738
Pentobarbital	2327827	0.9684
Lidocaine	2765218	0.9840

TABLE 25

A series of standards were prepared in the range 5 x 10^{-5} to 4 x 10^{-4}M. At concentrations above this the response became non-linear. In other systems this would signify detector overload. However, this is not thought to be the case here because non-linearity seems to occur to different extents for the same element in different compounds.

Plots were constructed of response versus concentration for each element. The plots for oxygen (Figures 33 and 34) clearly show a degree of structure dependence, as the slopes are not superimposable. Some of the lines are similar, but run parallel to each other, indicating a difference in response and sensitivity between the compounds. For example, the plots for lidocaine and caffeine are parallel, but the oxygen response for lidocaine is more sensitive. The slopes for seco- and pentobarbital are almost identical however, as are their structures. The plots overall are relatively widely spread with the difference between barbital (highest response) and cotinine (lowest response) being approximately 30%.

As stated earlier, at higher concentrations the plots became non-linear as response dropped off. This effect has been noted before (47) and can be seen in the plots here where some responses for 4 x 10^{-4}M are not as high as expected. This cannot be attributed to detector overload because the calibration curves depart from linearity at different concentrations for different compounds. One possible explanation therefore is that the production of oxygen atoms becomes non-linear at different concentations because efficiency of atom formation varies according to the nature of the parent molecule. Both results tables (Tables 20 and 24) for oxygen show that the response per unit oxygen tends to decrease with increasing concentration. This supports the theory that side reactions in the plasma decrease the amount of oxygen available for detection, such reactions being more likely at high concentrations when more atoms are present.

NITROGEN CONTAINING COMPOUNDS - OXYGEN CHANNEL 777nm
NEW DISCHARGE TUBE

FIGURE 33

NITROGEN CONTAINING COMPOUNDS - OXYGEN CHANNEL 777nm
OLD DISCHARGE TUBE

FIGURE 34

The timescale over which atomisation of the molecule in the plasma occurs is also important. On a narrow-bore capillary column the average peak width of eluates is 2-3 seconds. However, the diameter of the discharge tube is much greater than that of a gas chromatography column, decreasing the linear flow rate at the GC-AED interface. The base width of peaks, therefore, increases by up to 4 or 5 times on passing from the column into the plasma. The plasma itself is about 10mm long, therefore the atomisation of eluting molecules occurs over several seconds during which time molecules, reagent gases and atoms are all present. It is therefore possible that breakdown involves the formation of small molecular species, the structure of which will depend on the structure of the parent molecule. The structural dependency of the response will therefore vary according to the degradation pathways available to the molecule, the concentration of analyte and other reactive species, as well as residence time in the plasma. One species which could be formed during oxygen analysis is NO_2 as nitrogen is present in the auxillary gas used as a reagent gas for oxygen determination.

The results for the analysis using a new discharge tube (Figure 33) do go some way to support the above conclusions. For example, the slopes for the calibration lines for the old tube (Figure 34) are all less than those for the new tube, indicating reduced sensitivity. This suggests that more side reactions are occuring in the old dirty tube, therefore reducing the amount of oxygen available for detection. Side reactions are more probable in a dirty tube as more material is present, as opposed to a clean uncontaminated tube. However, in the previous phenol study the oxygen channel did not appear to be affected by the condition of the discharge tube. Therefore, the oxygen environment in phenols obviously affects the response in a different way to the oxygens' environment in this study. Here, most of the oxygens are present in carbonyl groups, whereas in phenols most are present in hydroxyl groups. The indication here is that when an oxygen

atom is present in a molecule in a carbonyl group the state of the discharge tube has an effect on response, whereas if hydroxyl groups are present, the discharge tube has very little effect on the oxygen response. With hindsight it would have been interesting to monitor the CO emission line at 241.36nm during these experiments.

The environment surrounding oxygen in a molecule obviously affects the response. For example, the response per oxygen for cotinine where the oxygen and nitrogen atoms are not directly bonded is 282 units (new tube, 5×10^{-5}M), whereas for 2-nitrophenol the response per oxygen is 28 units (new tube, 5×10^{-5} M). This may be due to the presence of the NO_2 moiety in the phenol which is likely to inhibit the atomisation of oxygen. NO_2 could also be formed during the atomisation of cotinine due to the presence of nitrogen in the oxygen reagent gas, however its effect is likely to be more pronounced in the phenol, because it is already present as part of the molecule.

The carbon responses for this set of compounds were also lower with the old tube (Figure 35) than with the new tube (Figure 36), showing the same reduced sensitivity seen with the oxygen responses.

The carbon environments are quite different in the target compounds. For example, caffeine has a xanthene-type structure, whereas in azobenzene the carbons form two benzene rings. In the barbiturates the carbons are present in six-membered rings and side-chains. Nicotine and cotinine are made up of a five- and a six-membered ring, but here the rings are not fused as they are in caffeine.

These two compounds would therefore be expected to give almost identical carbon responses. However, as Figure 35 shows this is not the case. In fact the

cotinine response is closer to the pentobarbital response than the nicotine. This pattern is repeated with the new tube (Figure 36).

Secobarbital and pentobarbital have almost identical structures, and their carbon responses are very similar, as were those for oxygen. However, on both the oxygen and carbon plots the barbital response is very different to those of seco- and pentobarbital. As the structures in Figure 31 show, barbital differs from the other two barbiturates in that it does not have a large alkyl side-chain. It therefore seems that the absence of this chain causes the barbital responses to differ from seco- and pentobarbital. This clearly indicates a degree of structural dependence.

When considering the nitrogen responses of the barbiturate, seco- and pentobarbital give almost identical responses with the old discharge tube. Barbital, however, gives a slightly elevated response. With the new discharge tube (Figure 38) the barbiturate responses are different, with barbital and secobarbital giving the closest responses.

Barbital gives a more sensitive response than seco- and pentobarbital on all three channels monitored, indicating that in this case the carbon, nitrogen and oxygen responses are all affected by structure.

Nicotine and cotinine should also give similar responses on the nitrogen channel. This is not the case however, as Figures 37 and 38 show. The carbonyl group adjacent to the nitrogen atom in the five-membered ring of cotinine therefore appears to have an effect on response.

Hence the intention to use a single standard for all nitrogen containing drugs was found to be untenable as the elemental response was found to be dependent on a

variety of factors. Calibration was therefore far more complex a procedure than was originally anticipated.

NITROGEN CONTAINING COMPOUNDS - CARBON CHANNEL 193nm
OLD DISCHARGE TUBE

FIGURE 35

NITROGEN CONTAINING COMPOUNDS - CARBON CHANNEL 193nm
NEW DISCHARGE TUBE

FIGURE 36

NITROGEN CONTAINING COMPOUNDS - NITROGEN CHANNEL 174nm COLD DISCHARGE TUBE

FIGURE 37

NITROGEN CONTAINING COMPOUNDS - NITROGEN CHANNEL 174nm
NEW DISCHARGE TUBE

FIGURE 38

4.1 Introduction

The first modern alcohol based perfume was Hungary Water which became a popular cosmetic in Europe around the end of the fourteenth century. It was distilled from rosemary and was still in use in Victorian times.

Towards the end of the nineteenth century the chemical industry became involved in perfume production. The first major success of this venture was the synthesis of odour-suitable aldehydes which led to the introduction of Chanel No 5 in 1921.

Today the perfumers have a wide range of synthetic ingredients at their disposal, as well as the natural products. However, in many ways the synthetic ingredients are better than the natural ones as they have better chemical and olfactory uniformity. This is because they are not subject to changing weather conditions and other natural phenomena. The main chemicals which are important in perfumery are alcohols, aldehydes, organic esters, ketones and related compounds. Certain nitrogen-containing compounds such as nitro musks are also of critical importance. The manufacture of aroma chemicals is not however confined to the production of perfumes. Fragrances are also manufactured for detergents, soaps, fabric softeners, bleaches, shampoos, deodorants, antiperspirants and talcum powders. Research into aroma chemicals is roughly divided into three areas. Firstly, there is the duplication of naturally occuring compounds, eg phenethyl alcohol which is present in rose oil. The second area of research is in the chemical modification of abundant naturally occurring materials, such as acetylated vetiver oil from vetivert oil and vanillin from lignin. Thirdly, there is the synthesis of aroma chemicals based on industrial organic feedstocks, such as nitro musks.

The ability to perform accurate trace analysis is essential for the perfume industry as many chemicals present in trace quantities are very important in

giving a natural product its full aesthetic value. If perfumers can quantify all the components present in a natural product, then a synthetic alternative can be produced. This is often desirable as natural products can be very expensive. As in all other manufacturing industries, quality control is very important in perfume production. Techniques such as refractive index and specific gravity determinations along with gas chromatography are used to help determine purity and maintain quality uniformity of fragrance.

During the last thirty years or so there has been a rapid advance in the capabilities of instrumental techniques for the separation and identification of volatile organics. The development of capillary gas chromatography columns and the ability to interface them directly to a mass spectrometer was of particular importance. This combination of techniques generates large quantities of data, so computer software is incorporated into the system to interpret the results. In GC-MS instruments the computer houses a library of thousands of mass spectra of different compounds to which results can be compared. These instruments, along with Fourier Transform nuclear magnetic resonance techniques, have allowed the discovery and analysis of minute quantities of odiferous substances, and have therefore revolutionised the analysis of essential oils and the synthesis of aroma chemicals.

Analytical techniques therefore have a vital role to play in the perfume industry. However, the techniques mentioned above cannot provide a complete picture. As the results in this chapter will show, the atomic emission detector can provide composition information complementary to the structural data given by GC-MS. For example, if the mass spectral data shows a certain compound contains nitrogen, but the AED shows no nitrogen is present, then all library guesses containing nitrogen can be eliminated. Also, the AED may detect minute quantities of trace compounds which the mass spectrometer could fail to detect.

4.2 Ysatis

Ysatis is a ladies' perfume. 'Genuine' and 'fake' samples of the perfume were analysed using the AED (Figures 39 and 40). The analysis was then repeated on a GC-MS instrument to identify the compounds present.

As the chromatograms show, the carbon channel responses resemble those of a flame ionisation detector. Both hydrogen responses closely mirror those of the carbon channel, as expected. The peaks for these two elements are, however, better resolved for the genuine sample compared to the fake. The chromatograms for the genuine sample are also more complex. The retention times differ between sample and between the GC-MS and AED results due to manual injection.

No sulphur or chlorine containing compounds were found in either sample, however several oxygen and a few nitrogen containing compounds were present. When the nitrogen channels were amplified, several smaller peaks were seen (see Figure 41). The GC-MS data was then used to compare the two samples to see which compounds, if any were present in both. The results are summarised in Table 26. Looking at the nitrogen containing peaks, it was found that the peak at MS retention time (RT) 19.667 for the genuine sample corresponded to the small peak at RT 19.484 for the fake sample. The best hits for these peaks from the mass spectral data showed them to be 2-amino methyl benzoate (917) (Figure 42). The large peak at RT 34.619 for the genuine sample was found to correspond to the peak at 34.454 on the fake sample. Mass spectral data suggested that both peaks could be 1-4-(1,1-dimethylethyl)-2, 6-dimethyl-35-dinitro-phenylethanone (836) (Figure 43). The major peak for the fake sample at 32.037 was shown to be 1-(1, 1-dimethylethyl)-3, 5-dimethyl-2, 4, 6-trinitrobenzene. When the nitrogen channels were magnified (Figure 41) a very

small peak at 32.2 could be seen for the genuine sample. This may have been due to the above compound in the fake sample, but the peak was too small to get reliable mass spectral data. Other small peaks could be seen on the 'genuine' chromatogram, but again these were too small to show up on the mass spectral traces. Attempts were therefore made to enlarge these peaks by overloading the column. However, this caused these small peaks to be obscured by neighbouring overloaded peaks.

Cl

FIGURE 39

FIGURE 40

FIGURE 41

YSATIS MASS SPECTROMETRY DATA

YSATIS - GENUINE			YSATIS - FAKE	
M.S. Retention time	GC/MS Best Hit		M.S. Retention time	GC/MS Best hit
14.701	Acetic acid, phenyl methyl ester		14.367	Acetic acid, phenyl methyl ester
16.634	3,7-dimethyl-6-octen-1-ol		17.100	1.6-octadien-3-ol-3,7-dimethyl-2-aminobenzoate
17.268	3,7-dimethyl-2-amonobenzoate-1,6-octdien-3-ol		18.150	7-hydroxy-3,7-dimethyl octanal
18.618	7-hydroxy-3,7-dimethyloctanal		19.484	Benzoic acid, 2-amino-methyl ester
19.667	Benzoic acid, 2-amino methyl ester		26.170	1,2-benzenedicarboxylic acid, diethyl ester
20.200	2-methoxy-4-(1-propenyl)-phenol		29.554	2-(phenylmethylene)-octanal
21.618	4,11,11-trimethyl-8-methylene-1-bicyclo 7.2.0 undec-4-ene		29.870	1H-cycloprop E azulene, decahydro-1,1,7-trimethyl-4-methylene
23.985	3,7,11-trimethyl-1,3,6,10-dodecatetraene		32.037	1-(1,1-dimethylethyl)-3,5-dimethyl-2,4,6-trinitrobenzene
26.835	Phenol, 2-methoxy-4-(2-propenyl)acetate		34.454	1-4-(1,1-dimethylethyl)-2,6-dimethyl-3,5-dinitrophenyl ethanone
34.619	1-4-(1,1-dimethylethyl)-2,6-dimethyl-3,5-dinitrophenyl ethanone			

TABLE 26

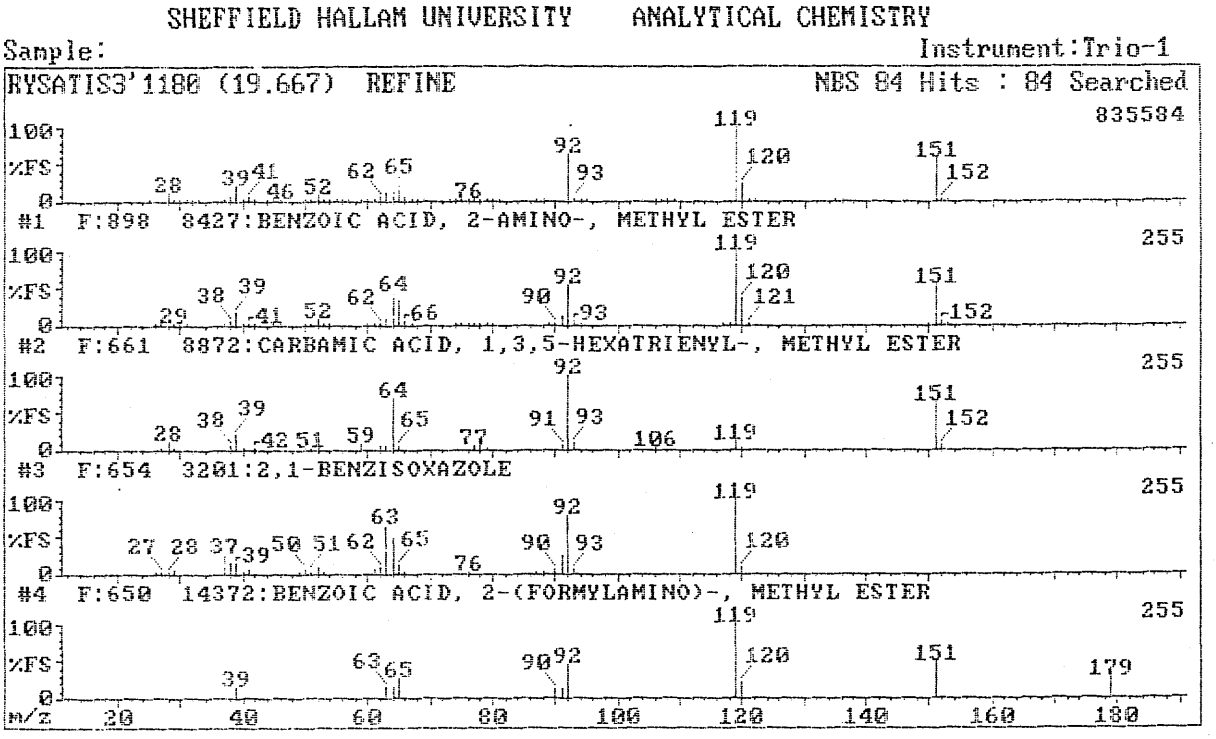
SHEFFIELD HALLAM UNIVERSITY ANALYTICAL CHEMISTRY
Sample:
Instrument:Trio-1
RYSATIS3'1180 (19.667) REFINE
NBS 84 Hits : 84 Searched
#1 F:898 8427:BENZOIC ACID, 2-AMINO-, METHYL ESTER
#2 F:661 8872:CARBAMIC ACID, 1,3,5-HEXATRIENYL-, METHYL ESTER
#3 F:654 3201:2,1-BENZISOXAZOLE
#4 F:650 14372:BENZOIC ACID, 2-(FORMYLAMINO)-, METHYL ESTER
%FS
m/z

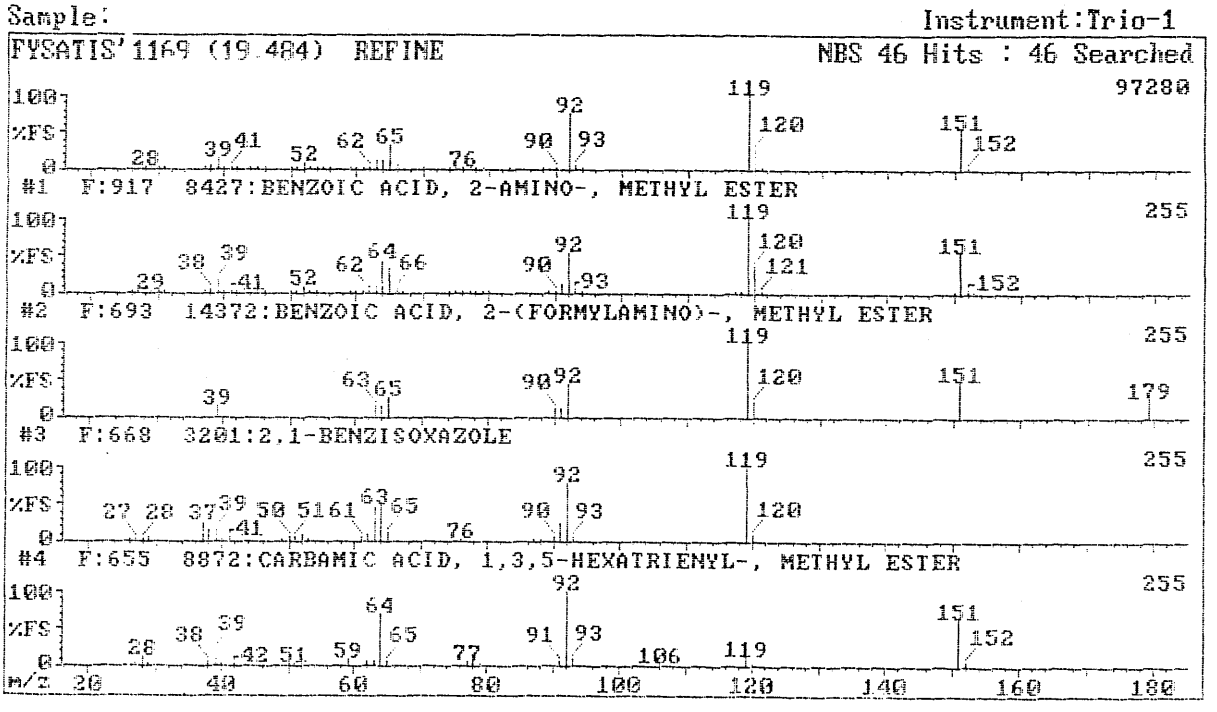
SHEFFIELD HALLAM UNIVERSITY ANALYTICAL CHEMISTRY
Sample:
Instrument:Trio-1
FYSATIS'1169 (19.484) REFINE
NBS 46 Hits : 46 Searched
#1 F:917 8427:BENZOIC ACID, 2-AMINO-, METHYL ESTER
#2 F:693 14372:BENZOIC ACID, 2-(FORMYLAMINO)-, METHYL ESTER
#3 F:668 3201:2,1-BENZISOXAZOLE
#4 F:655 8872:CARBAMIC ACID, 1,3,5-HEXATRIENYL-, METHYL ESTER
%FS
m/z

FIGURE 42

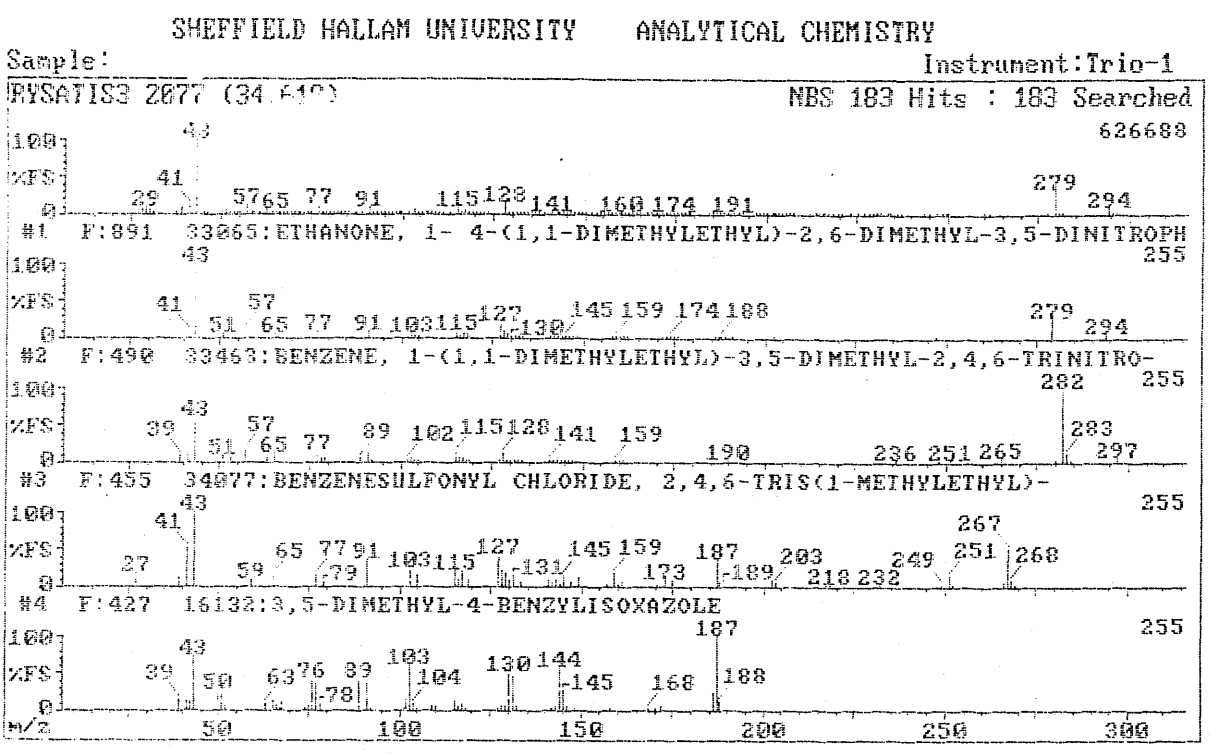
SHEFFIELD HALLAM UNIVERSITY ANALYTICAL CHEMISTRY
Sample:
Instrument:Trio-1
FYSATIS3 2077 (34.640)
NBS 183 Hits : 183 Searched
#1 F:891 33065:ETHANONE, 1- 4-(1,1-DIMETHYLETHYL)-2,6-DIMETHYL-3,5-DINITROPH
#2 F:490 33463:BENZENE, 1-(1,1-DIMETHYLETHYL)-3,5-DIMETHYL-2,4,6-TRINITRO-
#3 F:455 34077:BENZENESULFONYL CHLORIDE, 2,4,6-TRIS(1-METHYLETHYL)-
#4 F:427 16132:3,5-DIMETHYL-4-BENZYLISOXAZOLE
%FS
m/z

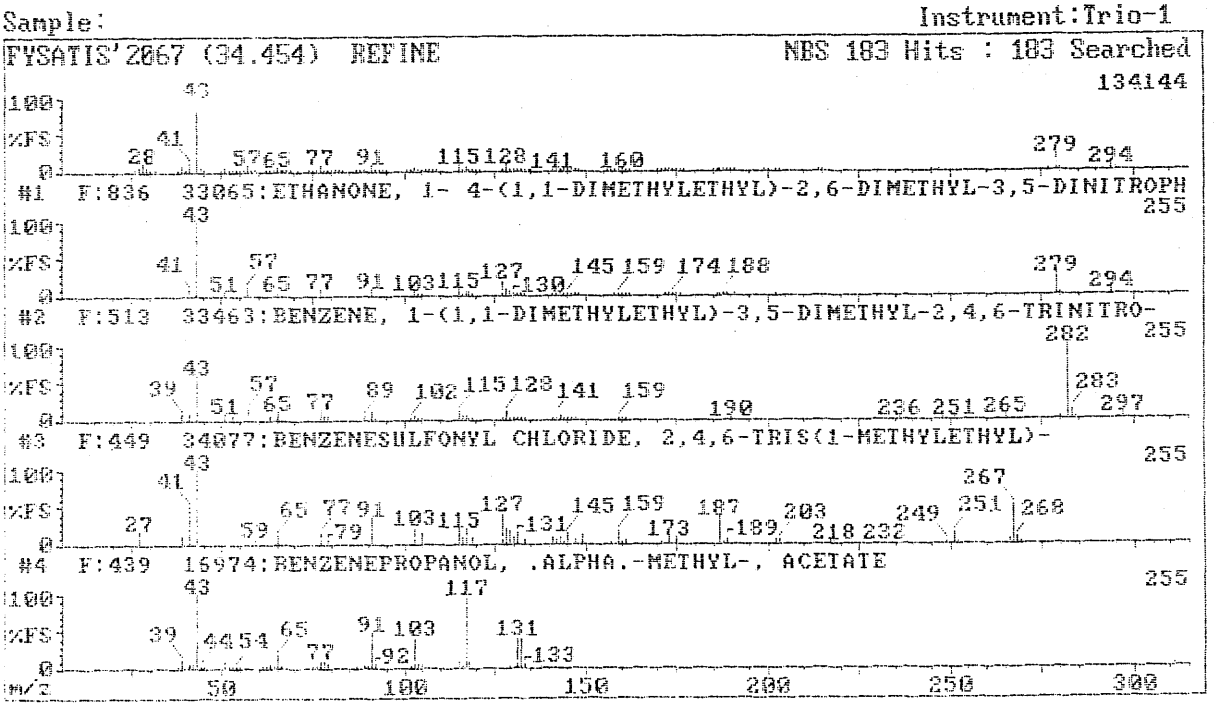
SHEFFIELD HALLAM UNIVERSITY ANALYTICAL CHEMISTRY
Sample:
Instrument:Trio-1
FYSATIS'2067 (34.454) REFINE
NBS 183 Hits : 183 Searched
#1 F:836 33065:ETHANONE, 1- 4-(1,1-DIMETHYLETHYL)-2,6-DIMETHYL-3,5-DINITROPH
#2 F:513 33463:BENZENE, 1-(1,1-DIMETHYLETHYL)-3,5-DIMETHYL-2,4,6-TRINITRO-
#3 F:449 34077:BENZENESULFONYL CHLORIDE, 2,4,6-TRIS(1-METHYLETHYL)-
#4 F:439 16974:BENZENEPROPANOL, .ALPHA.-METHYL-, ACETATE
%FS
m/z

FIGURE 43

4.3 Chanel No 5

A 'genuine' and two 'fake' samples of Chanel No 5 were analysed by GC-AED and GC-MS. One of the fakes was an alcohol based sample (fake #1) and one was a more viscous possibly glycol based sample (fake #2). The carbon channel chromatograms for the genuine perfume (Figure 44) and fake #1 (Figure 45) were similar. The chromatogram for fake #2 (Figure 46), however, was not very well resolved in places.

No sulphur containing compounds were found in the perfumes, but a chlorine containing compound was present in the genuine sample. However, this peak was very small on the mass spectral chromatograms and no chlorine containing match was given for this peak.

As the chromatograms show, all three samples contained both oxygen and nitrogen compounds. The mass spectral library was again used to try to match up these compounds (see Table 27).

The genuine perfume had a nitrogen containing component at RT 31.504 which was found to be 1-(1,1-dimethylethyl)-2-methoxy-4-methyl-3,5-dinitrobenzene (858) (Figure 47). This compound was not seen in the two other samples. The second nitrogen-containing peak in the genuine sample at RT 34.619 was given as 1, 4-(1,1-dimethylethyl)-2,6-dimethyl-3,5-dinitrophenylethanone (903) (Figure 48). This compound was also found to be the major nitrogen containing compound in the fake #1 sample at RT 34.602 (Figure 49), and was present in both Ysatis samples as well.

The smaller peak seen on the nitrogen channel for fake #1 at RT 23.652 was shown to be 7-(2,4-dinitrophenoxy)-2,3-dihydro-2,2-dimethylbenzofuran. The

RT here was similar to that of 2-amino benzoate which was present in both Ysatis samples. The mass spectral match for this peak in fake #1 could therefore be erroneous.

The mass spectral results for fake #2 were disappointing. The RT of the one nitrogen-containing compound corresponded to 1,4-(1,1-dimethylethyl)-2,6-dimethyl-3,5-dinitrophenylethanone seen in both the other Chanel samples. However, the mass spectral hits for this peak in fake #2 showed it to be due to nitric acid, 2-methylpropyl ester. This mass spectral identification could again be erroneous.

j#

ru ~ **FIGURE 44**

FIGURE 45

FIGURE 46

!LG)

TT	XT	T	TT	0
u	U	Li	LJ	0
0	0	0	0	0
I	l	■	■	0
ID	TT	n	a i	-rH

CHANEL MASS SPECTROMETRY DATA

CHANEL - GENUINE			CHANEL - FAKE#1	
M.S. Retention Time	GC/MS Best Hits		M.S Retention Time	GC/MS Best Hits
12.401	3,7-dimethyl-1,6-octandien-3-ol		12.367	3,7-dimethyl-1,6-octandien-3-ol
14.334	Acetic acid, phenylmethyl ester		14.250	Acetic acid, phenylmethyl ester
22.435	2H-1-benzopyran-2-one		18.235	7-hydroxy-3,7-dimethyloctanal
26.352	1,2-benzenedicarboxylic acid, diethyl ester		23.652	7-(2,4-dinitrophenoxy)-2,3-dihydro-2,2-dimethylbenzofuran
28.002	5-(2,3-dimethyltricyclo 2.2.1.02,6 hept-3-yl)-2-penten-1-ol		34.602	1,4-(1,1-dimethylethyl)-2,6-dimethyl-3,5-dinitrophenylethanone
31.504	1-(1,1-dimethylethyl)-2-methoxy-4-methyl-3,5-dinitrobenzene			
34.619	1,4-(1,1-dimethylethyl)-2,6-dimethyl-3,5-dinitrophenyl ethanone			

TABLE 27

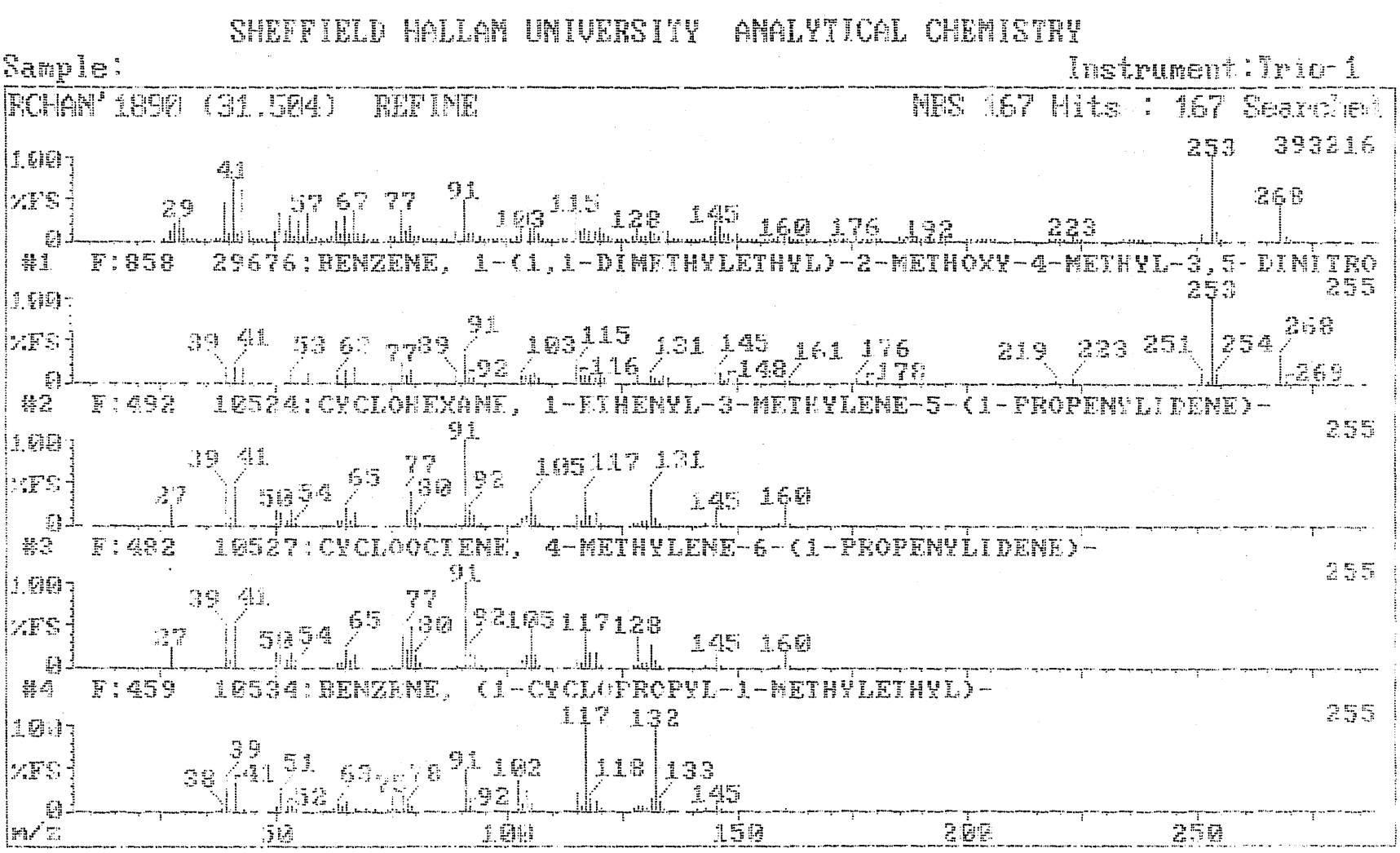
SHEFFIELD HALLAM UNIVERSITY ANALYTICAL CHEMISTRY
Sample:
Instrument:Trio-1
RCHAN'1890 (31.504) REFINE
NBS 167 Hits : 167 Searched
#1 F:858 29676:BENZENE, 1-(1,1-DIMETHYLETHYL)-2-METHOXY-4-METHYL-3,5-DINITRO
#2 F:492 10524:CYCLOHEXANE, 1-PHENYL-3-METHYLENE-5-(1-PROPENYLIDENE)-
#3 F:482 10527:CYCLOOCTENE, 4-METHYLENE-6-(1-PROPENYLIDENE)-
#4 F:459 10534:BENZENE, (1-CYCLOPROPYL-1-METHYLETHYL)-
M/Z

FIGURE 47

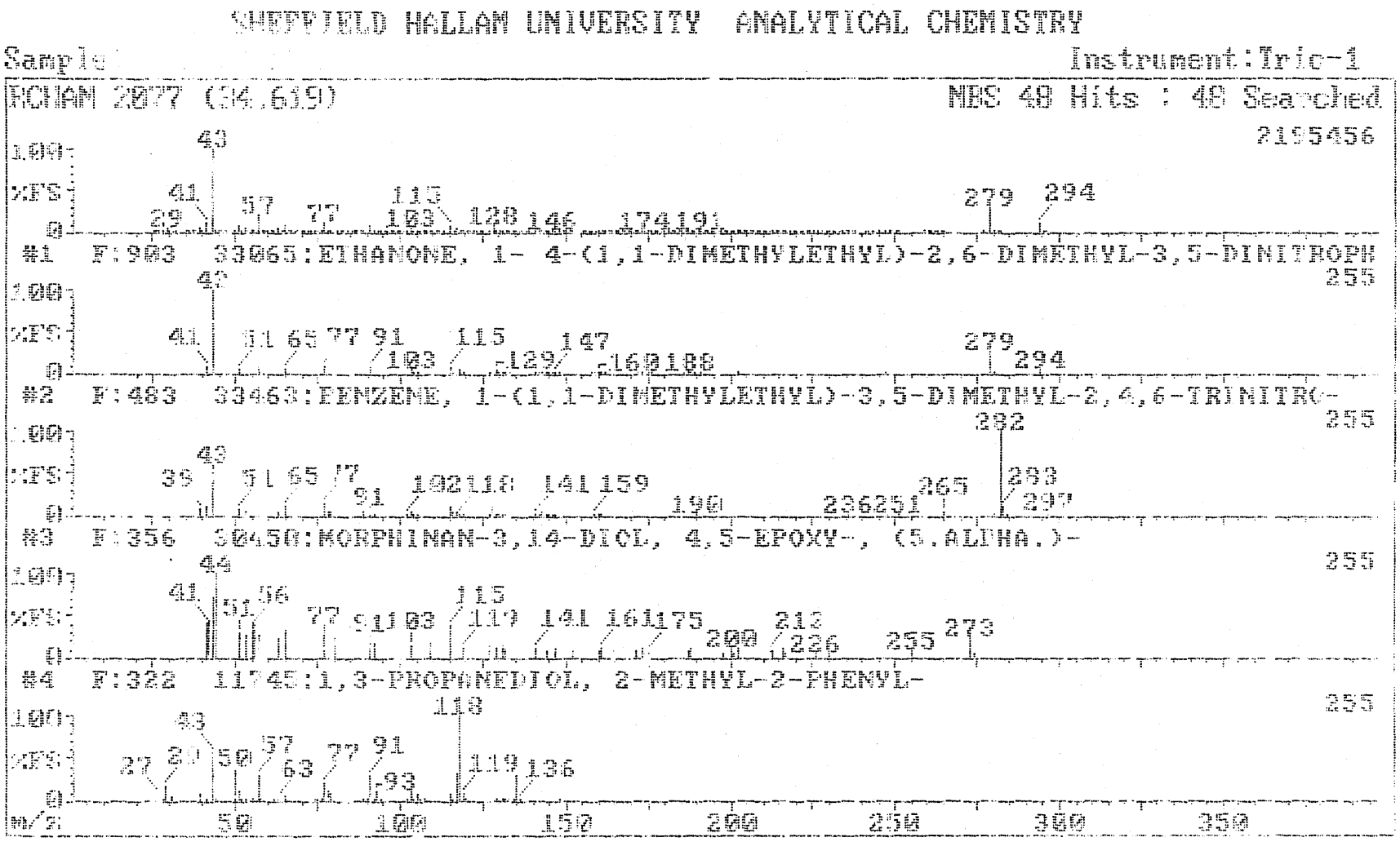
SHEFFIELD HALLAM UNIVERSITY ANALYTICAL CHEMISTRY
Sample
Instrument:Trio-1
RONAN 2877 (34.619)
NBS 49 Hits : 49 Searched
#1 F:903 33065:ETHANONE, 1- 4-(1,1-DIMETHYLETHYL)-2,6-DIMETHYL-3,5-DINITROPH
#2 F:483 33463:BENZENE, 1-(1,1-DIMETHYLETHYL)-3,5-DIMETHYL-2,4,6-TRINITRO-
#3 F:356 30450:MORPHINAN-3,14-DIOL, 4,5-EPOXY-, (5.ALPHA.)-
#4 F:322 11745:1,3-PROPANEDIOL, 2-METHYL-2-PHENYL-
m/z

FIGURE 48

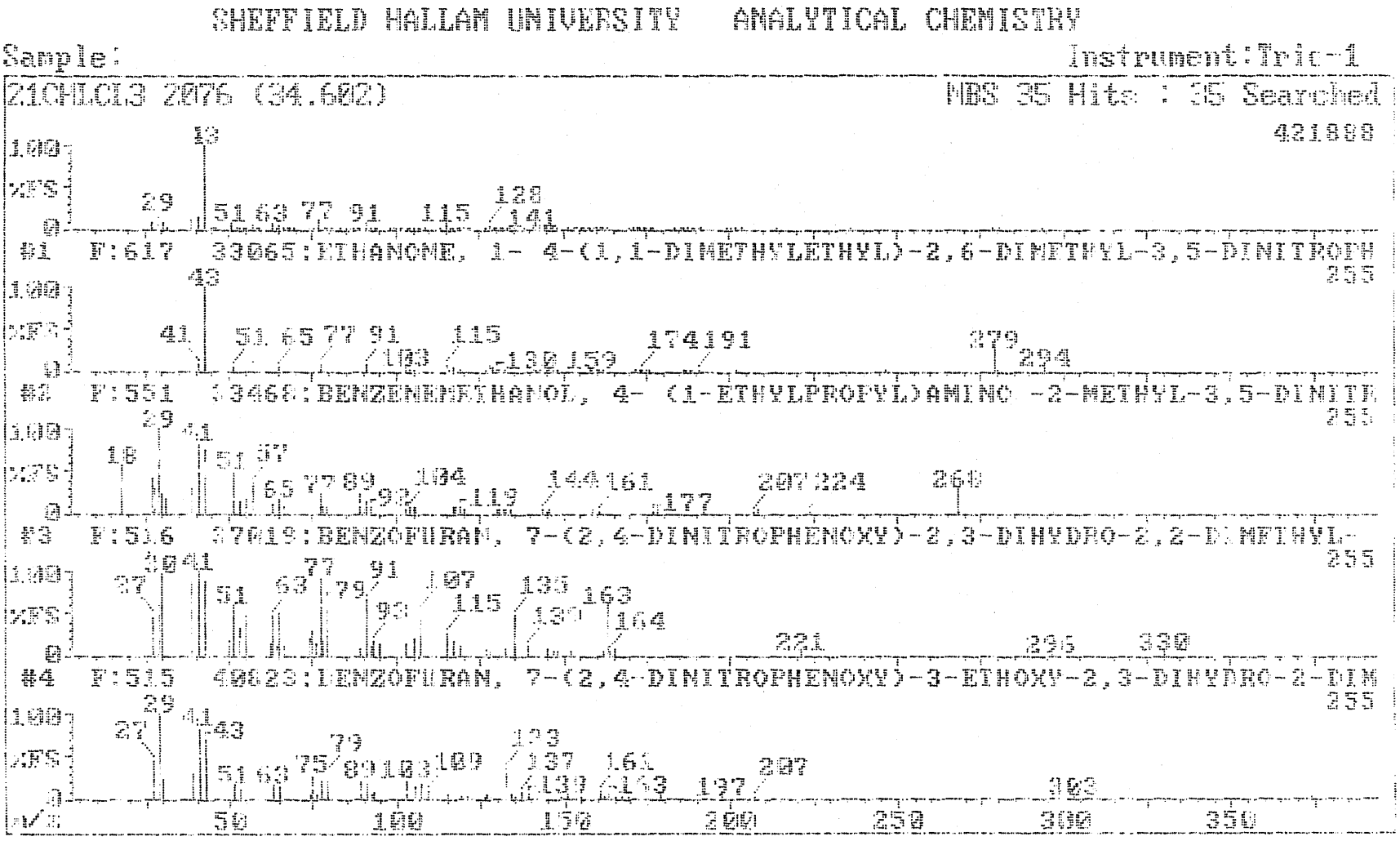
SHEFFIELD HALLAM UNIVERSITY ANALYTICAL CHEMISTRY
Sample:
Instrument:Trio-1
Z1CHLCI3 2076 (34.602)
NBS 35 Hits : 35 Searched
421888
#1 F:617 33065:KIHANONE, 1- 4-(1,1-DIMETHYLETHYL)-2,6-DIMETHYL-3,5-DINITROPH
255
#2 F:551 13468:BENZENEMETHANOL, 4- (1-ETHYLPROPYL)AMINO -2-METHYL-3,5-DINITR
255
#3 F:516 37019:BENZOFURAN, 7-(2,4-DINITROPHENOXY)-2,3-DIHYDRO-2,2-DIMETHYL-
255
#4 F:515 40623:BENZOFURAN, 7-(2,4-DINITROPHENOXY)-3-ETHOXY-2,3-DIHYDRO-2-DIM
255
%FS
m/z
50
100
150
200
250
300
350

FIGURE 49

4.4 Paco Rabanne

Paco Rabanne is a men's aftershave produced by the Paco Rabanne perfume house. A genuine and a fake sample were analysed by GC-AED and GC-MS (Figures 50 and 51).

Unfortunately the mass spectral data did not give many good matches for the samples. However, one reasonably good match was for 3,7-dimethyl-1,6-octandien-3-ol-2-aminobenzoate which was found by the mass spectrometer to be in both the genuine and the fake sample. However, the AED data showed that no nitrogen-containing compounds were present in either sample. The mass spectral library was therefore giving misleading information. When the results for the other perfumes were checked, it was found that the above compound has also been incorrectly matched to peaks in all but one of the samples. Therefore, without the AED results, incorrect assumptions could have been made about the content of the samples.

The AED could therefore be used to identify peaks of interest prior to analysis by mass spectrometry study.

CHAPTER 5

SULPHUR TRACE ANALYSIS

5.0 Analysis of Pre- and Post-Catalytic Refinery Streams

The samples analysed were light hydrocarbons from pre- (Figure 52) and post-catalytic (Figure 53) refinery streams. The catalytic process involved was desulphurisation. Each sample was compared to a mixed standard of benzene and toluene.

It was initially thought that only one sulphur containing compound was present in the pre-catalytic stream, this being thiophene. However, as the sulphur chromatogram for the 'before' sample shows, two other sulphur containing compounds were present in small quantities (Figure 54). It was thought that these compounds may have been dimethyl/ethyl thiophenes. As the chromatograms show, the catalytic process was successful in removing sulphur containing components of the refinery stream.

The sulphur chromatograms shown here are also a good illustration of the use of 'backamount' adjustments. The 'backamount' is the amount of the background chromatogram which is subtracted from the sample chromatogram to correct for interference peaks. Each element has its own value for the backamount which is set in the elements matched filter. The AED software allows the operator to adjust the backamount figure. This adjustment becomes necessary if negative peaks are present, as can be seen on the 'before' sulphur chromatogram (Figure 55). The two plots are of the sulphur channel before and after backamount adjustment. In this case, the backamount was too high, ie too much background was being subtracted, resulting in the negative peaks. When the backamount value was reduced, the amount of background subtracted was reduced, giving a flat baseline where the negative peaks were.

FIGURE 52

FIGURE 53

FIGURE 54

FIGURE 55

The pre-catalytic sample showed three unknown sulphur containing compounds, two of which were eluted with toluene. The next step was therefore to try to identify these unknown compounds which were thought to be methyl/ethyl thiophenes.

Three samples of the post-catalytic sample were spiked with 2-methyl, 3-methyl and ethyl thiophene. The spiked samples were then run and compared to pre-catalytic sample. Each sample was analysed for carbon, sulphur and oxygen. The following colour plot (Figure 56) shows the sulphur channel of the pre-catalytic sample and the three samples spiked with 100ppm 2-methyl, 3-methyl and ethyl thiophene.

The retention times of 2 and 3-methyl thiophene correspond to the two peaks seen at approximately 10 minutes on the pre-catalytic sample. The retention time for ethyl thiophene corresponds to another peak at approximately 19.5 minutes.

c ∞ ∞

∞

FIGURE 56

6.1 Introduction

One of the most often replaced parts of the AED is the discharge tube. As described earlier several features have been incorporated into the system to help prolong the life-time of the discharge tube, such as the use of reagent gases and solvent venting. However one of these features, the water cooling system, can itself cause problems when the discharge tube breaks.

As the diagram of the cavity shows (Figure 57a), the discharge tube is surrounded by a water jacket which cools the quartz tube by dissipating excess heat. The discharge tube effectively seals the water flow, preventing it from coming into contact with other parts of the cavity. However if the tube breaks or cracks, the seal is broken and the water is pumped through the gas lines. The water pump keeps going until it can no longer maintain the required flow rate. The flow rate only falls however when the water bath is empty, the water having been pumped round the entire system.

When this happens the gas lines must be blown dry, and the air-filter dried or replaced. Occasionally the discharge tube shatters producing small fragments of glass which are then carried around the system by the water. There have been two instances here when these tiny pieces of glass have lodged in the gas gauges and water pump. Unfortunately the glass could not be removed and the parts had to be replaced.

Regular maintenance can overcome these problems to a certain extent, but unforeseen breakages can still occur.

One way of minimising any damage done when a discharge tube breaks would be to incorporate a sensor into the water system. This could be built into the side of the water bath as shown in Figure 58, and connected to the pump. If the discharge tube broke, and the subsequent leak caused the water in the bath to

drop below a pre-determined level, the sensor could detect this and disable the pump, preventing water and broken glass being carried through the system.

The addition of a sensor would stop the bulk of the damage, but some water would still enter the system before the sensor disabled the pump. Two water traps could therefore be added to the cavity as shown in Figure 57b. These would lie in the path of the water flow. If the discharge tube broke the traps could stem the flow until the sensor disabled the pump.

We have also had problems with the gas union. As the diagram of the cavity shows (Figure 57a), three gas lines lead off from the main body of the gas union. On a previous occasion, one of these lines has broken at the attachment to the gas union. At this time the weld broke completely on one of the lines, and those on the other two lines cracked. It was thought that the welds may have been weakened by the cooling/reheating of the cavity which occurs when columns or discharge tubes are changed.

The gas lines are welded flush with the wall of the gas union. The welds would perhaps be stronger if the gas lines protruded slightly into the union. The wall of the gas line could therefore be welded rather than the edge, forming a stronger weld. Another possibility could be to have a screw-thread on the end of the gas lines. If a line cracked a new one could just be screwed in, rather than having to replace the whole gas union.

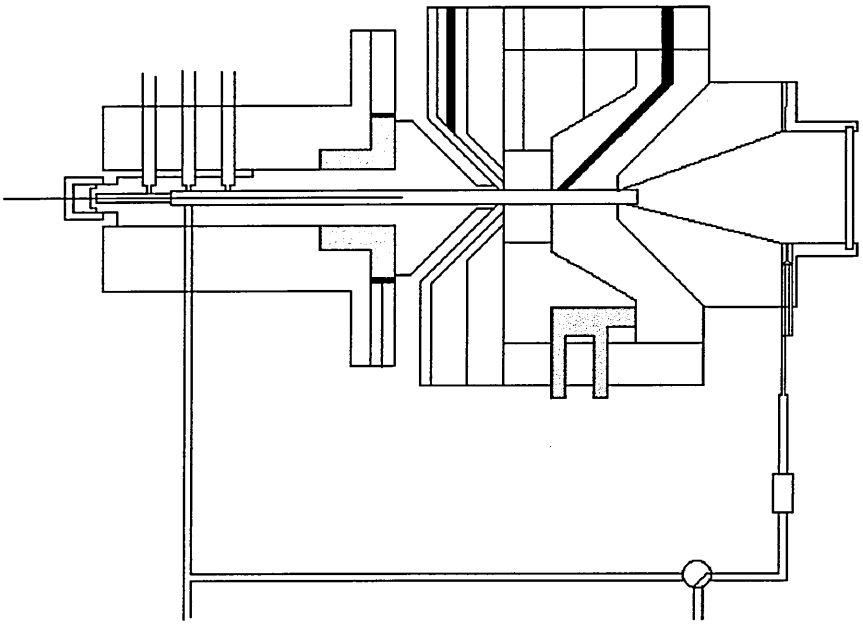

REENTRANT CAVITY
FIGURE 57a

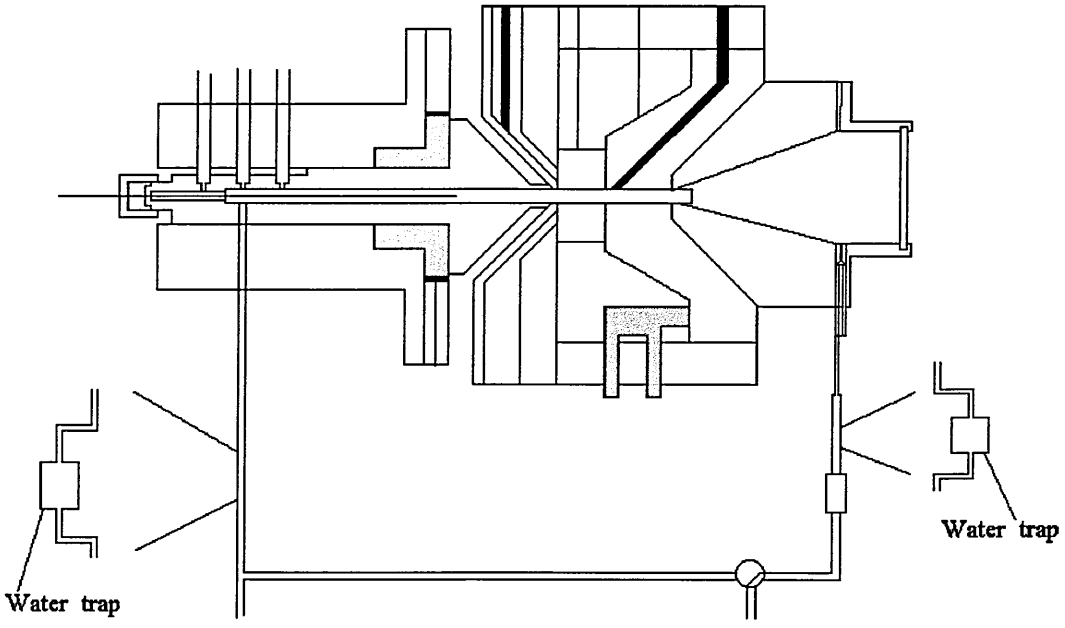

MODIFIED REENTRANT CAVITY
FIGURE 57b

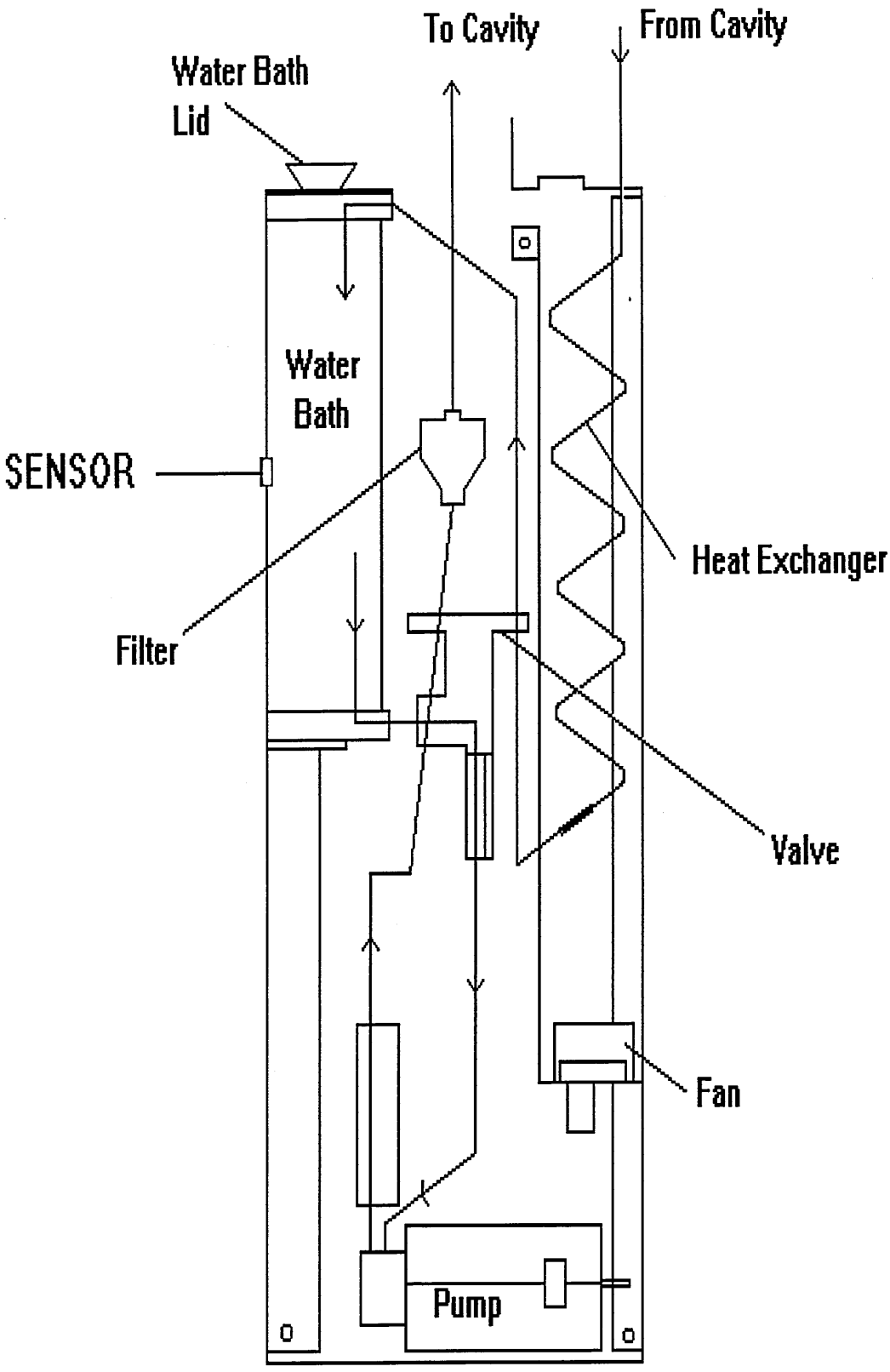
To Cavity
From Cavity
Water Bath
Lid
Water
Bath
SENSOR
Heat Exchanger
Filter
Valve
Fan
Pump

FIGURE 58

6.2 Reproducibility

Another operational problem was encountered when doing repeat injections. Low relative standard deviations (RSDs) were expected when using a fully automated system, as there is little or no opportunity for operator error.

However, when five repeat injections were made of a hydrocarbon mixed standard covering the concentration range 1 x 10^{-5} - 5 x 10^{-4}M, RSDs of between 6.6 and 12.6 were obtained (Table 28). Plots were constructed for each compound in the mix, ie Figure 59a shows the five injections of bibenzyl. The plots show that injections 1 and 4 give the closest results. As the tables show, the RSDs do not appear to increase with concentration, although the spread of the points on the graphs looks larger at the highest concentration.

The RSDs of the chloroanisole (Table 29) and barbiturate (Table 30) mixes are also shown. Overall, the values are higher than would be preferred for a fully automated technique. The oxygen responses are the worst, the RSD being much more random than for other elements. The values range from 3.1 to 16.7 for the chloroanisoles, and 3.0 to 16.4 for the barbiturates. No discernible pattern can be seen in the oxygen responses.

However, the RSDs of carbon and chlorine in the chloroanisoles are worst at the highest concentrations. This is also the case with the carbon and nitrogen responses of the barbiturates.

HYROCARBON MIX
RSD^ of Carbon Responses

	lxlO-5	5xl0"5	10-4	2xl0-4	5xl0-4
Bibenzyl	10.3	6.6	7.7	9.29	9.1
Diphenyl-ethylene	9.7	6.6	7.8	9.15	8.7
c-Stilbene	9.9	6.6	7.3	8.7	8.8
Diphenyl-acetylene	12.1	6.8	7.9	9.7	10.3
t-Stilbene	12.6	6.7	7.9	9.9	10.7

TABLE 28

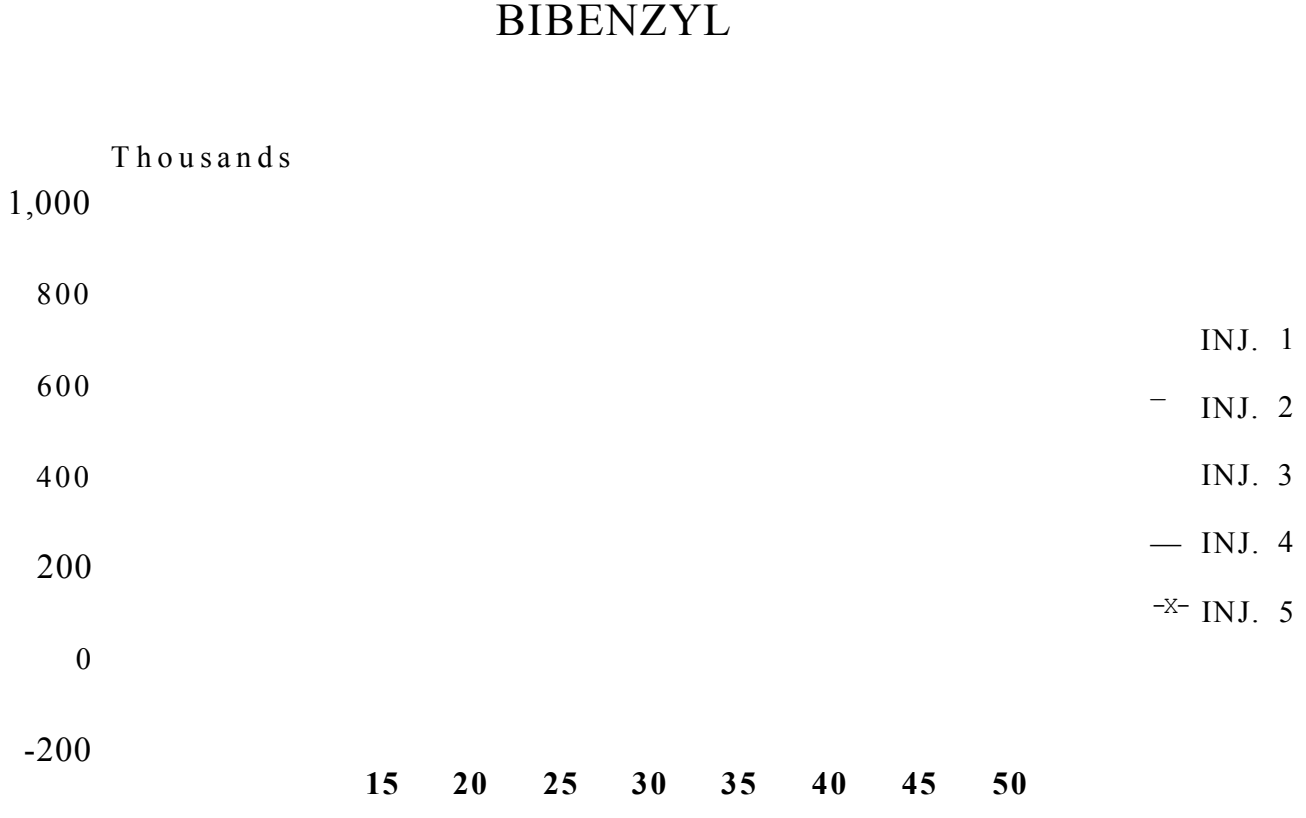

FIGURE 59a

FIGURE 59b

trans-STILBENE

FIGURE 59c

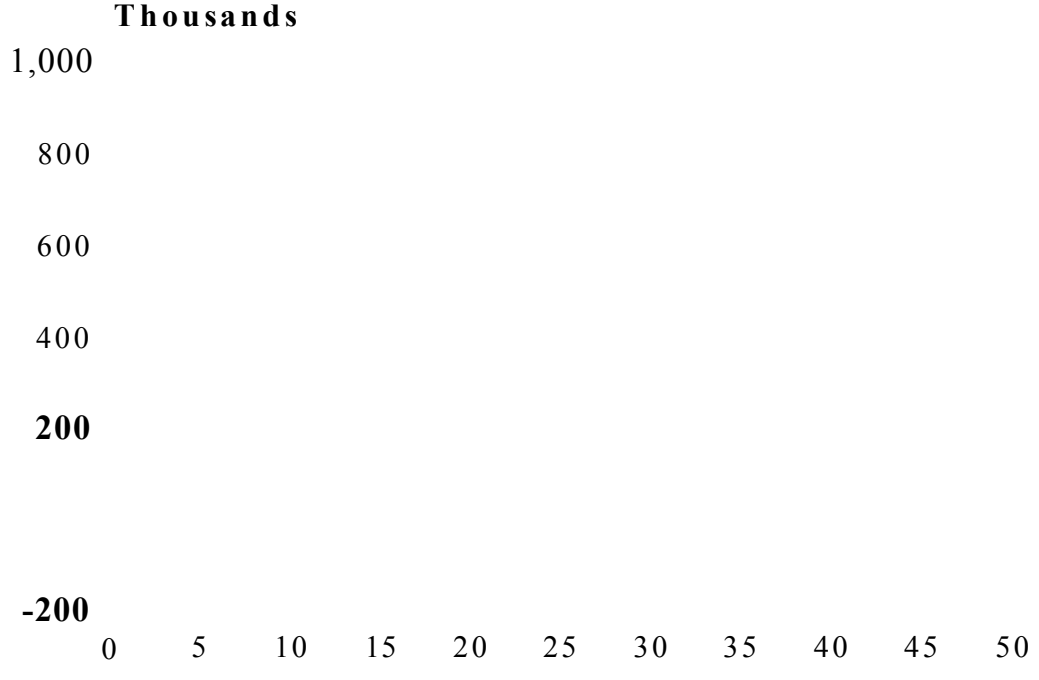

FIGURE 59d

DIPHENYLACETYLENE

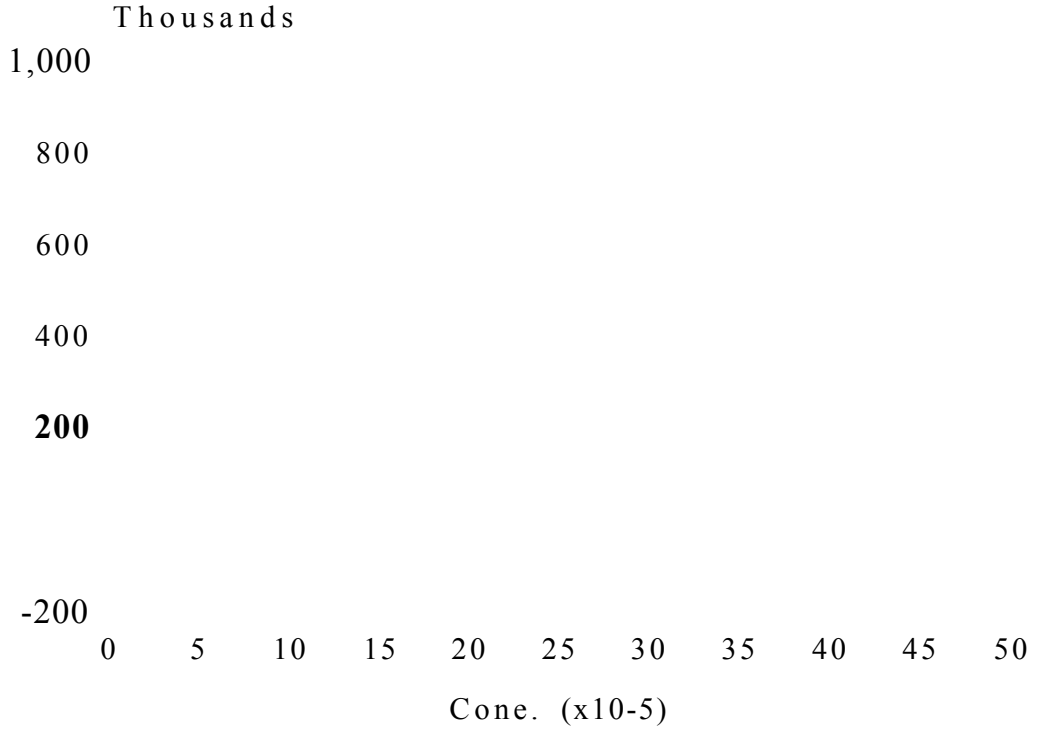

FIGURE 59e

CHLOROANISOLE MIX

RSD's of Carbon Responses

	$5x10^{-5}$	$1x10^{-4}$	$2x10^{-4}$	$5x10^{-4}$	$1x10^{-3}$
3,	7.2	8.3	9.0	5.4	11.3
4,	7.3	8.5	8.9	5.3	11.2
2,	7.2	8.3	9.1	5.4	11.3
2,6,	7.4	8.9	8.6	5.2	11.0
3,5,	7.6	9.5	8.1	5.5	10.8
2,5,	7.6	9.6	7.9	5.8	11.5
2,4,	7.7	9.6	7.9	5.3	9.9
2,3,	7.8	9.8	7.7	5.9	10.7
2,3,6,	7.9	10.4	7.2	5.7	10.3
2,3,4,	8.4	11.6	5.9	5.6	9.7
2,3,4,5,	9.0	13.0	4.6	5.4	8.8

RSD's of Oxygen Responses

	$5x10^{-5}$	$1x10^{-4}$	$2x10^{-4}$	$5x10^{-4}$	$1x10^{-3}$
3,	3.1	11.4	14.8	9.5	5.5
4,	11.5	10.7	11.9	9.8	5.6
2,	7.8	15.5	4.1	11.7	5.4
2,6,	11.9	9.4	12.7	11.0	5.4
3,5,	12.9	13.6	11.9	10.7	5.2
2,5,	16.4	10.0	5.4	6.4	5.8
2,4,	20.5	7.5	8.1	8.0	4.4
2,3,	11.1	6.9	10.8	12.4	4.4
2,3,6,	13.8	11.0	7.4	10.9	6.0
2,3,4,	6.1	6.3	19.4	13.3	5.5
2,3,4,5,	16.7	14.7	10.9	13.2	5.0

RSD's of Chlorine Responses

	$5x10^{-5}$	$1x10^{-4}$	$2x10^{-4}$	$5x10^{-4}$	$1x10^{-3}$
3,	5.7	7.9	5.7	11.6	11.0
4,	5.1	5.0	5.4	11.7	11.1
2,	2.6	6.7	5.7	11.5	11.1
2,6,	3.6	6.2	5.2	11.8	11.7
3,5,	3.7	7.0	5.2	11.6	12.1
2,5,	4.5	6.2	5.3	11.7	13.1
2,4,	5.2	5.7	5.3	11.2	12.0
2,3,	5.2	6.2	5.1	11.2	12.8
2,3,6,	4.8	5.9	5.5	11.0	13.1
2,3,4,	4.1	6.4	5.6	10.1	13.9
2,3,4,5,	5.8	6.8	6.4	9.0	14.5

TABLE 29

AZOBENZE/BARBITURATE MIX.

RSD's of Carbon Responses

	$5x10^{-5}$	$1x10^{-4}$	$2x10^{-4}$	
Azobenzene	7.3	8.2	4.0	11.9
Cotinine	7.8	8.7	4.4	14.5
Nicotine	7.7	8.7	4.6	14.9
Caffeine	6.4	8.8	4.7	13.1
Barbital	8.2	8.7	4.8	14.6
Secobarbital	8.1	8.4	4.6	13.7
Pentobarbital	7.7	8.4	4.5	14.6
Lidocaine	6.8	8.0	3.2	10.1

RSD's of Nitrogen Responses

	$5x10^{-5}$	$1x10^{-4}$	$2x10^{-4}$	
Azobenzene	6.2	12.2	4.9	14.9
Cotinine	7.0	12.4	5.4	14.5
Nicotine	6.2	12.6	5.5	15.7
Caffeine	6.9	11.7	4.5	13.3
Barbital	6.7	11.9	5.4	15.0
Secobarbital	7.3	11.2	4.9	13.4
Pentobarbital	6.7	11.9	5.3	14.5
Lidocaine	6.0	11.5	5.2	14.9

RSD's of Oxygen Responses

	$5x10^{-5}$	$1x10^{-4}$	$2x10^{-4}$	
Cotinine	15.7	7.2	9.3	14.0
Caffeine	7.7	5.6	7.7	12.3
Barbital	3.0	4.9	9.9	14.8
Secobarbital	7.0	7.9	7.3	11.2
Pentobarbital	10.3	6.0	7.8	11.9
Lidocaine	16.4	5.3	8.5	12.3

TABLE 30

One possible explanation for the high, random RSDs is that the injector is not reproducibly injecting the desired volume. However if this was the case, elements monitored in the same injection would have the same RSD. Carbon and nitrogen are monitored in the same injection in the barbiturate mix, but depending on concentration, the RSDs for these two elements range from 8.2 to 12.2 for the same injection.

Fluctuations in the plasma itself could also cause variation. Again however if this was the case the RSDs for carbon and nitrogen in the same injection would be similar.

The plasma therefore appears to respond to different elements in different ways. This leads into the compound independence issue discussed previously.

Another factor which may contribute to compound dependence and poor reproducibility is residence time in the plasma. Usually in GC separations peaks are very narrow, eg between 1 - 5 seconds. With AED detection peak widths are routinely between 10 and 20 seconds. This means that the front edge of the peak will spend longer in the plasma. It will therefore be exposed to reagent gases for longer. Obviously, the longer atoms spend in the plasma, the more opportunities exist for recombination or side reactions.

7.1 Conclusions

The GC-AED is a powerful technique for profiling hetero-atom containing compounds in complex matrices, as the results from the refinery samples show. The information provided by the AED is complementary to that proved by GC-MS, therefore the two techniques can be combined to achieve full characterisation of complex mixtures. This is illustrated by the perfume analysis described earlier.

It was found that the response of the AED to some elements is dependent upon the nature of the parent compound from which the element originates. For example, in a group of phenols elemental response appears to be virtually independent of molecular structure for chlorine, but structurally related for both carbon and oxygen. As carbon and oxygen combine to form CO, but chlorine does not undergo the corresponding reaction with either carbon or oxygen it is possible that the relative ease of formation of CO could influence both the carbon and oxygen elemental yields. Support for this conclusion comes from the poor oxygen response in 2-nitrophenol, which could easily generate NO_2 in the plasma, thus inhibiting oxygen yield.

The same effects were seen in a group of nitrogen-containing compounds, where carbon, oxygen and nitrogen responses all showed structure dependence.

The variation in the slopes of calibration lines, the departure from linearity at higher concentrations and the variation in response caused by contamination of the discharge tube support the argument that variation of breakdown pathway and the formation of relatively stable oxygen-containing small molecules in the plasma are responsible for the structure dependence seen.

No such compound dependence was seen for a group of chloroanisoles, indicating that polarity may also effect elemental yield.

Hence the results contained in this thesis refute the major advantage claimed for the atomic emission technique, namely that quantitation may be achieved from the elemental response alone because it is independent of the structure from which the atoms originate.

The choice of internal standard is, therefore, critical for calibration purposes. It is therefore recommended that close structural similarity is used as the primary criteria for selection. This point is clearly illustrated by the similarity of the slopes for pento and secobarbitals.

REFERENCES

1. M. Tswett, *Berichte der deutschen botanischen Gesellschaft*, **24**, (1906), pp 384. (Translation by H. H. Strain and J. Sherma, *Journal of Chemical Education*, **44**, (4), (1967), pp 238-242.)

2. L. S. Ettre, *Analytical Chemistry*, **43**, (14), (1971), pp 20A-31A.

3. A. J. P. Martin and R. L. M. Synge, *Journal of Biochemistry*, **35**, (1941), pp 1358-1368.

4. A. T. James and A. J. P. Martin, *Journal of Biochemistry*, **50**, (1952), pp 679-690.

5. E. R. Adlard, *Chromatographic Society Yearbook*, (1994), pp 21-24.

6. J. J. van Deemter, F. J. Zuiderweg and A. Klinkenberg, *Chemical Engineering Science*, **5**, (1956), pp 271-289.

7. W. H. F. Talbot, *Brewsters Journal of Science*, **5**, (1826), pp 77.

8. G. Kirchhoff and R. Bunsen, *Ann. Chim. Phys.*, **64**, (1862), pp 257.

9. W. Crookes, *Chemistry News*, **3**, (1861), pp 452.

10. W. Ramsey, *Journal of the Chemical Society*, **67**, (1895), pp 1107.

11. R. K. Skogerboe and G. N. Coleman, *Analytical Chemistry*, **48**, (7), (1976), pp 611A-620A.

12. F. C. Fehsenfeld, K. M. Evenson and H. P. Broida, *The Review of Scientific Instruments*, **36**, (3), (1965), pp 294-298.

13. A. T. Zander and G. M. Hieftje, *Applied Spectroscopy*, **35**, (4), (1981), pp 357-371.

14. A. J. McCormack, S. C. Tong and W. D. Cooke, *Analytical Chemistry*, **37**, (12), (1965), pp 1470-1476.

15. C. A. Bache and D. J. Lisk, *Analytical Chemistry*, **37**, (12), (1965), pp 1477-1480.

16. C. A. Bache and D. J. Lisk, *Analytical Chemistry*, **38**, (12), (1966), pp 1757-1758.

17. C. A. Bache and D. J. Lisk, *Analytical Chemistry*, **39**, (7), (1967), pp 786-789.

18. H. A. Moye, *Analytical Chemistry*, **39**, (12), (1967), pp 1441-1445.

19. W. R. McLean, D. L. Stanton and G. E. Penketh, *Analyst*, **98**, (1973), pp 432-442.

20. J. P. J. van Dalen, P. A. de Lezenne Coulander and L. de Galen, *Analytica Chimica Acta*, **94**, (1977), pp 1-19.

21. F. E. Lichte and R. K. Skogerboe, *Analytical Chemistry*, **45**, (2), (1973), pp 399-401.

22. C. I. M. Beenakker, *Spectrochimica Acta*, **31B**, (1976), pp 483-486.

23. C. I. M. Beenakker, *Spectrochimica Acta*, **32B**, (1977), pp 173-187.

24. H. A. Dingjan and H. J. de Jong, *Spectrochimica Acta*, **36B**, (4), (1981), pp 325-331.

25. C. I. M. Beenakker and P. W. J. M. Boumans, *Spectrochimica* Acta, **33B**, (1978), pp 53-54.

26. B. D. Quimby and J. J. Sullivan, *Analytical Chemistry*, **62**, (10), (1990), pp 1027-1034.

27. J. J. Sullivan and B. D. Quimby, *Analytical Chemistry*, **62**, (10), (1990), pp 1034-1043.

28. J. J. Sullivan and B. D. Quimby, *Journal of High Resolution Chromatography*, **12**, (1989), pp 282-286.

29. B. D. Quimby, M. F. Delaney, P. C. Uden and R. M. Barnes, *Analytical Chemistry*, **51**, (7), (1979), pp 875-880.

30. Zeng Ke-Wei , Ou Qing-Yu, Wang Guo-Chuen and Yu Wei-Lu, *Spectrochimica Acta*, **40B**, (1/2), (1985), pp 349-356.

31. B. D. Quimby, V. Giarrocco, J. J. Sullivan and K. A. McCleary, *Journal of High Resolution Chromatography*, **15**, (1992), pp 705-709.

32. J. J. Kosman and R. G. Lukco, *Journal of Chromatographic Science*, **31**, (1993), pp 88-94.

33. B. D. Quimby, P. C. Dryden and J. J. Sullivan, *Journal of High Resolution Chromatography*, **14**, (1991), pp 110-116.

34. S. A. Estes, P. C. Uden and R. M. Barnes, *Analytical Chemistry*, **54**, (1982), pp 2402-2405.

35. P. L. Wylie and B. D. Quimby, *Journal of High Resolution Chromatography*, **12**, (1989), pp 813-818.

36. R. Lobinski and F. C. Adams, *Analytica Chimica Acta*, **262**, (1992), pp 285-297.
37. R. Lobinski, W. M. R. Dirkx, M. Ceulemans and F. C. Adams, *Analytical Chemistry*, **64**, (1992), pp 159-165.

38. F. David and P. Sandra, *Application Note* 228-XXX.

39. B. F. Scott, Y. K. Chau and A. Rais-Firouz, *Applied Organometallic Chemistry*, **5**, (1991), pp 151-157.

40. K. B. Olsen, D. S. Sklarew and J. C. Evans, *Spectrochimica Acta*, **40B**, (1/2), (1985), pp 357-365.

41. E. Bulska and P. Tschopel, *Analytica Chimica Acta*, **271**, (1993), pp 171-181.

42. P. L. Wylie and R. Oguchi, *Journal of Chromatography*, **517**, (1990), pp 131-142.

43. Qinhan Jin, Fendi Wang, Chu Zhu, D. M. Chambers and G. M. Hieftje, *Journal of Analytical Atomic Spectrometry*, **5**, (1990), pp 487-494.

44. G. K. Webster and J. W. Carnahan, *Analytical Chemistry*, **64**, (1992), pp 50-55.

45. P. K. K. Louie, R. C. Timpe, S. B. Hawthorne and D. J. Miller, *Fuel*, **72**, (1993), pp 225-231.

46. Y. Liu, V. Lopez-Avila, M. Alcaraz and W. F. Beckert, *Journal of High Resolution Chromatography*, **16**, (1993), pp 106-112.

47. Y. Liu and V. Lopez-Avila, *Journal of High Resolution Chromatography*, **16**, (1993), pp 717-720.

48. R. Oguchi, A. Shimizu, S. Yamashita, K. Yamaguchi and P. Wylie, *Journal of High Resolution Chromatography*, **14**, (1991), pp 412-416.

49. S. Rowland, R. Evens, L. Ebdon and A. Rees, *Analytical Proceedings*, **30**, (1993), pp 87-88.

50. Huang Yie-ru, Ou Qingyu, Yu Wei-Le, *Journal of Chromatographic Science*, **28**, (1990), pp 584-588.

51. Huang Yie-ru, Ou Qingyu, Yu Wei-Le, *Journal of Analytical Atomic Spectrometry*, **5**, (1990), pp 115-120.

52. J. Th. Jelink and A. Venema, *Journal of High Resolution Chromatography*, **13**, (1990), pp 447-450.

53. S. Pedersen-Bjergaard, T. Norman Asp and T. Greibrokk, *Journal of High Resolution Chromatography*, **15**, (1992), pp 89-93.

54. A. L. P. Valente and P. C. Uden, *Analyst*, **115**, (1990), pp 525-529.

55. M. J. Perpall and P. C. Uden, *Spectrochimica Acta*, **42B**, (1/2), (1987), pp 243-251.

56. N. Kovacic and T. L. Ramus, *Journal of Analytical Atomic Spectrometry*, **7**, (1992), pp 999-1005.

57. P. L. Wylie, J. J. Sullivan and B. D. Quimby, *Journal of High Resolution Chromatography*, **13**, (1990), pp 499-506.

58. M. Zerezghi, K. J. Mulligan and J. A. Caruso, *Journal of Chromatographic Science*, **22**, (1984), pp 348-352.

59. D. B. Hooker and J. de Zwann, *Analytical Chemistry*, **61**, (1989), pp 2207-2211.

60. B. D. Quimby, P. C. Dryden and J. J. Sullivan, *Analytical Chemistry*, **62**, (22), (1990), pp 2509-2512.

61. D. Deruaz, A. Bannier, M. Desage and J. L. Brazier, *Analytical Letters*, **24** (9), (1991), pp 1531-1543.

62. Y. Zeng, J. A. Seeley, T. M. Dowling, P. C. Uden, M. Y. Khuhawar, *Journal of High Resolution Chromatography*, **15**, (1992), pp 669-676.

63. M. Y. Khuhawar, A. Sarafraz-Yazdi and P. C. Uden, *Journal of Chromatography*, **636**, (1993), pp 271-276.

64. H. Emteborg, N. Hadgu and D. C. Baxter, *Journal of Analytical Atomic Spectrometry*, **9**, (1994), pp 297-302.

65. D. L. Haas and J. A. Caruso, *Analytical Chemistry*, **56**, (1984), pp 2014-2019.

66. M. Cooke, D. A. Leathard, C. Webster and V. Rogerson, *Journal of High Resolution Chromatography*, **16**, (1993), pp 660-662.

67. A. Gelencser, J. Szépvolgyi and J. Hlavay, *Journal of Chromatography A*, **654**, (1993), pp 269-277.

68. F. David and P. Sandra, *LC-GC*, **5**, (12), (1992), pp 22-26.

69. E. Bulska, *Journal of Analytical Atomic Spectrometry*, **7**, (1992), pp 201-210.

70. S. Yamashita, R. Ozawa, K. Yamaguchi, Y. Hanai, T. Katou and P. Wylie, *Journal of High Resolution Chromatography*, **15**, (1992), pp 549-551.

71. J. A. Stäb, W. P. Cofino, B. van Hattum and U. A. T. Brinkman, *Fresenius Journal of Analytical Chemistry*, **347**, (1993), pp 247-255.

72. B. D. Quimby, M. F. Delany, P. C. Uden and R. M. Barnes, *Analytical Chemistry*, **52**, (1980), pp 259-263.

73. Taketoshi Nakahara, Syugo Yamada and Tamotsu Wasa, *Applied Spectroscopy*, **44**, (10), (1990), pp 1673-1678.

74. D. L. Haas and J. A. Caruso, *Analytical Chemistry*, **57**, (1985), pp 846-851.

75. C. Webster and M. Cooke, *Analytical Proceedings including Analytical Communications*, **31**, (1994), pp 237-240.

76. C. Webster and M. Cooke - accepted by *Journal of High Resolution Chromatography*.

77. J. T. Andersson and B. Schmid, *Fresenius Journal of Analytical Chemistry*, **346**, (1993), pp 403-409.

78. F. D. Rinkema, A. J. H. Louter and V. A. Th. Brinkman, *Journal of Chromatography A*, **678**, (1994), pp 289-297.

79. I. S. Krull, S. W. Jordan, S. Kahl and S. B. Smith, *Journal of Chromatographic Science*, **20**,(1982), pp 489-498.

80. M. S. Boukraa, D. Deruaz, A. Bannier, M. Desage and J. L. Brazier, *Journal of Pharmaceutical and Biomedical Analysis*, **12** (2), (1994), pp 185-194.

81. M. Zerezghi, K. J. Mulligan and J. A. Caruso, *Analytica Chimica Acta*, **154**, (1983), pp 219-226.

82. S. Pedersen-Bjergaard and T. Greibrokk, *Journal of Chromatography A*, **686**, (1994), pp 109-119.

83. S. Pedersen-Bjergaard, T. Norman Asp and T. Greibrokk, *Analytica Chimica Acta*, **265**, (1992), pp 87-92.

84. R. H. Dagnall, T. S. West and P. Whitehead, *Analytical Chemistry*, **44** (12), (1972), pp 2074-2078.

85. T. A. Gough, M. A. Pringuer, K. Sugden and K. S. Webb, *Analytical Chemistry*, **48** (3), (1976), pp 583-585.

86. K. S. Brenner, *Journal of Chromatography*, **167**, (1978), pp 365-380.

87. K. Tanabe, H. Haraguchi and K. Fuwa, *Spectrochimica Acta*, **36B** (7), (1981), pp 633-639.

88. H. A. Dingjan and H. J. de Jong, *Spectrochimica Acta*, **38B** (5/6), (1983), pp 777-781.

89. Ou Qing-Yu, Wang Guo-Chuen, Zeng Ke-Wei and Yu Wei-Lu, *Spectrochimica Acta*, **38B** (1/2), (1983), pp 419-425.

90. D. F. Hagen, J. Belisle and J. S. Marhevka, *Spectrochimica Acta*, **38B** (1/2), (1983), pp 377-385.

91. K. J. Slatkavitz, P. C. Uden, L. D. Hoey and R. M. Barnes, *Journal of Chromatography*, **302**, (1984), pp 277-287.

92. D. F. Hagen, J. S. Marhevka and L. C. Haddad, *Spectrochimica Acta*, **40B** (1/2), (1985), pp 335-347.

93. P. C. Uden, K. J. Slatkavitz and R. M. Barnes, *Analytica Chimica Acta*, **180**, (1986), pp 401-416.

94. J. C. Evans, K. B. Olsen and D. S. Sklarew, **194**, (1987), pp 247-260.

95. Wei-Le Yu, *Journal of Analytical Atomic Spectrometry*, **3**, (1988), pp 893-900.

96. J. E. Freeman and G. M. Hieftje, *Spectrochimica Acta*, **40B** (3), (1985), pp 475-492.

APPENDIX 1

COPIES OF PAPERS PUBLISHED FROM THIS THESIS

CONFERENCES ATTENDED

R & D Topics meeting, Bradford University, July 1993.

EuroAnalysis VIII at Edinburgh University, September 1993.

ISC 20 in Bournemouth, June 1994.

R&D Topics meeting, University of Hertfordshire, July 1994.

PUBLICATIONS

'Element - Selective Detection using Capillary Gas - Chromatography with Atomic Emission Detection.'
M.Cooke, D.A. Leathard, C. Webster, and V. Rogerson.
Journal of High Resolution Chromatography, 1993, **16** (No.11), pp 660 - 662.

'Use of Microwave-Induced Plasma-Atomic Emission Detection for the Quantitation of Oxygen Containing Compounds'.
C.Webster, and M.Cooke.
Analytical Proceedings and Communications, 1994, **31**, pp237 - 240

'Capillary Gas Chromatography with Atomic Emission Detection'.
C.Webster, and M.Cooke.
Chromatography and Analysis, 1994, **Oct/Nov,** pp 9-11

'Use of an Atomic Emission Detector to Study the Variation in Elemental Response for Chlorine, Carbon and Oxygen in Phenols'.
C.Webster, and M.Cooke.
Accepted by Journal of High Resolution Chromatography.

Element-Selective Detection using Capillary Gas Chromatography with Atomic Emission Detection

M. Cooke*, D.A. Leathard, C. Webster, and V. Rogerson
The Division of Chemistry, Sheffield Hallam University. Pond Street, Sheffield S1 1WB, UK

Key Words:

Atomic emission detection
Capillary GC
Environmental analysis
Element selective detection

Summary

Capillary GC coupled to an atomic emission detector (AED) provides a powerful new hyphenated technique for the separation and characterization of complex mixtures and compounds. The AED provides simultaneous and truly specific multi-element detection. The specificity of detection reduces the need for the complex sample pretreatment procedures which are necessary to reduce the interference from co-eluted substances which is experienced with detectors such as the FID and the ECD. A range of environmentally significant problems has been studied, including PCB analysis, the characterization of the reaction products of a novel waste treatment process, and the profiling of sulfur-containing species formed by the pyrolysis of various types of coal.

1 Introduction

The microwave-induced plasma atomic emission detector is but one form of the general technique of GC–atomic emission spectroscopy which has been extensively reviewed [1].

McCormack et al. [2] first demonstrated the technique of GC with an atomic emission detector (AED) in 1965. Since then the technique has developed slowly, primarily for technical reasons, but a key development occurred in 1976 when *Beenakker* [3] invented a cavity able to sustain a microwave-induced helium plasma at atmospheric pressure. Subsequent developments centered on improving plasma stability, optical technology, automation, and software. The incorporation of a photodiode array (PDA) [4] provides extremely high selectivity while maintaining sensitivities comparable with those of other GC detectors [5].

The capillary gas chromatograph is interfaced directly to a discharge cavity. A magnetron supplies microwave radiation to the cavity, inducing a helium plasma which is contained within a quartz discharge tube. The excess heat produced by the plasma is dissipated *via* a water cooling system to prolong the life of the discharge tube. As the eluent enters the plasma, the separated components are atomized and the outer shell electrons excited, promoting them to a higher energy level. When electrons decay back down to ground level they emit radiation at wavelengths characteristic of the elements concerned. The dispersed radiation is monitored by a PDA covering part of the range between 165–780 nm, enabling the simultaneous detection of a number of elements depending upon the location of the PDA in the focal plane. The complex spectral information is transferred to a computer where it is stored for future data manipulation, element identification, and chromatographic integration.

The simultaneous monitoring of carbon, nitrogen, and sulfur is useful for drug screening and characterization, as is the ability to monitor oxygen, chlorine, bromine, fluorine, arsenic [6], and metals such as mercury [7,8] for environmental applications. GC-AED is, in principle, able to provide elemental ratios giving information on empirical formulas [9]. In this respect the AED provides information complementary to that furnished by the mass spectrometer and hence provides comfirmatory identification data.

Three applications showing the use of the GC-AED have been studied–PCB analysis, the characterization of the reaction products of the wet air oxidation of 2-picoline, and the profiling of sulfur-containing species formed by the pyrolysis of coal.

2 Experimental

The GC-AED (Hewlett-Packard, Avondale, Pennsylvania, USA) consisted of an HP5890 capillary chromatograph interfaced to an HP5921A atomic emission detector and coupled to a ChemStation. Carrier (1 ml min^{-1}), make-up, and reagent gases were as recommended by the manufacturer. PCB standards were donated by the original manufacturers.

2.1 Sample Preparation and Analysis

2.1.1 PCBs

Sewage sludge was extracted with dichloromethane (20 mL) for 2 h in a Soxhlet apparatus and the extract reduced to *ca* 1 mL under a stream of dry nitrogen. 1 µL of the extract was injected splitless (60 s purge delay) on to a 25 m × 0.32 mm i.d. column coated with a 0.17 µm film of polydimethylsiloxane HP-1 (Hewlett-Packard). The column was programmed from 60 to 150 °C at 10 °min^{-1} and then to 300 °C at 5 °min^{-1}. Carbon, chlorine, and hydrogen were monitored at 496, 479, and 486 nm, respectively.

2.1.2 Oxidation of 2-Picoline

In a typical *Fenton* chemistry reaction [10] a mixture of dilute sulfuric acid, iron sulfate, and copper sulfate was refluxed under nitrogen and 2-picoline was added, followed by excess hydrogen peroxide. The reaction products were extracted with dichloromethane (4 × 15 mL) and reduced to *ca* 1 mL under a stream of dry nitrogen. 1 µL of the extract was injected splitless (60 s purge delay) on to a 10 m × 0.32 mm i.d. column coated with a 0.25 µm immobilized film of the polar polyethylene glycol Supelcowax (Supelco). The column was programmed at 10 °min^{-1} from 40 to 250 °C which was held for 10 min. Carbon, nitrogen, and oxygen were monitored at 193, 174, and 777 nm, respectively.

2.1.3 Coal Pyrolysis

Coal samples (0.5 mg) were pyrolyzed at 1123 K and transferred to the head of the polyethylene glycol column (Section 2.1.2) *via* a splitter (split ratio 100:1). The column was held at 40 °C for 10 min

after pyrolysis, programmed at 20 °min^{-1} to 120 °C, which was held for 6 min, then programmed at 20 °min^{-1} to 200 °C, which was held for 6 min, and finally programmed at 20 °min^{-1} to 280 °C, which was held for 6 min. Carbon, nitrogen, and sulfur were monitored at 193, 174, and 181 nm, respectively.

3 Results and Discussion

PCB analysis of environmental samples is complicated both by the presence of other chlorine-containing species in the extracts (*e.g.* organochlorine pesticide residues) and by the non-specificity of the traditional detector (ECD). The chlorine selectivity of the AED (479.0 nm) was used to analyze a standard PCB (Aroclor 1254, 10 µg mL^{-1} in hexane), giving the characteristic profile (not shown), and a sewage sludge extract spiked with Aroclor 1254 (10 µg mL^{-1}) (**Figure 1**). Analysis of the sludge extract revealed the absence of PCB, hence the spiked sample was analyzed to show the sensitivity of the instrument. Under these conditions the implied limit of detection for chlorine is equivalent to approximately 1 ng total PCB. The use of the snapshot facility (the emission spectrum for the peak of interest) confirmed the presence of chlorine (peaks at 479.0, 461.0, and 481.8 nm) in each component.

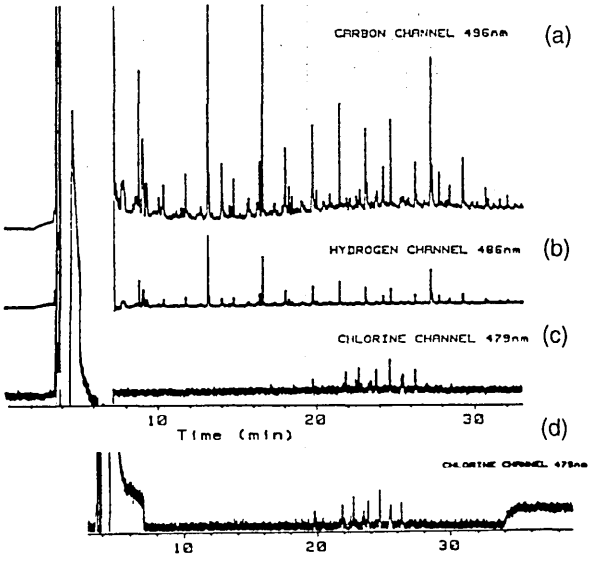

Figure 1
Analysis of sewage sludge extract spiked with Aroclor 1254; GC-AED responses from (a) carbon, (b) hydrogen, and (c) chlorine channels; chlorine trace (d) is that obtained from Aroclor 1254 sttandard.

Wet air oxidation is a technique which offers great promise for the disposal of waste chemicals. The process is intended to degrade molecules to simple biodegradable species such as ammonia, acetic acid, and methanol but little is known of the mechanism by which this occurs. Preliminary studies using 2-picoline (a typical nitrogen-containing heteroaromatic compound) as a model compound have been performed in an attempt to elucidate the pathway of the reaction process (**Figure 2**).

The chromatogram of the reaction mixture shows that a large number of less volatile, more complex compounds has been formed during the reaction. Three species containing both oxygen and nitrogen are present at t_R = 6.1, 12.1, and 13.2 min. In contrast there

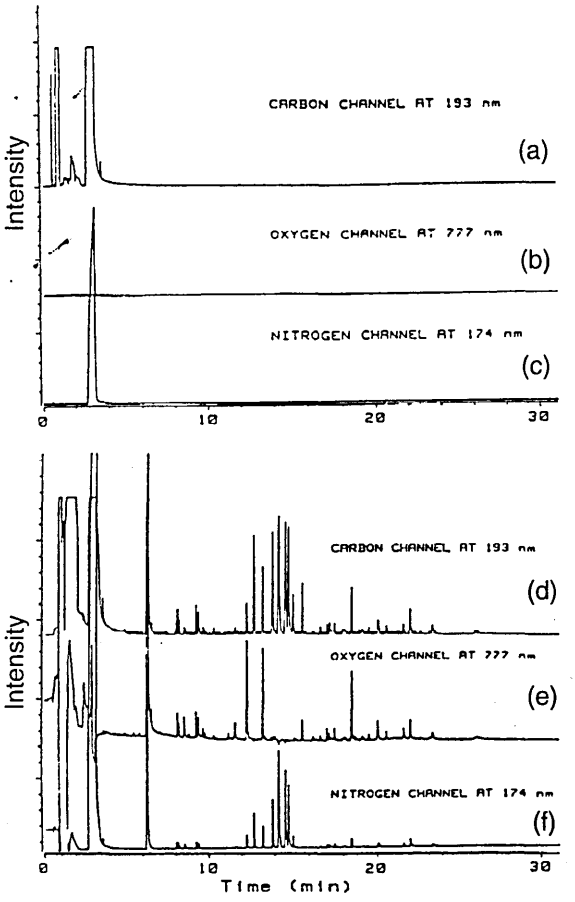

Figure 2
Characterization of the products from wet air oxidation of 2-picoline; (a), (b), and (c), are carbon, hydrogen, and chlorine channel signals from starting material; (d), (e), and (f), are carbon, hydrogen, and chlorine channel signals from analysis of reaction products.

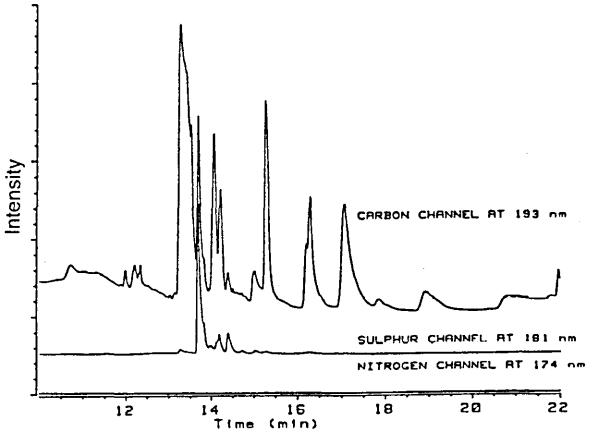

Figure 3
Characterization of the products resulting from the pyrolysis of coal at 1123 K: GC-AED responses from carbon, sulfur, and nitrogen channels.

is a group of five components which contain no oxygen eluting between 13.95 and 15.2 min. Most surprising is the appearance of several components, for example that at t_R = 15.5 min, which contain oxygen, carbon, and hydrogen but no nitrogen. It should be noted that separate injections are required for the oxygen-selective response and the carbon-and nitrogen-selective responses; the two selective chromatograms are then merged.

The combustion of sulfur-containing fossil fuels produces sulfur dioxide which is emitted to the atmosphere where it reacts to form acid rain. Characterizing fossil fuels by examining the organosulfur compounds produced on heating is a way of assessing their potential for producing sulfur dioxide when burnt. To simulate burning, a small amount of the coal is pyrolyzed and the carbon, sulfur, and nitrogen wavelengths monitored. As is apparent from **Figure 3** relatively few sulfur-containing compounds were produced; they were relatively non-polar and of low molecular weight. There was no evidence of the production of the larger polycyclic aromatic sulfur compounds of the type often found when crude oil is pyrolyzed. No nitrogen-containing compounds were observed.

4 Conclusion

GC-AED is a powerful technique for profiling heteroatom-containing compounds in complex matrices; it also requires minimal sample pretreatment. The information produced is complementary to that produced by GC-MS and hence the two techniques can be combined to achieve full characterization of complex mixtures.

Acknowledgments

We thank *Professor K. Bartle* of Leeds University (UK) for providing the coal pyrolysis samples and *Jacqueline Morris* of Sheffield Hallam University for performing the oxidation of 2-picoline.

References

[1] *L. Ebdon, S. Hill,* and *R.W. Ward,* Analyst **111** (1986) 1113.

[2] *A.J. McCormack, S.C. Tong,* and *W.D. Cooke,* Anal. Chem. **37** (1965) 1470.

[3] *C.I.M. Beenakker,* Spectrochim. Acta **31B** (1976) 483.

[4] *B.D. Quimby* and *J.J. Sullivan,* Anal. Chem. **62** (1990) 1027.

[5] *R.L. Firor,* American Laboratory May (1989) 40; Internat. Laboratory Sept. (1989) 44.

[6] *H. Haraguchi* and *A. Takatsu,* Spectrochim. Acta **42B** (1987) 235.

[7] *E. Bulksa, H. Emteborg, D.C. Baxter, W. Frech, D. Ellingsen,* and *Y. Thomassen,* Analyst **117** (1992) 657.

[8] *S.C. Hight* and *M.T. Corcoran,* J. Assoc. Off. Anal. Chem. **70** (1987) 24.

[9] *R.M. Dagnall, T.S. West,* and *P. Whitehad,* Anal. Chem. **44** (1972) 2075.

[10] *S. Ito, A. Mitarai, K. Hikino, M. Hirama,* and *K. Sasaki, J. Org. Chem.* **57** *(1992) 6937.*

Ms received: May 28, 1993
Accepted: September 27, 1993

Use of Microwave-induced Plasma Atomic Emission Detection for the Quantification of Oxygen Containing Compounds

Caroline Webster and Michael Cooke*
The Environmental Research Centre, Division of Chemistry, School of Science, Sheffield Hallam University, City Campus, Pond Street, Sheffield, UK, S1 1WB

An atomic-emission detector has been used to study the elemental response for oxygen for a series of compounds of markedly dissimilar molecular structure. Calibration curves over a range of concentrations have been generated and the variation in the slopes obtained. The slopes of these concentration *versus* response graphs indicate that the elemental response for oxygen varies with the molecular structure in which it is contained. Moreover, the condition of the plasma cavity discharge tube causes a variation in the slope, and hence the sensitivity of response, for the same compound. This observation may be attributed to molecular interference caused by non-instantaneous breakdown of the compounds in the plasma, resulting in incomplete, *i.e.*, non-ideal, elemental yield. The cause of molecular interference may be a lack of thermodynamic control at either the decomposition stage or during atom recombination, *e.g.*, the formation of CO from carbon and oxygen.

Although the coupling of a microwave-induced plasma (MIP) atomic emission spectrometer to a gas chromatograph was first reported in 1965[1] only recently has the technique become commercially available. Capillary gas chromatography coupled to an atomic emission spectrometer permits the latter to function as both a selective and a universal detector for gas chromatography. The atomic emission detector consists of a plasma source, typically of the Beenaker cavity type,[2] to render compounds down to their constituent atoms, and a diode-array detector to monitor line spectra from the individual elements formed. Although the cavity emits line spectra characteristic of each element present, the Hewlett-Packard system is limited to the monitoring of four elemental lines simultaneously. Additional information for other elements can be obtained by re-injecting the sample, collecting the additional data and then merging the two (or more) data sets for presentation purposes. Hence, the atomic emission detector (AED) may function as a multi-element detector. When operated in the carbon detection mode the response parallels that of the flame ionization detector and monitoring of nitrogen, phosphorus and sulfur emission lines produces a response similar to that for other selective gas chromatography detectors. The AED provides additional selectivity over the electron capture detector in that it can discriminate between the individual halogens, but the sensitivity is significantly less than that of the electron capture detector (ECD) for the same compound. Its range of selectivity is demonstrated by the ability to acquire the response for tin, lead and mercury organometallic compounds in a single sample, thus facilitating the determination of these environmentally significant organometallic compounds.[3]

Early work[4] using GC–MIP–AED indicated that a particular element could give a different molar response according to the molecular structure from which it originated, but this may have resulted from poor plasma stability. Subsequent work[5] demonstrated that, in different compounds of the chemical class, the response for carbon and for chlorine appeared to be independent of the molecular structure despite the low microwave powers employed. However, intercomparison of results obtained by using MIP–AED has been difficult because of the non-standard equipment used. The advent of a commercially available system (HP 5921-AED) combined with an HP 5890 GC and autosampler (HP 7673 A) has facilitated the study of elemental response and has provided the ability to highlight any inter-element or molecular effects should these occur.

The importance of this new hyphenated technique is two-fold. Firstly, it provides a simultaneous multi-element monitoring capability. Secondly, it allows the calculation of empirical formulae[6] and thus provides a complementary technique to GC–FTIR and GC–MS for the identification of unknowns in complex mixtures. However, it is necessary that, for element ratioing calculations, the atomic emission response must be truly independent of the molecular structures from which the atoms are derived. This criterion is often referred to as compound independent calibration (CIC) and, if it holds true, then any compound can be used to produce a calibration curve for quantification providing it contains the appropriate elements. Recent reports[7–10] on the reliability of CIC are almost equally divided on its validity with respect to C:H and C:Cl ratios, although two reports[8,10] agree that the C:N ratios in the classes of compound studied (nitroaromatics, alkylamines and heteroaromatics) were dependent to some extent upon molecular structure.

In this preliminary report we have used GC–MIP–AED to study the atomic responses of a series of compounds with markedly dissimilar structures, but each containing both nitrogen and oxygen in very different environments. The results obtained for C:N ratios confirm the variability previously observed. However, the results for oxygen reveal that not only does the molecular structure influence the response but that the condition of the discharge tube in which the plasma is generated also affects the relative oxygen response.

Experimental

The GC–AED (Hewlett-Packard, Avondale, Pennsylvania, USA) consisted of an HP 5890 capillary chromatograph interfaced to an HP 5921A atomic emission detector and coupled to a ChemStation. Helium carrier (1 ml min^{-1}) and reagent gases were as follows. For carbon and nitrogen analysis a mixture of O_2 and H_2 reagent gases was used. For oxygen analysis a mixture of H_2 and auxiliary (aux) reagent gas was used (aux ≡ 10% CH_4 in nitrogen). All reagent gases were introduced at a flow rate of 5 ml min^{-1}.

* To whom correspondence should be addressed.

The mixed standard was composed of cotinine, lidocaine, pentobarbital, secobarbital, barbital, caffeine, nicotine and azobenzene (Fig. 1) made up in dichloromethane. A range of concentrations were prepared, to cover the range from 5×10^{-5} to 5×10^{-4} mol l^{-1}, and 1 μl of each was injected splitless (40 s purge delay) on to a 25 m × 0.32 mm i.d. column coated with a 0.52 μm film of cross-linked 5% phenyl methyl silicone HP-5 (Hewlett-Packard). The column was programmed from 80 °C (4 min) to 280 °C at 20 °C min^{-1} and then held at 280 °C for 3 min. Carbon, nitrogen and oxygen were monitored at 193, 174 and 777 nm, respectively.

Results and Discussion

When an organic compound enters the plasma of the AED it is broken down into its constituent atoms, which are excited by the plasma energy and, upon returning to the ground state, emit line spectra. This emission energy is monitored at appropriate wavelengths for the elements of interest by the diode array detector. Because it is atomic emission which is measured, *i.e.*, an elemental response, the structure of the original molecule should not cause variation in the elemental response. Thus, for example, equimolar amounts of azobenzene and nicotine should produce identical responses as both contain two nitrogen atoms. It should therefore be possible to use azobenzene as a calibration compound for quantifying any nitrogen-containing compound. This procedure is known as compound independent calibration. To date, opinions vary as to whether compound independent calibration is valid. The response for halogens in chlorine and bromine containing compounds appears to be independent of structure,[7] but for carbon reports vary and for nitrogen the response is reported to be related to the parent molecule.[8,10] Little data for oxygen response has been reported previously but one report[11] demonstrates that the oxygen response is independent of molecular structure. However, these results apply to a small series of structurally similar compounds of one chemical class.

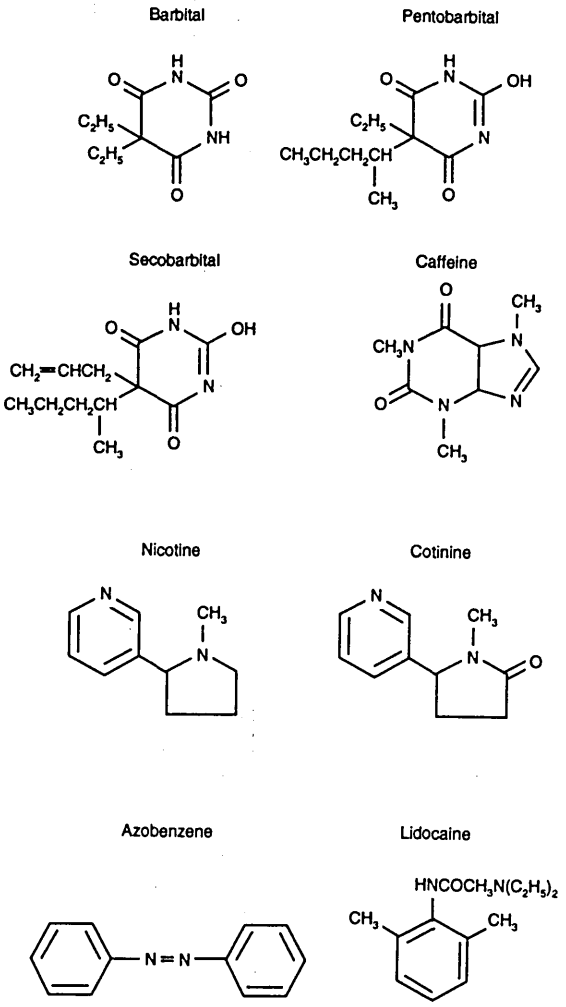

Fig. 1 Structures of the compounds used showing the different types of oxygen environment

A series of compounds containing both nitrogen and oxygen in differing structural environments was selected for study. The compounds selected were cotinine, caffeine, barbital, secobarbital, pentobarbital and lidocaine. Cotinine is a major metabolite of nicotine and contains a single oxygen in a carbonyl group adjacent to a nitrogen contained in a five-membered heterocyclic ring. Caffeine has a xanthene-type structure in which the four nitrogen atoms are contained in two rings. Three are amino nitrogens and one is imino in character. The two oxygens are both in carbonyl groups in the six-membered ring in a similar structural environment to that of cotinine. The three barbiturates have a similar core structure in which the oxygen atoms are contained in carbonyl groups, except for one hydroxy group in barbital. Both seco- and pentobarbital have relatively large alkyl side chains and hence are very similar in over-all structure. Lidocaine contains one tertiary amino nitrogen, one amido nitrogen and an oxygen in a carbonyl group which is not contained in a ring. The nitrogen and oxygen atoms of these compounds are therefore contained in markedly different environments (Fig. 1).

A series of mixed standard solutions was prepared to cover the concentration range from 5×10^{-5} to 5×10^{-4} mol l^{-1}. At concentrations above 5×10^{-3} mol l^{-1} the response becomes non-linear. Normally this phenomenon is associated with saturation of the detector but this is not thought to be the cause in this study (see below) because it occurs to differing extents for the same element in different molecular structures. The instrument was fitted with a new, *i.e.*, clean discharge tube, and the plasma and detector conditions were standardized for oxygen detection. Sequential injection of the standard solutions was made, in order of increasing concentration, the

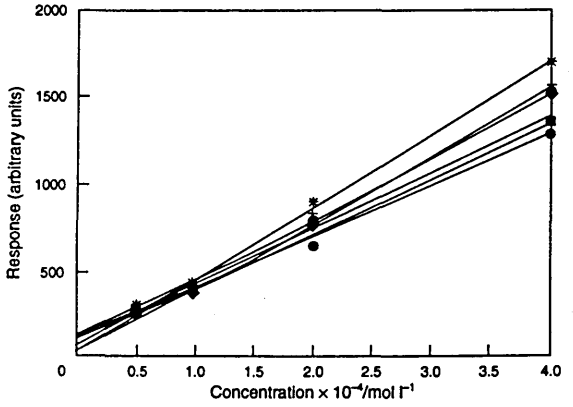

Fig. 2 Calibration lines for standard components using a clean discharge tube. Concentration range 0.5×10^{-4} mol l^{-1} to 4×10^{-4} mol l^{-1}. Response range 0–2000 units. ●, Cotinine; +, caffeine; *, barbital; ■, secobarbital; ×, pentobarbital; ◆, lidocaine

Table 1 Total oxygen response and response per unit oxygen using a clean discharge tube

	Concentration 5×10^{-5} mol l^{-1}		Concentration 1×10^{-4} mol l^{-1}		Concentration 2×10^{-4} mol l^{-1}		Concentration 4×10^{-4} mol l^{-1}	
	O (777 nm)	Resp. per O	O (777 nm)	Resp. per O	O (777 nm)	Resp. per O	O (777 nm)	Resp. per O
Cotinine (O_1)	282	282	369	369	652	652	1301	1301
Caffeine (O_2)	489	245	830	415	1674	837	3070	1535
Barbital (O_3)	754	251	1245	415	2697	899	5103	1701
Secobarbital (O_3)	754	251	1185	395	2374	791	4036	1345
Pentobarbital (O_3)	851	284	1167	389	2383	794	4161	1387
Lidocaine (O_1)	250	250	369	369	773	773	1518	1518

emission line for oxygen (777 nm) monitored and the response measured. From the data, calibration lines for oxygen in the six compounds were constructed (Fig. 2) and the response per oxygen atom at the various concentrations used was calculated (Table 1). Subsequently, the experiment was repeated with an old, *i.e.*, contaminated, discharge tube. In use the discharge tube becomes contaminated by deposits, primarily of carbon, generated by the reagent gases used to modify the plasma to promote elemental selectivity. The calibration lines obtained with a contaminated discharge tube are shown in Fig. 3 and the relevant data is given in Table 2. Peak areas were measured at all times.

If the elemental oxygen response is independent of the original molecular structure then the calibration lines should all have the same slope because any molecule would produce the same response per unit of oxygen. Clearly, this is not the case in either Fig. 2 or Fig. 3. The differences in slope are reproducible and are not attributable to variation of injection volume. The difference in slope (and hence of sensitivity of response) between barbital and cotinine is of the order of 30%. Note the close similarity of slope for seco- and pentobarbital. At higher concentrations (not shown) the lines become non-linear, implying overloading of the detector. However, a detector overload will begin to be apparent at the same concentration of oxygen for each compound as it is an oxygen detector. In this case, the calibration curves begin to depart from linearity at different concentrations. The probable explanation, therefore, is that the formation of oxygen atoms becomes non-linear at different concentrations because the efficiency of atom formation varies according to the nature of the parent compound, which will influence the breakdown pathway of the molecule to its constituent atoms. Both Tables 1 and 2 show that the response per unit of oxygen decreases with increasing concentration, which agrees with the theory that side reactions, which are more probable at a higher concentration of analyte in the plasma, are reducing the amount of elemental oxygen available for detection. The time-scale over which the degradation of the molecule in the plasma occurs is also important. On a narrow-bore capillary column the typical base width of a peak is of the order of 2–3 s. At the capillary column–discharge tube interface in the AED the diameter increases and hence the linear flow rate decreases. The base width thus becomes some 4–5 times greater. Although the addition of make-up gases is intended to moderate this broadening, it is still observed. The length of the plasma is of the order of 10 mm and thus the destruction of the molecules contained in an eluting peak occurs over several seconds, during which time molecules, reagent gases and atoms are all present. It is likely therefore that the breakdown involves the formation of small molecular species, particularly when oxygen is available in the presence of hydrogen and nitrogen. Hence, the dependence of the oxygen response will vary according to the degradation pathways available to the molecule, to the concentration of analyte and other reactive species and to residence time in the detector. The possibility also exists of atom recombination of carbon and oxygen.

Some evidence to support this theory is available. The use of a contaminated tube provides additional reagent material in the plasma and the potential for side reactions is correspondingly higher. The variation of microwave power to the plasma might also cause this effect to be observed, but we are unable to vary this parameter. The slopes of the calibration lines in

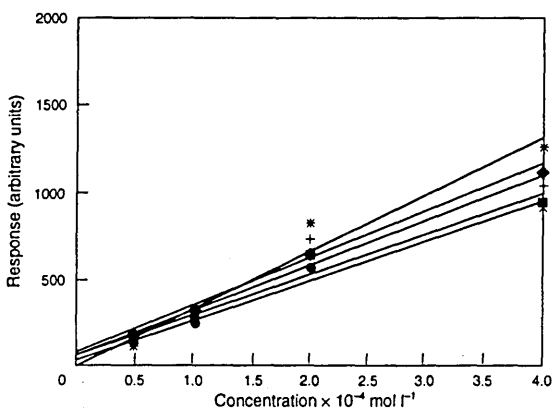

Fig. 3 Calibration lines for standard components using a contaminated discharge tube. Concentration and range as for Fig. 2. Symbols as in Fig. 2

Table 2 Total oxygen response and response per unit oxygen using a contaminated discharge tube

	Concentration 5×10^{-5} mol l^{-1}		Concentration 1×10^{-4} mol l^{-1}		Concentration 2×10^{-4} mol l^{-1}		Concentration 4×10^{-4} mol l^{-1}	
	O (777 nm)	Resp. per O	O (777 nm)	Resp. per O	O (777 nm)	Resp. per O	O (777 nm)	Resp. per O
Cotinine (O_1)	130	130	217	217	557	557	930	930
Caffeine (O_2)	269	135	513	257	1454	727	2076	1038
Barbital (O_3)	350	117	800	267	2439	813	3762	1254
Secobarbital (O_3)	342	114	766	255	1917	639	2789	930
Pentobarbital (O_3)	292	97	794	267	1941	647	2766	922
Lidocaine (O_1)	181	181	296	296	736	736	1131	1131

Fig. 2 are all less than for a new clean tube, indicating reduced oxygen sensitivity, *i.e.*, reduced oxygen concentration in the plasma. The response per unit oxygen values in Table 2 are all lower than for Table 1. Moreover, the relative proximity of atoms in a molecule influences the elemental response. The unit oxygen response in cotinine, where the oxygen and nitrogen atoms are not directly bonded, is of the order of 280 units (new tube) at 5×10^{-5} mol l^{-1}, whereas in 2-nitrophenol (new tube, 5×10^{-5} mol l^{-1}) it is of the order of 55 units per oxygen.[11] In 2-nitrophenol the $-NO_2$ moiety already exists and hence is likely to inhibit the formation of free oxygen to a greater extent than in the degradation of cotinine. Perhaps the best evidence in support of the concept that small, relatively long lived, molecules are formed as intermediates in the plasma of the AED and thus inhibit free element formation comes from the use of the AED to monitor the molecular emission of ^{13}CO (λ = 171 nm) as a technique for quantification of ^{13}C labelled drugs. Clearly, molecular carbon monoxide must be produced in sufficient quantity during the degradation of the parent molecule for this process to occur.

Conclusions

The response of the atomic-emission detector to oxygen is dependent upon the nature of the parent compound in which the oxygen is contained. The condition of the discharge tube also influences the response. The variation in slope of calibration lines, the departure from linearity at higher concentrations, and the variation in response caused by contamination of the discharge tube, support the argument that variation of breakdown pathway and the formation of relatively stable oxygen-containing small molecules in the plasma are responsible for the observed departure from an independent elemental response. Consequently, the choice of an internal standard for calibration purposes becomes critical, and it is recommended that close structural similarity is used as the primary criterion for selection. The similarity of slope for pento- and secobarbital (both new and old tubes) serves to illustrate this point. A similar parallelism of response has been observed for the carbon response of 2-chloro- and 2-nitrophenol.[12]

References

1 McCormack, A. J., Tong, S. C., and Cooke, W. D., *Anal. Chem.*, 1965, **37**, 1470.
2 Beenakker, C. I. M., *Spectrochim. Acta*, 1976, **31B**, 483.
3 Rogerson, V., and Leathard, D. A., personal communication.
4 van Dalen, J. P. J., de Lezenne Coulander, P. A., and de Galen, L., *Anal. Chim. Acta*, 1977, **94**, 1.
5 Zerezhi, M., Mulligan, K. J., and Caruso, J. A., *J. Chromatogr. Sci.*, 1984, **22**, 348.
6 Perpall, H. J., and Uden, P. C., *Spectrochim. Acta*, 1987, **42B**, 242.
7 Huang, Y., Ou, Q., and Yu, W., *J. Chromatogr. Sci.*, 1990, **28**, 584.
8 Jelink, Th., and Venema, A., *J. High Resolut. Chromatogr.*, 1990, **13**, 447.
9 Kovack, N., and Ramus, T. L., *J. Anal. Atom. Spectrom.*, 1992, **7**, 999.
10 Pedersen-Bjergaard, S., Asp, T. N., and Grubrokk, T., *J. High Resolut. Chromatogr.*, 1992, **15**, 89.
11 Quimby, B. D., Giarrocco, V., and Sullivan J. J., *J. High Resolut. Chromatogr.*, 1992, **15**, 705.
12 Webster, C., and Cooke, M., in preparation.

Paper 4/02496F
Received April 27, 1994
Accepted June 13, 1994

CAPILLARY GAS CHROMATOGRAPHY WITH ATOMIC EMISSION DETECTION

by Caroline Webster and Michael Cooke, The Environmental Research Centre, Sheffield Hallam University, UK

Keywords: Atomic emission detection, Multi-element analysis, envoironmental analysis

Biography

Caroline Webster is a graduate of Sheffield Hallam University, holds an MSc from Loughborough University and is presently completing her PhD studies at Sheffield Hallam University.

Michael Cooke graduated from Bristol University in 1967 and completed his PhD in 1969. Post-doctoral research in the UK and the USA resulted in an academic position at Bristol University where he worked with Gordon Stone for some years. In 1988 he left to work in industry, first in Germany and, subsequently, in North Wales. In 1991 he was appointed Professor of Analytical Science at Sheffield Hallam University. His main research interests are in separation science.

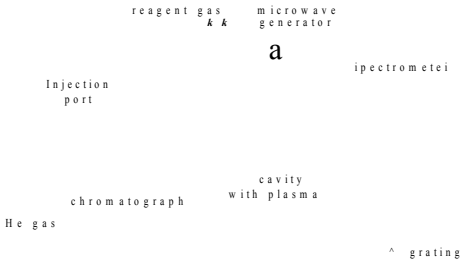

Fig. 1. GC-AES block diagram.

Fig. 2. The HP 5921A AED uses atomic emission spectroscopy to detect dements eluting from a gas chromatograph. A helium plasma fragments all compounds, with the excited atoms producing characteristic emission lines. A mirror focuses each element's unique optical emission line onto the spectrometer's entrance slit. A concave holographic diffraction grating disperses the light according to wavelength and brings it to a focus along a flat focal plane.

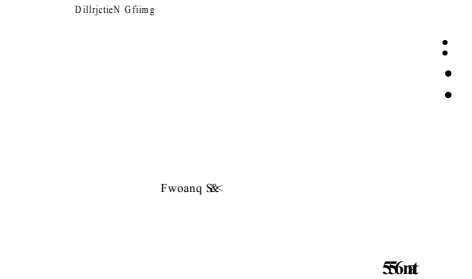

Fig. 3. A photodiode array, which can be positioned at various points along the focal plane, simultaneously measures the light from as many as *six elements. The powerful software of the Hewlett Packard Chem-Station translates the data into real-time, background-correcting chromatograms. All of this technology offers the highest sensitivities and selectivities for element detection.*

Introduction

Capillary gas chromatography and atomic emission spectroscopy can be combined to provide a powerful hyphenated analytical technique for the separation and characterisation of complex mixtures. The technique consists of a conventional capillary gas chromatograph interfaced to an atomic emission spectrometer. Various types of atomic emission spectrometer have been used (1) but the one which is now available commercially utilises a microwave-induced plasma as the spectral source. The potential of this coupled system was first demonstrated by McCormack *et al* (2) in 1965. Since then the technique has developed slowly, primarily for technical reasons relating to plasma cavity design. The development of the Beenakker cavity (3) provided a sustainable, microwave-induced helium plasma operating at atmospheric pressure. Spectroscopic detection can be achieved at a single wavelength using conventional optical spectroscopic equipment but the incorporation of a photodiode array (4) permits simultaneous multi-element detection. A complete GC-AED system therefore consists of an autosampler, a capillary gas chromatograph, interfaced via a heated transfer line directly to the cavity which acts as the spectral source. Spectral collection is by diode array detection and the complete system (Fig. 1) is controlled from a microprocessor. The ftill spectral range of the diode array detector is 165-780 nm but only a small 'window' within this range can be monitored at any one time. Up to four elements can be studied simultaneously providing each has a spectral line which falls within the detection 'window'. Hence the AED has several advantages over other types of gas chromatography detector. For example it is a specific oxygen detector with the oxygen response being acquired by monitoring the line at 777 nm. Sulphur can also be monitored at 181 nm but the response is linear over four decades in contrast to the performance of the flame photometric detector. The AED can also be used to detect halogens. Here the major advantage over the electrolytic conductivity detector and the electron capture detector lies in the ability to discriminate between the response for fluorine, chlorine, bromine (and iodine) rather than give a total halogen response. However, the sensitivity is inferior to that provided by the electron capture detector. Organo-mercury, -tin and -lead compounds can be detected at the appropriate wavelengths (253.6 nm for mercury, 303.42 nm for tin and 405.8 nm for lead). Deuteration can be detected as can the presence of ^{13}C-labelled compound via monitoring of the ^{13}CO emission line at 241.36 mm

The software incorporated into the microprocessor (an HP Chemstation) makes the calculation of elemental ratios possible, leading to information about the partial empirical formulae and hence provides complementary information to that given by GC-MS. Care should be exercised when using this procedure. Elemental spectral response should, in theory be independent of the molecular structure from which the atoms originate. Whilst this does appear to hold true for compounds of *similar molecular structure* there is increasing evidence to suggest that the spectral response does vary for compounds of markedly dissimilar chemical structure (5,6). Two reasons are possible. Incomplete breakdown of the mole-

cules in the plasma leaving a proportion of small molecules (eg CO) instead of atoms would result in incomplete spectral yield (for carbon in this example). The ability to monitor the *molecular* emission of CO indicated that breakdown is not necessarily total. Secondly, recombination of atoms in the plasma could also produce a non-ideal elemental response. The former explanation is clearly structurally dependent whereas the latter is more likely to be related to the concentration of the appropriate atoms in the plasma.

The process of atom formation, spectral response and detection forms the heart of the atomic emission detector. The helium carrier gas passes the GC eluent from the oven via a transfer line to the cavity housing the detector which consists of a microwave induced helium plasma. High purity helium is used as the plasma support gas, as any impurities can give quite intense spectra, leading to a high background. Helium flow rates are usually in the range 20-100 ml/min, much lower than the 10-20 ml/min flows required for inductively coupled plasma sources.

The compounds entering the plasma are atomised and the outer shell electrons are then raised to an excited state. As they return to the ground state they emit light of a wavelength characteristic of the element present. The light produced by the atoms is then dispersed by the grating into its component wavelengths and measured by a light sensor, in this case a photodiode array. The helium plasma is formed in a narrow quartz discharge tube, (1 mm id) into which the end of the GC column passes (Fig. 2).

The discharge tube is the most delicate part of the instrument, and several features have been added to prolong the lifetime of the tube:

Firstly, water is circulated around the cavity to dissipate the excess heat produced by the plasma. This decreases erosion of the inner surfaces of the cavity by preventing interaction of the samples with the tube walls. Background emissions are also reduced, for example a decreased cavity temperature reduces oxygen and silicon emissions by decreasing volatilisation from the tube itself.

Secondly, a solvent venting procedure is used. This stops solvent entering and extinguishing the plasma by diverting the column flow away from the detector. If the plasma is extinguished by incorrect solvent venting, the AED automatically tries to relight itself, weakening the discharge tube. The solvent vent is controlled by a solenoid valve which is operated from the Chemstation.

Thirdly, reagent gases are automatically added to the plasma support gas when the elements to be monitored have been chosen. They are added in small concentrations to prevent carbon deposits on the walls of the discharge tube. As the tube is so narrow any small deposits would produce severely distorted peaks and affect the sensitivity of the instrument. They may also contribute to non-ideal qualitative spectral response.

At the other end of the discharge tube is the spectrometer window through which the emitted light passes to the sensor (Fig. 3). As the light enters the spectrometer it is focused through a slit by a mirror, and then dispersed by a curved holographic grating. The grating is curved to allow dispersion onto a flat focal plane, along which the photodiode array (PDA) slides. Although this plane covers the range 170-780 nm, to achieve the desired resolution the PDA only covers a specifically chosen portion of the spectrum at any one time. So, when the elements of interest are chosen prior to a run, the PDA is positioned to cover the emission wavelengths of those elements. Fig. 3 shows the groups of elements which can be monitored simultaneously in one injection. For example, nitrogen, phosphorus, sulphur and carbon can be monitored in one injection. However, if oxygen were present a second injection would be required. The Chemstation then merges the data from the two chromatographic runs.

Therefore it is possible to identify all the elements present in compounds leaving the gas chromatograph. The data can be presented in two ways. The plot of the detector output, ie light intensity at a certain wavelength over time gives a chromatogram, and the spectral detector's output across a range of wavelengths at a specific moment in time produces an emission spectrum. Hence, the spectrum or 'snapshot' shown in Fig. 4 is the full uv spectrum of the peak marked on the chromatogram. The snapshot shows the spectral lines of the elements monitored and confirms elemental identity. It is best represented as a 3-D plot. This spectrum is of a sulphur-containing compound and shows the expected elemental lines around 181 nm, giving conclusive proof of the presence of sulphur. The AED can therefore provide quantitative data from the chromatograms, and qualitative data from the snapshot spectra.

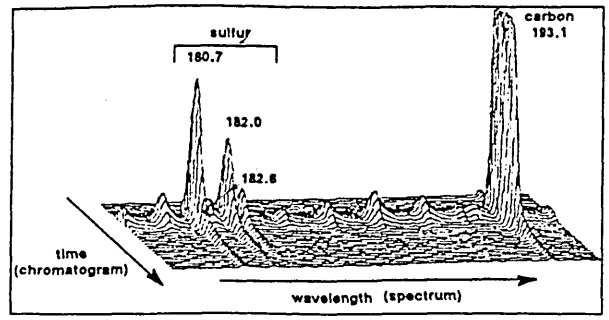

Fig. 4. Overview of GC-AES 1-8

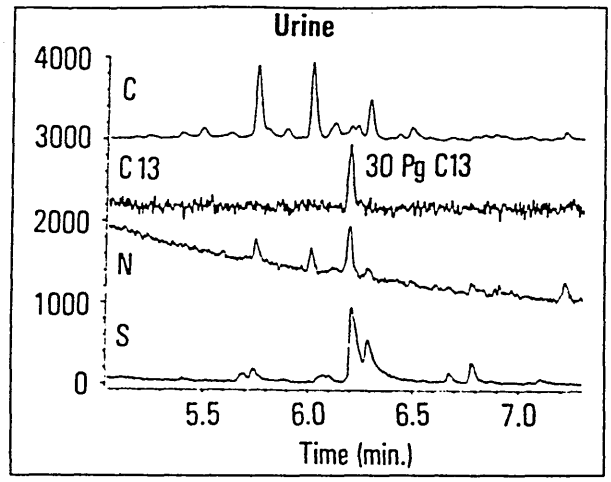

Fig. 5. HP 5921A AED chromatograms show extraordinary sensitivity and selectivity. This chromatogram clearly identifies a single peak revealing the presence of Carbon-13 spiked into a urine extract.

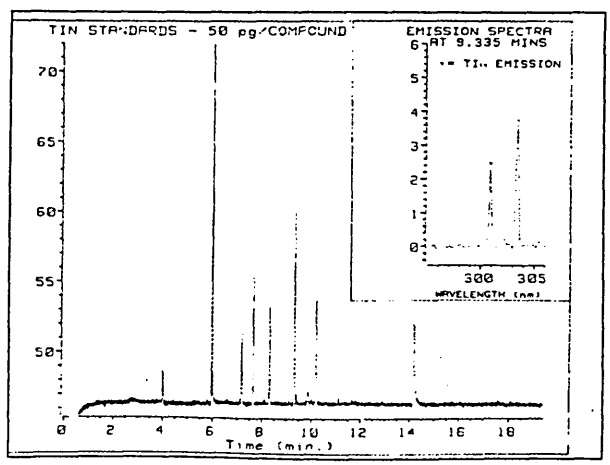

Fig. 6.

Applications

The ability to analyse by GC-AED can be useful in several areas:

(a) *Screening for waste disposal.* In this area it is very important to know if the waste is halogenated. This can be discovered quickly and easily using the AED, which can distinguish between individual halogens. Valuable ele-

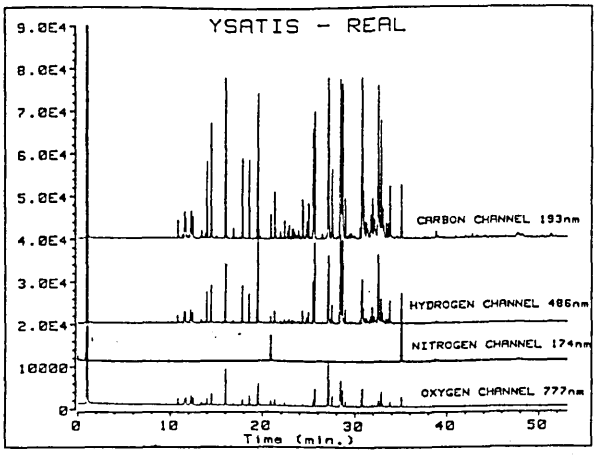

Fig. 7a.

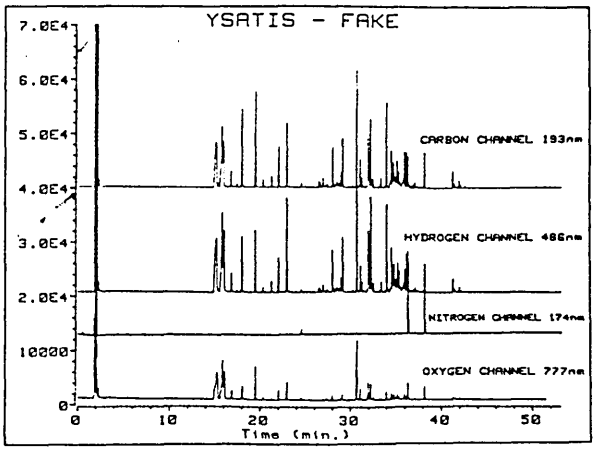

Fig. 7b

mental information can also be collected to help with the mass spectral analysis in eliminating some library matches. For example, if the AED run shows no sulphur to be present, all sulphur-containing library matches can be eliminated.

(b) Drug tracing and analysis. In drug metabolism studies, the drug in question is often labelled with a radioisotope such as deuterium or ^{13}C. The metabolites can then be identified by mass spectrometry in the case of deuterated compounds or using a radiochemical detector for ^{13}C. Both methods are time-consuming, and the radiochemical detector poses the problem of disposal of the scintillant fluid often added to boost photon emission from labelled compounds. The AED can however distinguish between isotopes of the same element (Figure 5) making the analysis much simpler. Another advantage of the AED for drug analysis is in monitoring nitrogen which is present in many drugs. While the AED is less sensitive than the nitrogen-phosphorus detector, it allows for the monitoring of other elements such as specific halogens and oxygen to give a more complete picture.

(c) Organometallic compounds of environmental significance are easily and selectively detected with the AED. The analysis of trace levels of organometallics in the environment is becoming increasingly important. For example, the EEC list of priority pollutants contains 8 organotin compounds. Tin compounds can be detected using the AED at 303 nm (Figure 6) at the femtogram level which is a considerable improvement over GC-MS sensitivity.

(d) Multi-element profiling of the headspace vapour from perfume samples not only reveals which is the fake or synthetic equivalent, but also reveals the presence of possibly harmful additives such as nitro-musks. In Fig. 7A the headspace chromatogram of the genuine Ysatis perfume is recorded. Four elemental responses (carbon, hydrogen, nitrogen and oxygen) are shown. In Fig. 7B the equivalent response for the fake perfume is displayed. Several points should be noted. Firstly, the complexity of the fake perfume carbon response (equivalent to the FID response in conventional capillary GLC) is remarkable. The fake perfume is a serious attempt to copy the original rather than merely imitate, and hence reproduce, the keynotes of the aroma. The similarity of the two oxygen response traces reinforces this view with many compounds being common to both samples. Clear differences are observed for the nitrogen-containing compounds and these are displayed in Fig. 8. Note that the lower trace is displaced to the right by approximately three minutes for clarity. Peaks 1, 2 and 3 have the same retention times although the concentration of 1 relative to 3 is much reduced in the fake sample. The reverse is true for compound 2. GC-MS data suggest that these are nitro-musks or closely related compounds. Note also the appearance of a range of low concentration nitrogen-containing compounds in the real sample. This complexity is absent in the fake sample. Differences between the two samples do exist, primarily amongst the minor components, but the fake sample is quite a good copy.

Conclusion

The advantage of the AED lies in its ability to act as a truly element-specific detector. Hence it is a particularly useful technique for screening samples as it highlights those compounds which contain hetero-atoms. It is particularly useful as a comparison technique and as such may be viewed as a complementary technique to GC-MS. For example, comparison of perfume samples rapidly establishes real from fake materials because the nature of the nitrogen-containing compounds varies. Likewise the distribution of the oxygenated compounds varies, even though the TIC from the mass spectrometer may be superficially similar. Arguably, the need to use high purity helium as carrier gas is a drawback.

The strategy, therefore, is to use the AED to screen complex mixtures to highlight components of interest because of their heteroatom content. This process gives information about elemental composition. Use of gas chromatography-mass spectrometry to identify the highlighted components provides additional structural information from the mass fragmentograms. The combined information from the two techniques often allows elimination of the ambiguous assignments made by mass spectral libraries.

References

1. Ebdon, L, Hill, S., and Ward, R. W, *Analyst*, 1986, **111**, 1113.
2. McCormack, A. J., Tong, S. C., and Cooke, W. D., *Anal. Chem.*, 1965, **37**, 1470.
3. Beenakker, C. I. M., *Spectrochim Acta*, 1976, **31B**, 483.
4. Quimby, B. D., and Sullivan, J. J., *Anal. Chem.*, 1990, **62**, 1027.
5. Webster, C., and Cooke, M., *Analyt, Proc. and Commun.*, in press.
6. Webster, C., and Cooke, M., *HRC*, in press.

Authors details: Caroline Webster and Michael Cooke, Sheffield Hallam University, City Campus, Pond Street, Sheffield S1 1WB. Tel: 0742 533086.

Acknowledgement
Figures 1,2,3,4 and 5 reproduced with the kind permission of Hewlett Packard.

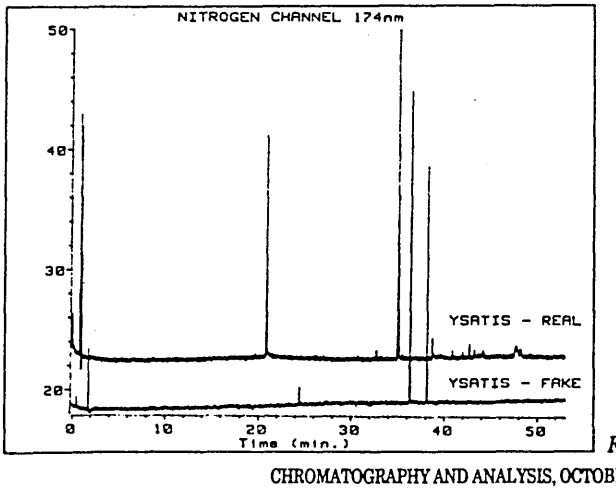

Fig. 8.

USE OF AN ATOMIC EMISSION DETECTOR TO STUDY THE VARIATION IN ELEMENTAL RESPONSE FOR CHLORINE, CARBON AND OXYGEN IN PHENOLS

Caroline Webster and Michael Cooke*
The Environmental Research Centre
Division of Chemistry
School of Science
Sheffield Hallam University
City Campus
Pond Street
Sheffield S1 1WB UK

Submitted to: Journal of High Resolution Chromatography as a Short Communication

Keywords: Capillary Gas Chromatography, Atomic Emission Detection, Elemental Response, Compound Independent Calibration

Abstract

A series of chlorophenolic compounds have been studied using capillary gas chromatography with atomic emission detection. Various molar concentrations of the mixed standard compounds were analysed and the elemental responses for carbon, chlorine and oxygen were collected. Calibration curves for element against concentration were plotted to reveal variations in the elemental responses. The spectral lines used were carbon (193 nm), oxygen (777 nm), and chlorine (479 nm). None of the elements studied gave responses which were completely free of the influence of molecular structure. Discharge tube contamination generally reduced sensitivity for carbon, chlorine but not, apparently, for oxygen which increased slightly.

Introduction

The coupling of a capillary gas chromatograph to a microwave induced plasma-atomic emission spectrometer (MIP-AES) gives a powerful hyphenated technique which can provide complimentary information to that available from gas chromatography-mass spectrometry. Use of a diode array detector in the spectrometer permits the simultaneous detection of up to four elements and thus provides truly element specific detection (1). Hence the atomic emission detector duplicates the functions of all the common gas chromatography detectors and, in addition, can provide selective detection of individual halogens as well as for metals such as tin, lead and mercury. Of particular importance is the ability of the AED to provide information which permits the determination of

* author for all correspondence

empirical formulae (2-7). In theory the helium microwave induced plasma operates at a sufficiently high temperature to decompose the compounds eluting from the gc column into free atoms which are then excited and emit line spectra upon returning to the ground state. Hence the emission yield should be related to the element concentration in the plasma and should not be influenced by the molecular structure which preceded the formation of the elements. If this does not occur and partial breakdown, or scavenging of the elements produced by side reactions, occurs then the emission response will vary according to the amount and nature of these processes. Early reports on the independence of elemental response relative to the structure of the parent molecule reveal both ideal (8) and non ideal (9) behaviour. In particular van Dalen et al (9) have shown that the hydrogen response may be non-linear with an apparent increase in relative response at higher concentrations.

Quantitation in gas chromatography is generally achieved using a reference compound. In order to match responses and also chromatographic behaviour it is conventional to use a reference compound of similar character to the compounds to be determined. However the MIP-atomic emission detector should, in theory, give elemental responses which are independent of compound structure. Hence the reference compound need only contain the elements of interest because the response measured by the detector will be independent of the molecular structure. This procedure has been called 'compound independent calibration (CIC)' (2). Recently, however, the validity of CIC has been questioned (10-12) and the procedure has been found to be unreliable when heteroatoms such as nitrogen (11) and oxygen (12) are present.

This paper describes the results obtained by studying the responses for carbon, chlorine and oxygen in a set of phenolic compounds using a commercially available gas chromatograph - atomic emission detection system. The effect of discharge tube contamination is also discussed.

Experimental

The GC-AED (Hewlett-Packard, Avondale, Pennsylvania, USA) consisted of an HP5890 capillary chromatograph interfaced to an HP5921A atomic emission detector and coupled to a ChemStation. Helium carrier (1ml min^{-1}) and reagent gases were as recommended by the manufacturer.

The mixed standard was composed of 2-chlorophenol, 2,4,6 tri-chlorophenol, 4-chloro-3-methyl phenol, 2-nitro phenol and 2,4-dinitro phenol made up in dichloromethane. A range of concentrations were prepared to cover the range 5×10^{-5} to 4×10^{-4}M and 1µl of

each was injected splitless (40s purge delay) onto a 25m x 0.32mm i.d. column coated with a 0.52μm film of cross linked 5% phenyl methyl silicone HP-5 (Hewlett-Packard). The column was programmed from 80°C (4min) to 280°C at 20°C min^{-1} and held for 3min. Carbon, nitrogen and oxygen were monitored at 193, 174 and 777nm respectively.

Results and Discussion

The compounds used in this study were 2-chlorophenol, 2-nitrophenol, 2,4,6-trichlorophenol, 4-chloro-3-methyl phenol and 2,4-dinitrophenol. Unfortunately, the 2,4-dinitrophenol proved to be undetectable at low concentrations and data was obtained for the two strongest concentrations only. Mixed standard solutions over the concentration range 5 x 10^{-5}M to 5 x 10^{-4}M were used throughout this study. The instrument was operated using standard reagent gas mixtures and conditions. A new discharge tube was installed in the instrument and the mixed standards were chromatographed in increasing order of concentration. Data was collected for the carbon response (193 nm), the chlorine response (479 nm), the oxygen response (777 nm) and the nitrogen response (174 nm). Hence two separate injections were made and the data for the oxygen response was merged with the data for the other three elements. From the data obtained calibration curves of response against concentration were plotted for carbon (Figure 1A) for chlorine (Figure 2A) and for oxygen (Figure 3A). Subsequently the data for each elemental response was collected when the discharge tube was contaminated by frequent use and this data is shown graphically in Figures 1B, 2B and 3B.

The response per atom of carbon using a clean discharge tube (Figure 1A) shows that 2-chlorophenol and 4-chloro-3-methylphenol produce virtually identical sensitivities, that is, the slopes for the compounds are the same, but that the carbon response for 2,4,6-trichlorophenol is less and that for 2-nitrophenol is even lower as is evidenced by the vertical displacement of the respective calibration lines. A structurally independent response would yield individual calibration lines which were fully superimposed. When a contaminated discharge tube is used (Figure 1B) the similarity of response between 2-chlorophenol and 4-chloro-3-methylphenol remains as does the lower response for the trichloro compound and the lowest response for the 2-nitro-phenol. However, the slopes for all four compounds are reduced by some 25%. Not only do the slopes for carbon vary between those obtained from a clean discharge tube and a used discharge tube (Table 1) but there are differences in relative response with respect to molecular structure. Consider the responses for 2-chlorophenol and for 2-nitrophenol. The lines are parallel but <u>not</u> superimposed. Superimposition would mean that the carbon response was independent of the molecular structure. The vertical separation of the two lines indicates that the absolute

response for the carbon atoms in 2-nitrophenol is less than that for the carbon atoms in 2-chlorophenol suggesting that the elemental carbon yield for these compounds differs.

When chlorine is considered, a similar picture is observed. With a new, ie clean, discharge tube (Figure 2A) all three compounds respond similarly with little difference in chlorine response between compounds. With a contaminated tube (Figure 2B) the slopes of all three lines decreases by approximately 20%. This difference in response with respect to the condition of the discharge tube is reflected in the decrease in the slopes of the calibration lines (Table 1) yet the correlation coefficients remain acceptable (Table 2). For chlorine the vertical separation of the calibration lines, representing the elemental response for chlorine in each structure is relatively small indicating that chlorine response is relatively independent of structure. This is to be expected as chlorine is unlikely to form stable intramolecular compounds during structural degradation of the parent compound.

When oxygen is considered (Figures 3A and 3B) the results are different. Although the correlation coefficients appear to be acceptable (Table 2). The response is best represented as a non-linear response. The shape of the curve is that previously observed by van Dalen et al (9) for hydrogen. There are small variations in response between new and used discharge tubes but the differential response per unit oxygen within this group of compounds is evident from the non-superimposability of the response curves. Note that for both clean and contaminated discharge tubes it is the 2-chloro compounds which deviate the most from a non-linear response. Hence, the response per atom of oxygen for 4-chloro-3-methylphenol is greatest whilst that for 2-chlorophenol and 2-nitrophenol is lowest.

Inter-molecular elemental responses also highlight differences. The oxygen atoms in the 2- substituted phenols behave identically whereas the carbon atoms in the same compounds give responses which differ by some 12% on average. In contrast the chlorine atoms in these compounds behave in a similar manner and their response appears to be virtually independent of the structure in which they are contained.

The possibility that contamination of the injection port of the chromatograph was causing discriminatory loss of compounds was considered. However, such discrimination would manifest itself on a compound dependent basis (possibly related to compound polarity) and not on an elemental dependent basis as is observed. However, to check for polarity and positional substitution effects a series of chloroanisoles (methoxyphenols) is being studied (13).

Conclusions

The elemental responses of carbon, chlorine and oxygen in a group of phenols in the atomic emission detector is related to the condition of the discharge tube for carbon and chlorine and, to a lesser extent, for oxygen. A contaminated tube reduces the response per unit atom for both carbon and chlorine. Elemental response appears to be virtually independent of molecular structure for chlorine but structurally related for both carbon and oxygen. As carbon and oxygen can combine to form CO but chlorine does not undergo the corresponding reaction with either carbon or oxygen it is possible that the relative ease of carbon monoxide formation during the breakdown of the molecules in the plasma influences both the carbon and oxygen emission yields. Evidence for the formation of CO in the plasma comes from the use of the line at 171.0 nm to monitor the emission from ^{13}CO in isotopically labelled compounds (14). Supporting evidence for this conclusion comes from the relatively poor oxygen response in 2-nitrophenol which contains the $^{-}NO_2$ moiety and thus can easily generate NO_2 thus inhibiting complete yield of molecular oxygen. Hence the presence of oxygen in a molecule will cause the carbon response to vary from that for a non-oxygen containing equivalent compound. Such variations should be noted when selecting compounds for quantitative purposes when using atomic emission detection.

References

(1) P C Uden, Element-Specific Chromatographic Detection by Atomic Emission Spectroscopy, *ACS*, Washington DC, 1992.

(2) J J Sullivan and B D Quimby, *HRC*, **12**, (1989), 282.

(3) P L Wylie, J J Sullivan and B D Quimby, *HRC*, **13**, (1990), 499.

(4) P L Wylie and R Oguchi, *J Chromatogr*, **517**, (1990), 131.

(5) A L P Valente and P C Uden, *Analyst*, **115**, (1990), 525.

(6) H Yieru, O Qingyu and Y Weile, *J Anal At Spectrom*, **5**, (1990), 115.

(7) N Kovacic and T L Ramus, *J Anal At Spectrom*, **7**, (1992), 999.

(8) M Zerezhi, K J Mulligan and J A Caruso; *J Chromatogr Sci*, **22**, (1984), 348.

(9) J P J van Dalen, P A de Lezenne Coulander and L de Galen; *Anal Chim Acta,* **94**, (1977), 1.

(10) Th Jelink and A Venema, *J H R C*, **13**, (1990), 447.

(11) S Pedersen-Bjergaard, T N Asp and T Grenbrokk, *J H R C*, **15**, (1992), 89.

(12) C Webster and M Cooke, *Analytical Proc and Commun* **31**, (1994), 237.

(13) C Webster and M Cooke in preparation.

(14) B D Quimby, P C Dryden and J J Sullivan, *Analyst Chem*, **62 (22)**, (1990), 2509.

Legends to Figures

Figure 1 A Calibration curves for the carbon responses using a new discharge tube

B Using a contaminated discharge tube

Figure 2 A Calibration curves for the chlorine response using a new discharge tube

B Using a contaminated discharge tube

Figure 3 A Calibration curves for the oxygen response using a new discharge tube

B Using a contaminated discharge tube

Table 1 Slopes of calibration lines for carbon, oxygen and chlorine using new and old discharge tubes.

Table 2 Correlation coefficients for calibration lines for carbon, oxygen and chlorine using new and old discharge tubes.

Table 1

	New Discharge Tube			Old Discharge Tube		
Phenol	**Carbon**	**Oxygen**	**Chlorine**	**Carbon**	**Oxygen**	**Chlorine**
2-Chloro	9.87	2.73	4.00	5.95	3.20	3.24
2-Nitro	9.30	2.84	-	5.63	3.30	-
4-Chloro-3-Methyl	9.65	3.16	3.94	6.04	3.68	3.16
2,4,6-Trichloro	9.39	2.85	3.79	5.71	3.26	2.97

All slopes x 10^7 for Carbon, x 10^6 for Oxygen, x 10^6 for Chlorine

Table 2

	New Discharge Tube			Old Discharge Tube		
Phenol	**Carbon**	**Oxygen**	**Chlorine**	**Carbon**	**Oxygen**	**Chlorine**
2-Chloro	0.9978	0.9672	0.9965	0.9986	0.8887	0.9939
2-Nitro	0.9980	0.9975	-	0.9976	0.9836	-
4-Chloro-3-Methyl	0.9981	0.9975	0.9985	0.9957	0.9865	0.9951
2,4,6-Trichloro	0.9985	0.9975	0.9988	0.9962	0.9791	0.9957